Assessing Deterioration of ADSS Fiber Optic Cables Due to Corona Discharge

Final Project Report

Power Systems Engineering Research Center

A National Science Foundation
Industry/University Cooperative Research Center
since 1996

Power Systems Engineering Research Center

Assessing Deterioration of ADSS Fiber Optic Cables Due to Corona Discharge

Final Project Report

George G. Karady, Project Leader
Johnny Madrid, Researcher
Arizona State University

PSERC Publication 02-17

May 2002

Information about this Project

For information about this project contact:

George G Karady
Salt River Chair Professor
Arizona State University
Department of Electrical Engineering
P.O. Box 875706
Tempe, AZ 85287-5706
Phone: 480 965 6569
Fax: 480 965 0745
Email: karady@asu.edu

Power Systems Engineering Research Center

This is a project report from the Power Systems Engineering Research Center (PSERC). PSERC is a multi-university Center conducting research on challenges facing a restructuring electric power industry and educating the next generation of power engineers. More information about PSERC can be found at the Center's website: http://www.pserc.wisc.edu.

For additional information, contact:

Power Systems Engineering Research Center
Cornell University
428 Phillips Hall
Ithaca, New York 14853
Phone: 607-255-5601
Fax: 607-255-8871

Notice Concerning Copyright Material

Permission to copy without fee all or part of this publication is granted if appropriate attribution is given to this document as the source material. This report is available for downloading from the PSERC website.

© 2002 Arizona State University. All rights reserved.

Acknowledgements

The work described in this report was sponsored by the Power Systems Engineering Research Center (PSERC). We express our appreciation for the support provided by PSERC's industrial members and by the National Science Foundation under grant NSF EEC 0001880 received under the Industry/University Cooperative Research Center program. We also express our appreciation for the support provided by the Bonneville Power Administration. Thanks are also given to Mr. Monty W. Tuominen, Bonneville Power Administration, who contributed to this project.

Executive Summary

Utilities have reported failures of ADSS (All Dielectric Self-Supporting) fiber optic cables installed on high voltage lines. The high electric field on those lines generates continuous corona discharge at the end of supporting armor rods. This discharge leads to cable deterioration. In a polluted environment, dry-band arcing causes cable deterioration when fog or dew occasionally wet the cable. This report presents a novel experimental technique to assess cable deterioration due to dry-band arcing. A long-term laboratory test replicated the dry-band arcing cause of fiber optic cable deterioration. The failure mechanism was identified and the cable life expectancy was estimated. A result of this project is the development of a novel test method to evaluate damage of ADSS fiber optic cables when dry-band arcing occurs.

This report uses text from the Masters thesis of Mr. Johnny Madrid who was supported by this project.

Table of Contents

Chapter 1	Introduction	1
I.	Problem description	1
II.	Dry-band arcing development	4
III.	Consequences of dry-band arcing on fiber optic cables	5
IV.	Reason for a standardized test	6
V.	Characterization method of dry-band arcing damage	7
VI.	Changes in the telecommunication media	10
VII.	Products and choices	11
VIII.	Importance of quality	12
IX.	The scope of the problem	15
X.	Copper versus fiber optic	16
XI.	Philosophical task for an electrical corrosion test method	17
Chapter 2	Literature review	19
I	Introduction	19
II	The electrical environment	20
III	Electromagnetic compatibility modeling	21
IV	Electromagnetic model transformation	23
V	Effects of pollution on fiber optic cable sheath	26
VI	Pollution level characterization on fiber optic cables	28
VII	Electrical test methods for sheathing material	30
VIII	Dry-band arcing effects on the aging of sheathing material	35
IX	Conclusions	36
Chapter 3	Experimental dry-band arcing test setup and procedure	38
I	Introduction	38
II	Test objects	38
III	Experimental set-up	39
IV	Cable setup	40
V	Spray system	41
VI	Galvanized metallic tank	43
VII	Protection system	43
VIII	Cables, impedance, and salinity	48
IX	Labview™ data acquisition and control system	49
X	Hardware and software interface	52
XI	Conclusions	53

Table of Contents (continued)

Chapter 4 Initial dry-band arcing verification tests 55
- I Introduction 55
- II Initial metrics and apparatus 55
- III Series 1: 0 Ω limiting impedance, tap water wetting 57
- IV Series 2: 0 Ω limiting impedance, tap water wetting 60
- V Series 3: 1.65 mΩ limiting impedance, tap water wetting 62
- VI Series 4: 150 kΩ limiting impedance, salt water wetting 63
- VII Comparison of series 1 – 4 test results 68
- VIII Long-gap tests with 10 kVrms. supply 69
- IX Test on cables ‘a’ and ‘f’ 74
- X Conclusions 81

Chapter 5 Correlation between dry-band arcing and time-to-failure 83
- I Introduction 83
- II Categorization of dry-band arcing events 83
- III Data acquisition parameters 86
- IV Tests performed and metrics used 88
- V Test on cable ‘a’ – series i results 93
- VI Test on cable ‘a’ – series ii results 100
- VII Test on cable ‘f’ – series iii results 105
- VIII Test on cable ‘f’ – series iv and v results 112
- IX Test on cable ‘f’ – series vi results 120
- X Conclusions 129

Chapter 6 Conclusions and recommendations 131
- I Dry-band arcing damage 131
- II The need of a test procedure 131
- III Future research and development 132

References 133

Chapter 1

Introduction

I. PROBLEM DESCRIPTION

Utilities frequently use ADSS (All Dielectric Self-Supporting) fiber optic cables installed on transmission lines 10-20 feet below the high voltage conductors. An armor rod assembly supports the cable at each tower as shown in Figure 1. The rods surround the cable and distribute the mechanical loads evenly. Discussions during an IEEE workshop indicated that the failure of ADSS fiber optic cables in high electric field environments is an industry-wide problem. Several corporations such as, Bonneville Power Administration, Houston Light and Power, Consolidated Edison, and others in England and Germany observed surface deterioration on ADSS cables installed on HV structures.

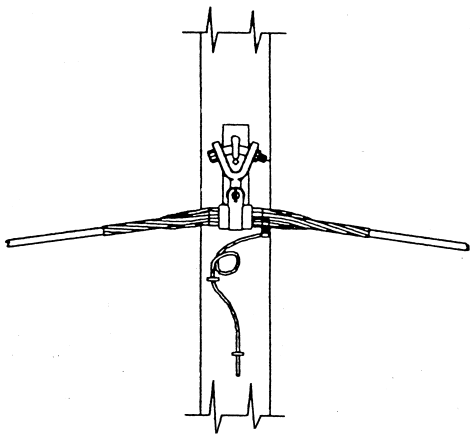

Figure 1. Armor rod assembly for fiber optic cables

The experimental results and the review of literature indicated that dry-band arcing, due to longitudinal electric fields in combination with pollutant levels of varying severity accumulating on the surface of cables, especially when wet, have caused most of the cables to deteriorate and eventually fail. The objectives of the case in study are the development of the following:

1. Develop a new test method that will define and represent environmental conditions experienced by fiber optic cables strung along high-voltage networks experiencing different degrees of pollution levels, particularly in salty areas.
2. Compare the performance of different fiber optic cable sheaths subjected to dry-band arcing test under controlled conditions.
3. Study and compare the effects of current-limiting impedances used in exposing the cable's sheath to high voltage.
4. Give the results of a methodology used to analyze the acquired leakage current data and consider its outcomes correlated to the failure characteristics of the fiber optic cables due to dry-band arcing.

There are analytical methods, based on the geometry and voltage levels, that allow the power utilities to determine the optimum stringing positions for any given tower and power line configuration. The analytical methods are based on electromagnetic theory such as the one used by Bonneville Power Administration (BPA) 0. Voltage potential profiles around the towers are used to help determine a convenient point with the lowest space potential as shown in Figure 2.

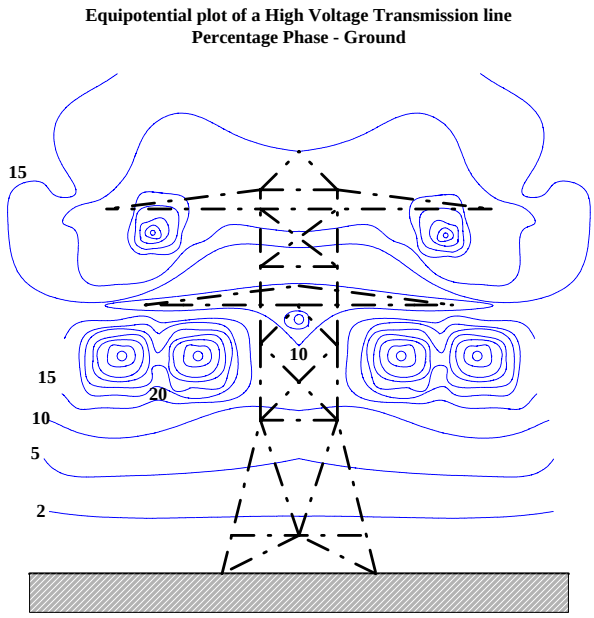

Figure 2. Typical 2D equi-potential plot of a high voltage transmission line

Armor rod assemblies are attached to transmission line structures and support the fiber optic cables. The cables are effectively grounded to the earth through these suspension points via the structure's design. Depending on the placement of the cable with respect to the high voltage conductors, the conductor's voltage, and pollution on the cable's sheath an induced voltage and current will flow over most of the cable's suspended length. This type of configuration, as shown in Figure 3, gives rise to various physical phenomena, namely, corona, microsparking, and dry-band arcing, especially near the tower, as the current is greatest there [2]. Fiber optic cables strung in these electrically hostile environments must last for a predicted life in excess of 25 years [3]. An experimental setup is needed to verify and compare the expected lifetimes for various cable sheath materials under the influence of dry-band arcing as encountered in its natural environment.

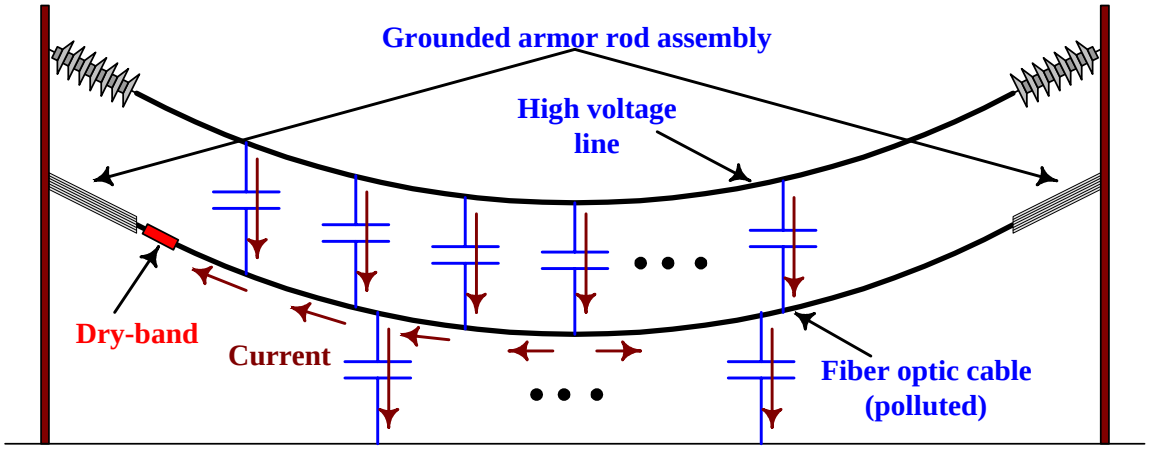

Figure 3. Fiber optic cable high voltage line configuration

II. DRY-BAND ARCING DEVELOPMENT

Dry-band arcing will develop under the conditions already mentioned and the cable's outer sheath can be degraded as a result of arc current flowing along the cable's sheath induced by the high electric field from the high voltage transmission lines. Due to the relative geometric position of the high voltage conductors and the fiber optic cable, the fiber optic cable will be capacitively coupled between the line and earth. The voltage difference between the high voltage line(s) and the fiber optic cables implies a charge distribution on the fiber optic cable. This is because there can be no voltage without an electric field. The concept of an electric field is attributed to the interaction between charged bodies. This idea of charge distribution when voltages are present is not described by circuit theory alone and necessitates a process of simulating the physical phenomenon. In general, the simulation of a physical phenomenon is referred to as modeling. Over prolonged periods of time the electric fields will cause enough dry-band arcing stresses to occur and degrade the fiber optic cable's sheath and cause it to fail.

Figure 4 shows a typical two-dimensional configuration of the relative voltage and current distributions along a suspended fiber optic cable on a high voltage transmission network. The magnitude of the induced voltage and current will depend on the installation position, transmission line loading, conductor sag and phasing, and accumulated contamination on the fiber optic cable.

III. CONSEQUENCES OF DRY-BAND ARCING ON FIBER OPTIC CABLES

Cables in service from various regions around the world, especially near coastal areas, have largely imputed failures to dry-band arcing. Dry-band arcing occurs on the outer sheath of fiber optic cables, even though the ADSS cable is electrically non-conductive. Dry-band arcing can be largely attributed to the contamination that accumulates on the outer sheath, which can be considerably conductive. One of the outer sheath's functions is to provide protection for the aramide material that is wrapped around another inner structure underneath the cable's outer sheath. The aramide material gives the cable its required tensile strength that allows the cable to be self-supporting. The aramide yarn is by far the strongest synthetic fiber next to a spider's web. Deterioration of the outer sheath will expose the aramide to the environment and degrade its tensile strength characteristics. Exposing the aramide material to arcing activity will cause degradation to occur by the high temperature of the arc. This will then lead to the fiber optic cables to drop out of service by collapsing under its own weight.

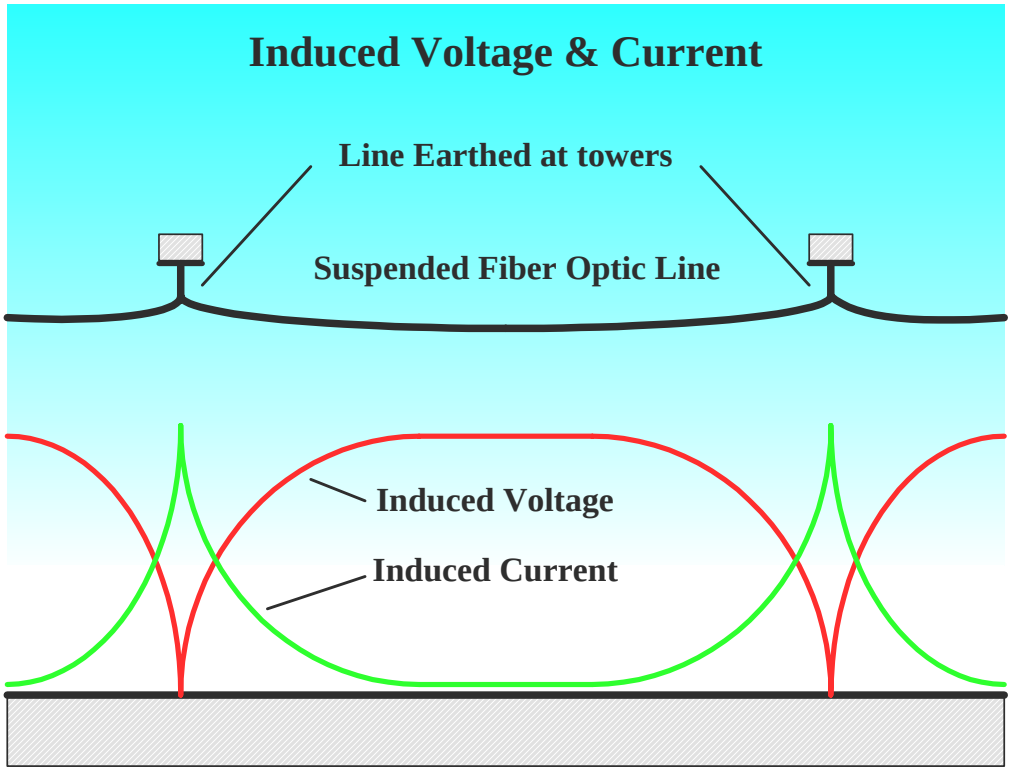

Figure 4. Induced voltage and current on a suspended fiber optic cable

IV. REASON FOR A STANDARDIZED TEST

Various companies manufacture ADSS cables and assert that their products outer sheath is suitable for high voltage applications. In order to validate their specifications, an independent test procedure is needed to investigate the effects and performance of various fiber optic cable's outer sheath under dry-band arcing. The materials used in the cable's outer sheath are not the same from manufacturer to manufacturer. A test procedure and analysis technique have been implemented and used to rank the assortment of cables with regard to the performance to dry-band arcing. The test procedure along with its results and its relative advantages and disadvantage is the main focus of this

thesis. A set of measurable metrics will be used to simulate environmental conditions encountered by the fiber optic cables in nature. The cable rankings will be a function of how well the individual cables perform relative to each other under the same measured metrics.

V. CHARACTERIZATION METHOD OF DRY-BAND ARCING DAMAGE

The method used to characterize the cable degradation is based on the damage caused by the dry-band arcing occurring on the outer sheath of the cable. The fiber optic cables are installed in a laboratory test setup and energized to a specified high voltage. A water solution is sprayed periodically on the energized fiber optic cable by an automated computer system to initiate dry-band arcing and allowed to dry naturally. The most useful experimental apparatus for testing fiber optic cable sheaths against dry-band arcing is shown in Figure 5. This setup simulates the effects of dry-band arcing on the fiber optic cables as encountered in the field. In this setup, the high voltage and low voltage electrodes are fixed directly to the cable's sheath and a 60 Hz (AC) voltage is supplied to the high voltage electrode through a series current limiting impedance. Much care must be considered by making sure that the concentration of the NaCl (sodium chloride) water solution does not change drastically during the test. Changing the conductivity of the water solution may adversely change the rate of degradation of the cable's sheath for a fixed high voltage level. This change in conductivity increases the risk of introducing an aging mechanism that could be drastically different from the actual environment encountered by the ADSS fiber optic cable in service. Therefore the NaCl water solution concentration is kept as constant as possible.

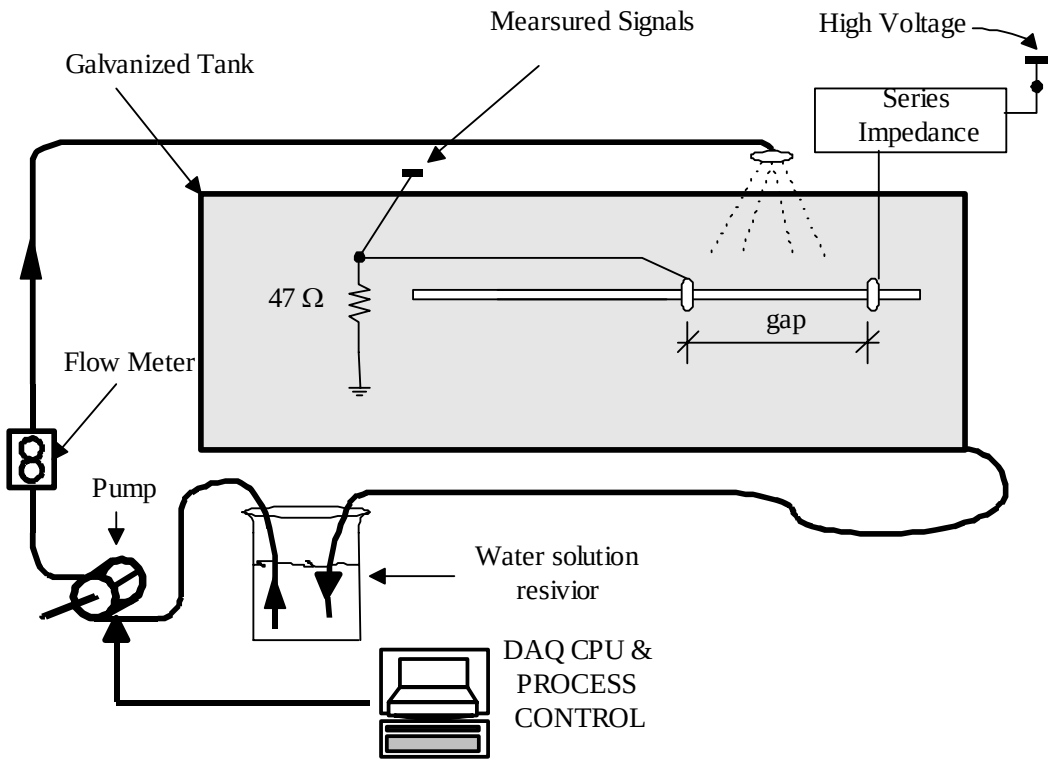

Figure 5. Apparatus for testing cable samples in the laboratory

The water solution is used to simulate the pollution that accumulates on the cable as strung on high voltage networks. The wet/dry periods caused by the spray and dry-band arcing processes is cyclical. Dry-band arcing will eventually degrade the cable's outer sheath and cause the sheath to fail. The failures are a function of time and therefore evaluated in terms of the time-to-failure (TTF). Several other factors are involved in the failure mechanism caused by the dry-band arcing. These factors are categorized into several metrics that can be measured and quantified. The metrics can be adjusted to match those encountered in nature and determine their effects on the failures. The dry band arc current flowing along the cable sheath is measured by an automated data acquisition system. The acquired data is then analyzed off-line and correlated to the TTF.

The method used to analyze the acquired data is founded on the events developed in the dry-band arcing process that undergo during the wet/dry cycles. The events are categorized into the following three qualitative outcomes:

1. *AC period*, this occurs when the current is predominantly sinusoidal. This type of activity takes place during the time prior to the onset of dry-band arcing
2. *Arcing period*, this event follows the *AC period* activity. In this period the cable has undergone the drying process and dry bands have formed to initiate dry-band arcing.
   a. *60 Hz type.*
   b. *Pulse type.*
3. *Noise period*, this occurs when dry-band arcing has ceased, and negligible current is induced through the cable's sheath.

The three periods that categorized above are shown in Figure 6. The two types of arcing events under the *Arcing period* have not been studied in detail in regard to the amount of damage caused on the cable's sheath.

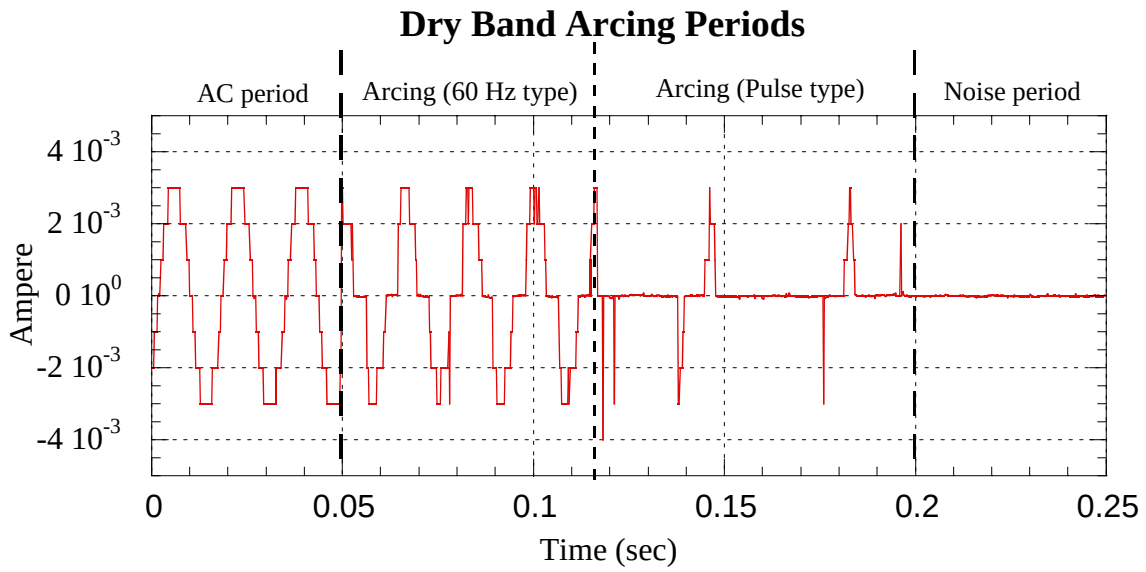

Figure 6. Dry-band arcing periods

VI. CHANGES IN THE TELECOMMUNICATION MEDIA

The advent of fiber optic communication technology has led to a rapidly changing telecommunications industry. Fiber optic cable is one media type for the growing communication industry. Presently, there are more than 220 fiber optic cable companies around the world. Optical communication enables faster and higher-quality information transmission. The fiber optic cable was first introduced in 1950s and can carry high volume of information, about 40 million words in a single second. Fiber optic cable can transmit approximately 40,000 messages simultaneously and copper cable can transmit approximately 3,700 messages at one time. Presently, due to technological limitation in the electronic industry, a fiber optic cable is capable of transmitting 20,000 messages. Fiber optic cable does not conduct electricity and is not affected by electromagnetic waves, which makes fiber optic cable transmission safe and reliable. The size of fiber

optic cable is comparable to the size of copper cable but have much greater bandwidth than copper cables. In 1974, Furukawa Electric became the world's first manufacturer of optical fiber cable [4]. ADSS fiber optic cables began to be installed on overhead power lines around 1979. Since then manufactures are continually introducing new products, transmission technologies, and cables.

In today's advanced telecommunication cable systems, conventional communication systems, such as copper-based wiring systems, are considered as becoming phased out. Copper-based wiring systems will still be used in some applications and definitely be the dominant infrastructure for many more years to come, for example in residential homes.

VII. PRODUCTS AND CHOICES

There are many manufactures, over 220, providing serviceable fiber optic cable products [5]. There are many service providers considering upgrading or replacing cable and equipment and sometimes do not consider the costs and benefits associated with the new fiber optic cable systems, especially in high voltage environments. These service providers can greatly benefit from an impartial test not associated with any supplier or manufacturer. The test can be used to analyze their fiber optic cables and make objective recommendations about the various cable's sheath under test as encountered in high voltage distribution and transmission networks. An analysis of a fiber optic cable's sheath under high electrical stress evaluates functionality, damage, customer

requirements, and life expectancy in the context of quality, service reliability, availability of products and hardware, and economics.

VIII. IMPORTANCE OF QUALITY

A quotation that is very relevant in the quality assurance tests is, "Quality is a race without a finish line," and should be used for all recommendations, reports, and analyses related to design, workmanship, testing, and hardware. This quote is one of the most popular themes of the United States Quality Movement. It is a concise, polished statement that speaks of the continuous improvement of a job never finished. A test procedure that can compare different fiber optic cables for high voltage networks is very valuable to the power utilities and customers. The utilities can determine which fiber optic cable is of better quality from the test results. The tests performed to compare and validate which manufacture produces a fiber optic cable with a sheath of withstanding dry-band arcing the best is a very extensive and important task.

One of the main business philosophies is defining the responsibilities of a test procedure to be standardized and help the consultant evaluate design and technical projects in the ongoing research of understanding the damage of fiber optic cable's sheath caused by the dry-band arcing phenomenon. The evaluation may also include the objective recommendation or purchase of products and hardware to meet a customer's present and future requirements by comparatively ranking the cable's performance with regard to incurred dry-band arcing damage. In the last ten years, the telecommunications industry has been experiencing an era in which the typical customer can be connect to a

terminal and communicate with almost anyone around the world instantly. In time, satisfied customers will identify who the real winners in the telecommunications arena are. In the meantime, however, many companies sometimes fail to understand the importance of quality, service, reliability, and economics. A compromise must be met in order to provide the best possible solution in an ever-growing field.

Many trade journals, articles, white papers, and panels, to name just a few, reverently discuss the merits of competing products and hardware but only a few discuss the test methods employed to characterize the fiber optic cable's sheath against dry-band arcing as discussed in Chapter 3. A better source of important product characteristics and specifications are standards organizations, such as the Telecommunications Industry Association (TIA) [6], the American National Standards Institute (ANSI) [7], the International Organization for Standardization (ISO) [8], International Electrotechnical Commission (IEC) [9], and the Institute of Electrical and Electronics Engineers (IEEE). Presently the IEEE has a standard draft for ADSS fiber optic cable for use on overhead utility lines [10]. Ongoing recommendations are being put forth to come up with a standard test procedure to characterized fiber optic cable sheath damage caused by dry-band arcing. An IEEE joint working group has been formed to come up with a standard. The present IEEE working group is structured as shown in Figure 7. The IEEE is currently the only professional society that is working on standardizing a test method for dry-band arcing on fiber optic cables in high voltage environments.

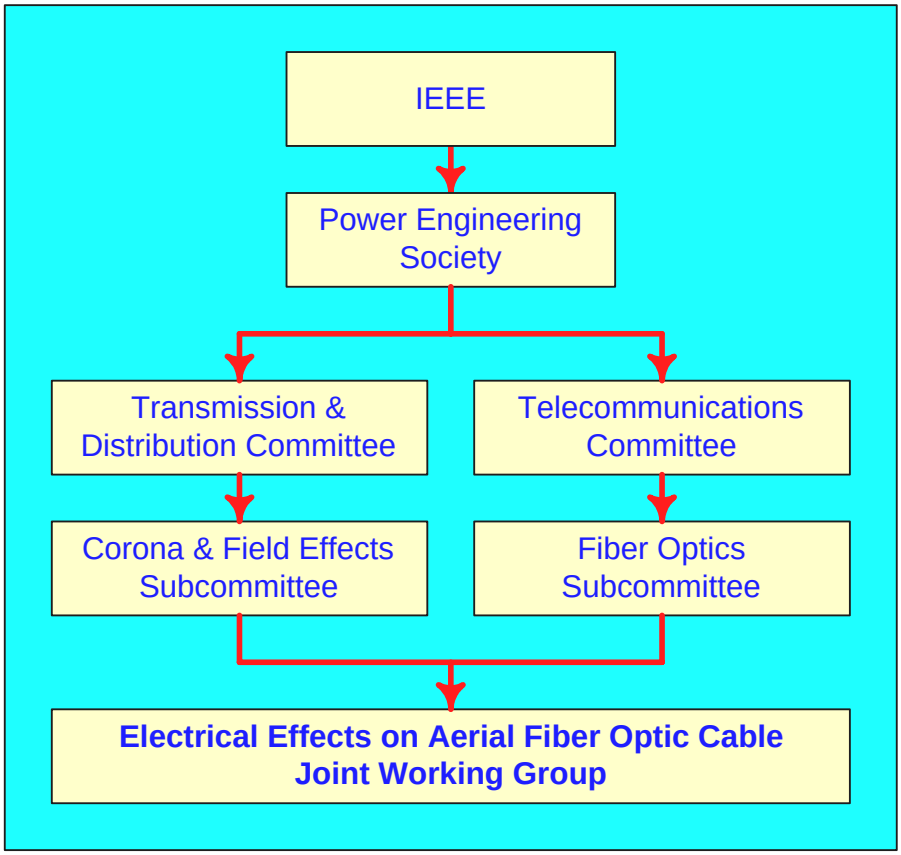

Figure 7. IEEE committee structure

There are various methods used by customers to determine which products to choose for their application(s). A very common way to differentiate between products is to examine their respective guarantees, but sometimes the guarantees can be definitively deceiving. There is a manufacture that states it has an aerial ADSS fiber optic cable designed for aerial self supporting installation under extreme wind and ice load conditions that can be used in high voltage applications up to 500 kV. They also state that their product has a special sheath material is used to counter dry-band arcing [11]. Therefore the need of an independent test to verify the manufactures guaranteed specifications. Manufactures that cover life cycle, bandwidth, operations, environmental

specifications, and management are helping customers make a long-term investment. High-performance cabling is only as good as its guarantee. The test procedure use to test the cable's sheath against dry-band arcing will help in determining its lifetime serviceability.

The ADSS cables are of particular interest to power utilities since existing power distribution and transmission infrastructure networks are being used as installation elements. The cable’s sheath provides protection from moisture and extreme temperatures to the aramide yarn material, and may also have fire resistance material allowing it to run directly to the wiring closet. Cost savings results from the elimination of splice enclosures and reduced need for connectors and labor due to the single type of cable.

IX. THE SCOPE OF THE PROBLEM

Most problems in signaling systems are exposed to electrical and magnetic interference, especially in the harsh environments that exist in high voltage networks. Exercising correct planning and design procedures is of the utmost importance to the useful lifetime expectancy and overall reliability of an existing or proposed telecommunication cabling system. The specifications for proposed facility growth and system efficiency require an identification and test procedure that will ensure the employed design functions as designed.

Design is the primary concern for the engineer as opposed to analysis for the scientist. With today's world of telecommunications expanding into all of our daily lives,

a great deal of effort must be put into the design of fiber optic cable systems in order for it to operate properly in high voltage environments. High voltage networks are known to be hostile to the fiber optic cables installed near the power lines and, in some benign instances, to human health. The power lines generate external fields and currents. The external fields are merely unwanted by-products of their function and are referred to as unintentional radiators.

The coexistence of electrical systems is a science in itself, known as electromagnetic compatibility (EMC). Modeling of electromagnetic systems is a field exclusively for electromagnetic scientists and engineers. Power systems, in real life, act simultaneously as an electromagnetic interference (EMI) source and receptor, which affect the existence of the fiber optic cables installed on high voltage networks. In addition, a review of compliance with current codes and standards must be completed and fully understood to warrant the safety of people and property. Present or proposed cable systems are regulated by city, state, or federal codes, and in most cases must also meet the standards of the Occupational Safety and Health Administration (OSHA), the Environmental Protection Agency (EPA), Federal Communication Commission (FCC), and the National Electrical Safety Code (NESC).

X. COPPER VERSUS FIBER OPTIC

Voice signals have been transmitted over copper-wire systems since the late 1800's. Considering today's transmission speeds of millions of bytes, it would be easy to relegate copper-wire systems to the history museums. In reality, however, exchange

carriers are still using standard gauge copper wire, and some research laboratories are issuing white papers declaring that copper-wire systems can deliver higher frequency signals over given bandwidths. Customers planning work on existing or proposed communication networks must ask whether copper will comply with their changing needs and be able to adapt to the new systems entering the growing field of the information age.

Technology is currently providing copper-network investments with a new lease on usage for several more years. Such systems as Digital Subscriber Line (DSL) technologies can be implemented over standard and unconditioned copper facilities. The advantages of DSL systems include that no new electronic circuits are required or need to be deployed in the loop. The DSL technology allows the carrying of higher-speed data without extensive arrangements or special accommodations.

As fascinating as fiber may seem, copper may still be a top competitor and hold its own as a viable media in today's communication needs. Both types of media can be cost-effective for the customer, and both are essential means of transporting information that complement each other in a well-designed telecommunications system.

XI. PHILOSOPHICAL TASK FOR AN ELECTRICAL CORROSION TEST METHOD

Dry-band arcing is acknowledged to take effect on polluted fiber optic cables installed in high voltage environments as the cables sheath dries. Another recognized fact known about dry-band arcing activity is it will lead to cable sheath erosion that ultimately exposes the aramide strength member to be weakened by environmental effects and thereby causing a catastrophic failure of the fiber optic cable altogether. Such

catastrophic failures are not widely reported or discussed in the literature due to commercial reasons. Commercial reasons of this type is one of the methodological problems that hinders the proliferation of an independent test procedure to comparatively rank different manufacture's fiber optic cables in an acceptable and standard test method. Some manufactures will not risk their business revenues based on a test method that would degrade or even disqualify their products from being marketed for what they were originally intended to be used as. Therefore it is of utmost importance to be able to simulate actual environmental and electrical conditions by a laboratory test setup that will not abate but attest to the manufacture's quality of their fiber optic product's performance. The test method will inherently push the manufactures to improve their products to outperform their competitors resulting in an overall improvement and higher quality of products. This line of reasoning forms the basis for a standardized test procedure since there is myriad of fiber optic cable manufactures to chose from. Eventually it breaks down to an economical problem since the amount of revenue that can be lost from a fiber optic cable dropping out of service is remarkably high. In today's world of information and speed, this could be devastating even to the common person either directly or indirectly.

Chapter 2

Literature Review

I. INTRODUCTION

ADSS fiber optic cables were originally developed in West Germany and the Netherlands and have been in operation on power lines of up to 110 kV_{rms} successfully for a number of years of service [12]. Attempts of installing ADSS cable on voltage levels of 220 kV led to cable sheath failures in less than a year after installation. Examination of the damage in these early failures exhibited, what seemed to be electrical damage near the supports. Various theories ensued and tried to explain and solve the events leading to the cables dropping out of service. Dry-band arcing is now generally acknowledged to be the main cause of damage sustained by the cables strung in a high voltage environment [13]. Research at Arizona State University in joint efforts with Western Power Administration (WAPA), and Electric Power Research Institute (EPRI) has developed an experimental setup to simulate the dry-band arcing electrical damage observed on the fiber optic cable's sheath. Bonneville Power Administration (BPA) also contributed to the study. The following paragraphs discuss and summarize recent methods and techniques posed by experts in the field in attempts to solve the problem and test different manufacture's ADSS cables against dry-band arcing.

II. THE ELECTRICAL ENVIRONMENT

An electric field exists where there are voltages. When there are voltage differences, there is energy stored in the electric and magnetic fields. This energy cannot be ignored or dissipated instantaneously. The geometry formed by the high voltage transmission line(s) and the ADSS fiber optic cables sets up a set of capacitances that store and transfers the energy from the high voltage conductor(s) to the ADSS cable. In many cases the dissipation or decay of the stored energy is developed by the electric field from the high voltage line is considered to be the driving force of the induced currents causing dry-band arcing on the fiber optic cable [2]. Electrical and magnetic fields exist in high voltage networks and pose dry-band arcing problems to most nearby ADSS cables. The physical geometry of an electrical setup will considerably dictate how much dry-band arcing will be exposed or experienced by the adjacent fiber optic cable. Controlling electrical fields is considered to prevent damage to occur on the cable. This subject of arc control, namely grounding and shielding, is explained by using basic physics and cannot be approached by using circuit theory alone. One reason that circuit theory alone cannot be used is because the geometry of a structure is rarely treated as it appears in the physical world. The geometry is at the heart of understanding the interference process as in the case of dry-band arcing on ADSS fiber optic cables.

There are many topics that cannot be treated using circuit theory. Some examples that can be included in this subject are lightning phenomena, microwave transmission, antenna radiation, noise on power distribution systems, skin effect, shielding affectivity, aperture penetration, dry-band arcing, et cetera.

III. ELECTROMAGNETIC COMPATIBILITY MODELING

There are two approaches that basically encompass the foundation to deriving a working model that can be used to describe the natural behavior of the phenomena of dry-band arcing in a scientific manner: the inductive approach and the deductive approach. The inductive approach is one that follows the historical development of the subject by starting with some observations from experiments and then inferring from them laws and theorems. On the other hand, the deductive approach postulates a few essential relations for an idealized model. Particular laws and theorems can then be derived from the postulated relations. The relations and model's validity is verified by their ability to predict outcomes that check with experimental observations. The two conceptual frameworks of inductive and deductive reasoning enabled the development of the computer model developed at Arizona State University, which will be discussed later in the next section.0

Modeling the physical and electrical parameters of a suspended ADSS fiber optic cable on high voltage networks is a very formidable task to be undertaken. The steps of deliberating the physical environment, which are then abstracted and converted to mathematical entities, typically to be an element of, or compatible with, rules and equations forming the basis of the numerical model explained in the next section. Obtaining such a model greatly helps in gaining an understanding of how to simulate the environment in the laboratory with agreeable results. The main picture of the system configuration is depicted in Figure 8, which shows the tower, phase conductors, ADSS fiber optic cable, self-capacitances, and mutual capacitances. Note that there is also a

capacitance present between phase-to-phase conductors and phase-to-ground, but are not included in the modeling since they do not affect the induced currents.

Having a representative model enables further investigation of the physical metrics most dominating that affect the events leading to dry-band arcing under the aforementioned electrical environment. An in depth inspection of the analytical results gives rise to simplification of the total model.

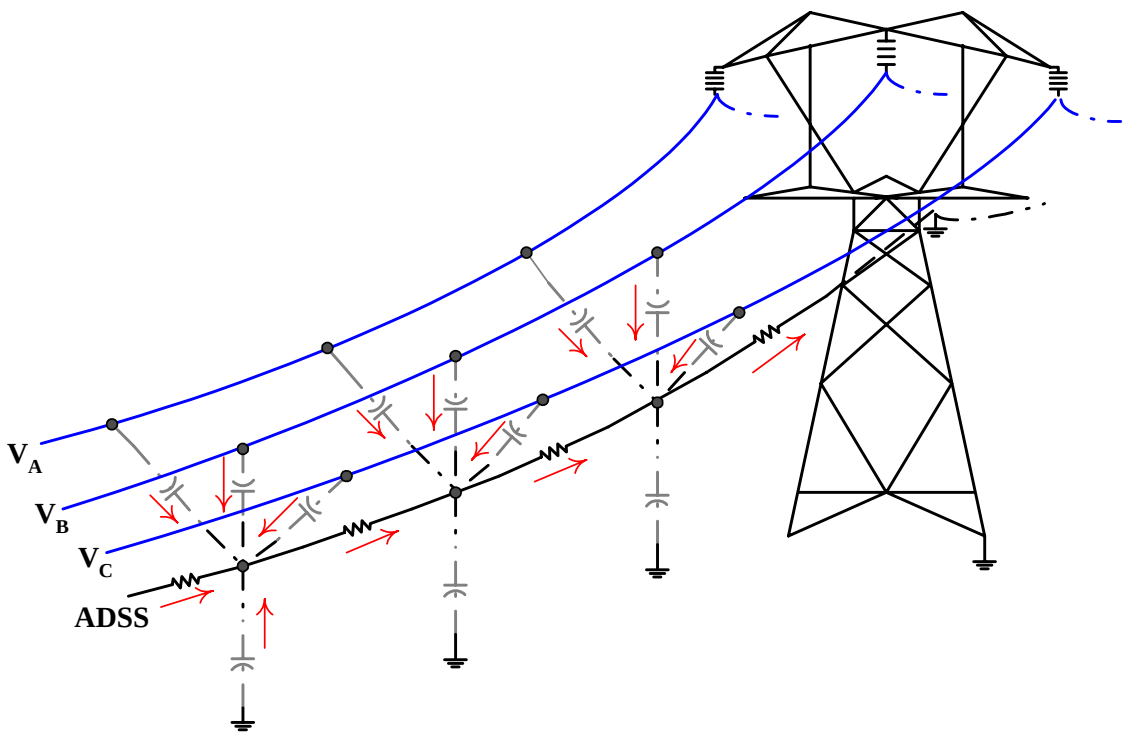

Figure 8. Representative Transmission and ADSS Circuit Model

IV. ELECTROMAGNETIC MODEL TRANSFORMATION

Electromagnetic modeling is a very intensive field of study. The rudiments of electromagnetic modeling may be simply defined as the transformation of the physical design into a representative geometry.

Presently there are three methods used to model the fiber optic cables strung on high voltage networks. All of the methods have been developed independently by engineers studying the problem. The results generated by these analytical methods are very much in agreement to one another, which is not a surprise given the circumstances. One method uses a different approach as described in [14]. The other method, developed at Arizona State University and Bonneville Power Administration, transforms the physical parameters to a mathematical representation to predict dry-band arcing on fiber optic cables installed on transmission lines 3 – 6 meters (10 – 20 feet) below high voltage conductors [15]. This method has been developed to represent the polluted fiber optic cable in the high voltage environment. An equivalent circuit of polluted fiber optic cable is used as an electrical model and simulated on a computer. The model can include and conform to a few of the principal entities that dominate the dry-band arcing process. The algorithm used can include:

1. Effects of non-uniform pollution
2. Cable sag
3. Open circuit calculations
4. Mitigation devices using semiconductor rods (linear representation)

5. Tower (support) capacitance.

Kirchoff's Current Law (KCL) is used to derive node point equations for the equivalent circuit. An equivalent mathematical expression for the energy source is also derived. This equivalent energy source is one of the main parameters obtained from the model. The section of an equivalent circuit of a polluted fiber optic cable per unit length is shown in Figure 9. This equivalent circuit is derived from the representative transmission and ADSS Circuit shown in Figure 8. The equivalent circuit shows a capacitance made up of the sum of a self-capacitance and four mutual capacitances, C_{0g}, and three mutual capacitances, C_{01}, C_{02}, C_{03}. A discrete number of sectional equivalent circuits may be arranged in series to approximate the physical geometry of the three-phase electrical and ADSS system as represented in Figure 8.

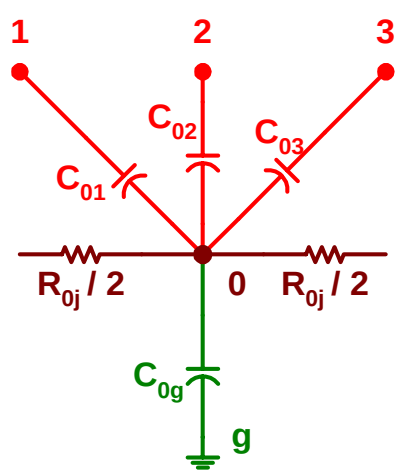

Figure 9. Equivalent circuit of polluted fiber optic cable, sectional

The accumulated pollution may be relatively conductive and is represented as a sectional resistance of finite value, R_{0j}. The equivalent circuit in Figure 9 also shows the phase conductors labeled 1, 2, and 3. From this equivalent circuit model an additional important parameter may be obtained, namely the energy source voltage. The energy source is deduced by replacing the three-phase conductors and mutual capacitances by a Thevenin equivalent source. Representing the energy source by a Thevenin equivalent circuit simplifies calculation and gives the key voltage and capacitance values practicable in an experimental test. The Thevenin equivalent is basically a single-phase system reduced from the three-phase equivalent circuit of Figure 9. The single-phase equivalent circuit is shown in Figure 10. The other key parameter obtained from the analysis of the equivalent is the prototypical values of polluted fiber optic cable. With these three values of voltage, source capacitance, and polluted cable resistance enables the implementation of a laboratory setup to simulate the electrical effects experienced by a fiber optic cable near the high voltage conductors in a power transmission network. Note that the capacitively induced current that flows along the polluted cable sheath is driven by the electric field radiated from the high voltage power lines. The induced current magnitude will also be a function of the pollution level on the fiber optic cable's sheath. The equivalent circuit can be represented and implemented as shown in Figure 11.

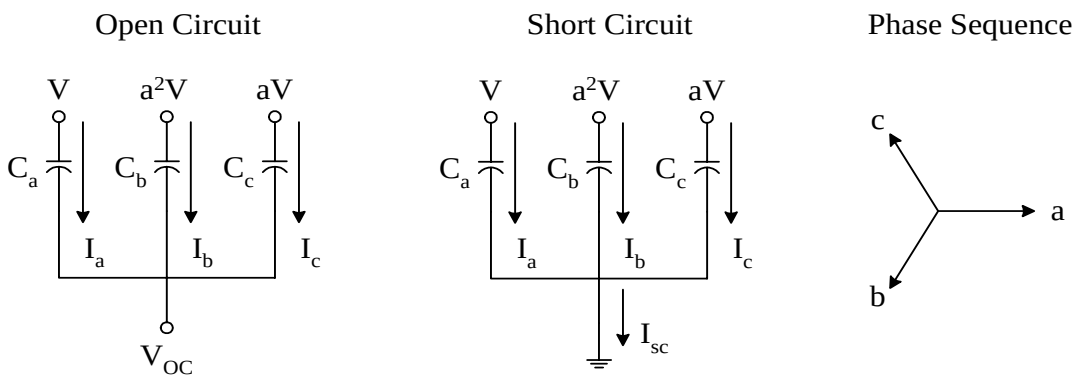

Figure 10. Single-phase equivalent circuit

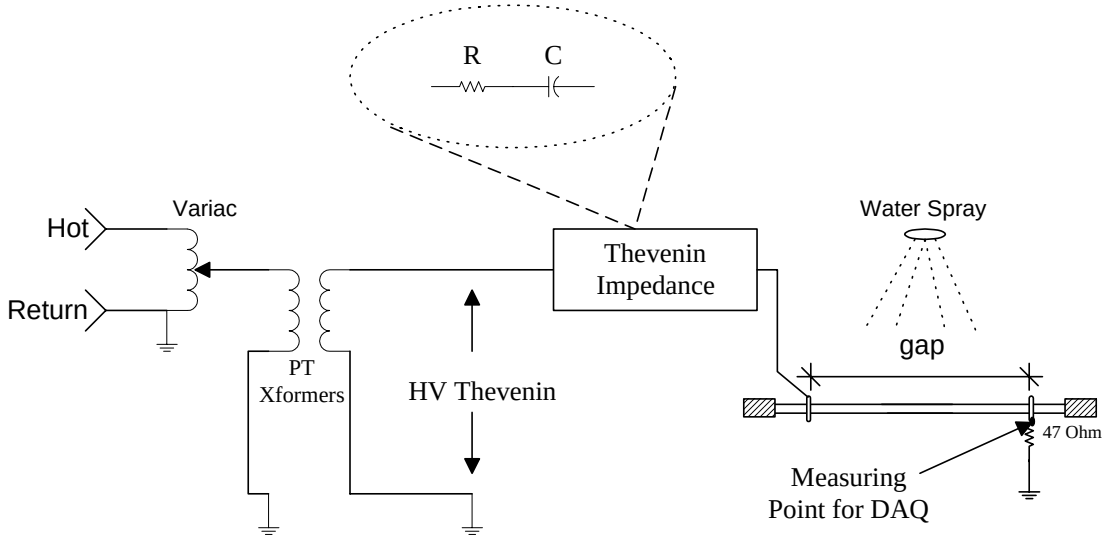

Figure 11. Implementation using equivalent Thevenin voltage and Thevenin impedance

V. EFFECTS OF POLLUTION ON FIBER OPTIC CABLE SHEATH

The pollution level is independent of the energy source, but is a dominant parameter regarding the magnitude of the induced current. The fiber optic cable's sheath is electrically non-conductive. ADSS fiber optic cables are effectively independent of the function of the high voltage power networks. The ADSS cables may be installed on

electrical power transmission networks without disruption thus quite cost effective both to the power utilities and the customers. The installation method for ADSS fiber optic cables is fully developed. The development of this type of fiber optic cables for use in high voltage networks is discussed in greater detail in [3]. The calculations in this paper suggest that currents in the order of 10 mA would be capacitively induced on this type of cable with a wet or polluted sheath and enough to cause considerable damage to the cable's sheath in a faulty designed system. In [16] it is stated that a magnitude of below 0.5 mA is the threshold for dry-band arcing to occur, and damage will not be prevalent. For a wet polluted cable at a given level of induced voltage, the leakage current is highly dependent on the resistance per unit length of accumulated contamination and the cable's sheath. This figure of merit may explain why cable sheath degradation subject to marine type pollution are more prone to damage than cables subjected to pollution levels of a lesser degree. There is a deficiency in the amount of data from actual fiber optic cable installations with regard to the duration, frequency and magnitudes of dry-band arcing current, which is quite important in the evaluation of accelerated test procedures. A study in regard to this lack of data is discussed and in the years between 1987 and 1989 two independent trials of ADSS cables were mounted on a double-circuit, 400 kV power line [17]. The 1987 trial was at Fawley on the south coast of England and the 1989 trial was at Hunterston on the west coast of Scotland. From these two independent studies, an increased awareness of the causes and conditions leading to the degradation of fiber optic cables helped in the development of an experimental setup to be implemented in the laboratory and simulate dry-band arcing degradation on fiber optic cables. Weather

conditions were monitored using conventional instruments while measuring the actual leakage current induced along the cable. It is noted that leakage currents do not always flow even when the amount of moisture was high enough to sustain it, but only when the pollution in the moisture was high enough. This gives a very good correlation between the leakage current and the specific resistance of the pollution layer accumulated on the cable's sheath. As expected, relatively high current levels were seen only after rainfall or when the relative humidity approached 100%. Another important finding confirmed from the trials in [17] was that dry-band arcing did not occur when current levels were less 0.3 mA. The pollution layer established on the surface of installed fiber optic cables strung along power transmission networks is a very difficult parameter to quantify and dependents on many factors such as geographical and environmental conditions.

VI. POLLUTION LEVEL CHARACTERIZATION ON FIBER OPTIC CABLES

Assessing the possibility of dry-band arcing damage to occur on fiber optic cables installed on overhead power lines is a primary concern. The situation is complicated further by the rigor of forecasting and verifying the actual pollution's electrical resistance accumulated on an installed fiber optic cable. The electrical resistance of the pollution directly influences the leakage current's magnitude flowing along the cable's sheath. In [18] it is estimated that the resistance of a dry fiber optic cable is in the range of 10's of Mega-ohms per meter (MΩ/m). The cables electrical resistance will vary widely depending on the pollutants present in rainfall, dew, and dirt that may accumulate on the cable's sheath over time. An estimation of 10^5 Ω/m is stated for humid marine locations,

whereas areas inland and away from industrial activity may be 10^7 Ω/m. Other situations, even in the cleanest areas, may be encountered such that electrical pollution levels of 10^6 Ω/m could easily be achieved. Presently there is no proven device that can accurately measure and quantitatively assess the type of pollution levels encountered by the cables installed on high voltage networks. At the time of this thesis, research at Washington State University was designing and constructing a calibrated portable transducer for measuring contamination levels on an ADSS cable's sheath in the range of 10^5-10^7 Ω/m in a high voltage environment [19]. The pollution level alone does not give an adequate indication of dry-band arcing occurrence, since the energy source will greatly dictate how much current will be induced through the pollution layer. The classification of the relative pollution levels on an in-service fiber optic cable is shown in Table 1. Further investigation is still needed in order for the arbitrary pollution levels to be associated with a given geographical area and be meaningful with respect to the amount of damage to be expected from the dry-band arcing phenomena. There is only limited success in reliably correlating any particular environmental factor that predominates in the occurrence of dry-band arcing on fiber optic cables installed on power transmission networks, since the amount of recorded environmental data in regard to this type of electrical activity is very limited.

Table 1. Classification of pollution levels on fiber optic cables

Cable's Pollution Resistance (Ω/m)	**Associated Pollution Level (Arbitrary)**	**Possible Geographical Significance**
10^5	Light	Rural
10^6	Medium	Industrial
10^7	Heavy	Marine

There are three factors known to be paramount in the development of dry-band arcing that may be established as metrics for an accelerated electrical degradation test procedure. The three paramount metrics are:

1. An equivalent source voltage dependent on geometric configurations and conductor to earth voltage.
2. A wet/dry cycle that emulates the frequency of precipitation dependent on geographical location.
3. The pollution level accumulated on the fiber optic cable.

VII. ELECTRICAL TEST METHODS FOR SHEATHING MATERIAL

Many materials undergo either chemical or mechanical changes under the stress driven by the forces of electrical energy. Much research has been performed in the field of material strength and their effects caused by electricity. The development and process

of a suitable sheathing material to withstand high electric fields in the application of a 400 kV power transmission system is discussed in [20]. The sheath material used was subjected to two forms of environmental tests. The environmental tests used to qualify the sheath material for use in the 400 kV application. The environmental tests performed were a salt fog test according to the proposed International Electrotechnical Commission (IEC) of 1000 hours exposure and a 1% NaCl water solution. The second test was an ultraviolet (UV) light exposure cycle according to American Society for Testing and Materials (ASTM) G53-84 specifications. A test voltage of 25 kV RMS, 50 Hz was applied to each of the samples tested. The results varied in erosion and tracking. A 1 km length of cable with an optimum level of alumina trihydrate (ATH) filler and UV stabilizer, was installed on 132 kV power transmission network in the East Midlands Electricity Board area at Londonthorpe near Grantham. Unfortunately, the environmental tests performed and discussed in [20] do not prove to be adequate for dry-band arcing. This method lacks the wet/dry cycle necessary to simulate the frequency of dry-band arcing. Dry-band arcing very seldom occurs during a continually wet pollution layer, since a leakage current path is always present. The UV test may be incorporated into an accelerated test method, but there is no standard test procedure applicable for ADSS fiber optic cables in high voltage environments. Further data is needed to be able to substantiate the effects of UV environmental tests in conjunction with dry-band arcing aging.

The tests to qualify sheathing materials used on ADSS fiber optic cables in high voltage applications can be categorized into mechanical and electrical tests. In [21] the

properties that the sheathing material should exhibit over the temperature range encountered while in service are listed as:

1. Sufficient mechanical strength to withstand handling during installation and abuse when installed.
2. Stability against UV, rain and pollutants.
3. Chemical compatibility with other materials present in the cable.
4. The ability to transfer clamping forces to the strength member from the devices used to clamp the cable to the supports.
5. Reasonable cost and processing.
6. Immunity to the electrical environment seen in service.

It is also stated that the first three properties can be tested by standard techniques that are well established in the field of plastic test methods. The fourth property is difficult task to model and calculate and must be tested experimentally on long-bed tensile testing machines. The electrical environmental test is a more severe requirement for materials in this type of high voltage application, since the cables must be in service for the specified lifetime of the cable under harsh electrical stress. The fiber optic cable sheath material in [21] was tested for tracking resistance in a broad range of experiments. One of the original tests used was similar to IEC 112 with a 50 Hz, 500 V supply and a gap length of 4 mm and controlled drops of a 0.1% NH_4Cl and stated that the results are difficult to interpret. The definition of a failure is not very practical without the supervision of someone to actually stop the test and look at the sample. The test method should be able

to test numerous cables and with minimum human intervention, basically an automated test system. It is stated that the test setup most useful for materials is very similar to the one described in this thesis and shown pictorially in Figure 5. The results of their test state that no damaging activity occurs when the cable is well wetted or when it is dry. This is a very important piece of information in analyzing the electrical activity and correlating it to the damage caused. It was also found that, in general, the rate of degradation of polymer material varies with different wetting cycles and varies for different materials. Therefore, to be able to compare different materials, the test method must be under a wide range of such diverse condition. The reason for this is because some materials will age most rapidly under continual fine spray while others are damaged faster under longer drying periods.

An experimental test setup is described in [22], which uses a setup as shown in Figure 5. Subjecting the energized cables to an intermittent water spray induced dry-band arcing. The spray duration used in the setup discussed in [22] comprised of two seconds at two-minute intervals. The definition of failure is based on an subjective judgement. The stated failure is when sheath degradation has proceeded to a stage where the central cable core is just exposed, but no significant degradation of the core itself has occurred. Due to this objective definition of failure they considered ten samples and analyzed them using Weibull analysis.

In [23] a correlation between the laboratory test and a field trial is discussed. The setup is similar the one used at Arizona State University as shown in Figure 5. The effects of gap length and voltage were studied. The spray cycle used was with an on time

of 2 seconds and an off time of 1 minute and 58 seconds with no limiting impedance. The wet/dry cycle used is defined by the following criteria:

1. The spray cycle shall be of sufficient duration to thoroughly wet the sample.
2. The drying cycle shall be such that all electrical activity has ceased before the next spray cycle commences.

The Hunterston field trial of 1990 is discussed and states that a fiber optic cable strung on a 400 kV transmission line successfully lasted for an 18-month period with a mid-span induced voltage of 10-12 kV. The cable was then repositioned to a mid-span of 25 kV. During the trial tests the leakage current were being recorded along with the rainfall frequency. In the six months of operation in the 25 kV mid-span voltage, the maximum leakage current recorded was 1.2 mA and an average of 0.5 – 0.6 mA. An interesting observation made was that electrical activity does not occur after every period of rainfall. This has also been observed in the laboratory.

Another paper discussing experimental test methods to compare sheathing material against dry-band arcing is [24]. The experimental setup used is similar to the one used at Arizona State University. It is stated that the results of dry-band arcing depend on the material on which it occurs and the arcing seen on ADSS is not the same as that seen on traditional high voltage insulators. It is suggested that the use of a current-limiting impedance more realistically represents service conditions than a low impedance source. The suggestion of arc compression is said to accelerate the damage,

as has also been the case for experiments performed at Arizona State University's dry-band arcing laboratory setup.

VIII. DRY-BAND ARCING EFFECTS ON THE AGING OF SHEATHING MATERIAL

There are many scenarios to consider and study in the events leading to dry-band arcing on a fiber optic cable's sheath installed on a high voltage network. There are many geometric configurations, geographical conditions, and meteorological parameters that can not be forecasted and sometimes measured. This leads to the need of an experimental setup that can simulate the various conditions and make modeling and analyzing the development and process of arcs on different sheathing materials understandable. The aging phenomena caused by dry-band arcing is not fully understood to allow guidelines that are agreed upon and applied to experimental tests and comparatively rank cable sheathing materials against dry-band arcing. The study on the effects of dry-band arcing aging on ADSS fiber optic cables in high electric fields is discussed in [25], stating that cable failure tend not to be widely publicized. Carter and Waldren have suggested that currents higher than several milliamps cause less damage, because the arcing tends to extend the dry bands faster and thereby reducing the arcing time [2]. This is one reason that dry-band arcing with currents in the range of a few milliamps cause the greatest damage. Rowland and Nichols suggest that the reason arcing with higher currents do not cause considerable damage is because the arcing is not confined to the minimum dry band region and the arc roots can stray over the electrolyte surface. Lower currents tend to cause arcs to be more localized and in a sense less 'jumpy'. Rowland and Nichols also suggest that moisture can accumulate and cause droplets to run along the cable in such a

way that an existing arc between them can be extinguished by continually shortening the arc length. The results of Rowland and Nichols are general and they state that one of the disadvantages of their analysis is the definition of the exact time of failure is arbitrary and ill defined. Their results state that the rate of damage by higher currents of several milliamps is dependent on the sheathing material.

IX. CONCLUSIONS

For a test method to be worthy of qualifying fiber optic cable sheathing material for different manufactures and be relative to lifetime predictions, the failures must be based on actual conditions that are encountered by the cables in service. Based on the available literature, there is not a standard test method to qualify fiber optic cable sheathing materials against dry ban arcing damage. The study of dry-band arcing on fiber optic cables installed on high voltage transmission networks is fairly new, dating back about a decade and a half. A few studies in the UK have been performed to determine the effects of dry-band arcing on cables deliberately installed in high voltage environments with equipment to collect data that could be used to correlate to failures. There is still much more research needed to fully understand cable failures and have a standard test method that mimics the failures. The problem is that actual field failures is not exactly known.

A mathematical model has been derived that gives the Thevenin voltage and Thevenin impedance that can be used in a laboratory experimental setup. These two parameters is good basis for the development of a test that can be used rank different

fiber optic cables in regard to dry-band arcing. Also the effects of pollution are of great influence in the damage produced by the arcing. The pollution has been categorized into three different levels, high, medium, and low. The pollution levels are estimated values and need to be measured in order to obtain useful information to be able to be applied in the laboratory test.

Chapter 3

Experimental Dry-Band Arcing Test Setup and Procedure

I. INTRODUCTION

A laboratory experimental setup has been developed and built to test and rank different fiber optic cables against dry-band arcing. Herein is the description of the test setup used to qualify and rank six different fiber optic cables provided by different manufactures. The manufacture's anonymity will be kept due to proprietary reasons. A startup manual is included in Appendix A, which contains information on the hardware and software.

II. TEST OBJECTS

Fiber optic cables from six manufacturers are used to test their sheath's immunity to dry-band arcing. Table 2 shows the physical diameter and sheath color of each cable used as test samples. The cables tested in this thesis are identical to those tested in the 1997 and 1999 Western Area Power Administration (WAPA) project reports submitted by Arizona State University, which determined the corona resistance and dry-band arcing failures respectively. An additional cable, labeled F, was not included in the 1997 WAPA report.

Table 2. Cable diameter and sheath color of test objects

Cable	Diameter	Sheath Color
A	0.705 inch	Black
B	0.570 inch	Black
C	0.625 inch	Black
D	0.645 inch	Red
E	0.640 inch	Black
F	0.577 inch	Black

III. EXPERIMENTAL SET-UP

To simulate environmental conditions representative of the fiber optic cable's posture on high voltage networks, an experimental setup subjects the cables to particular preconditions for dry-band arcing to occur. An experimental setup was built indoors in Arizona State University's Instrumentation Laboratory. Figure 12 shows the high voltage electrical connections and Figure 5 shows the experimental setup. The water reservoir contains water that may contain NaCl to simulate the effects of the surrounding polluted environment and the flow rate is measured using an in-line flow meter. The entire setup was placed in a grounded cage to prevent personnel to come in contact with the high voltage. A PC equipped with a National Instruments™ multifunction IO (input/output) card and LabVIEW™ software is used to control the high voltage electrical system, the pump system, the data acquisition system (DAS), plus a set of safety features [26]. This setup is designed to accommodate up to five cables to be tested simultaneously.

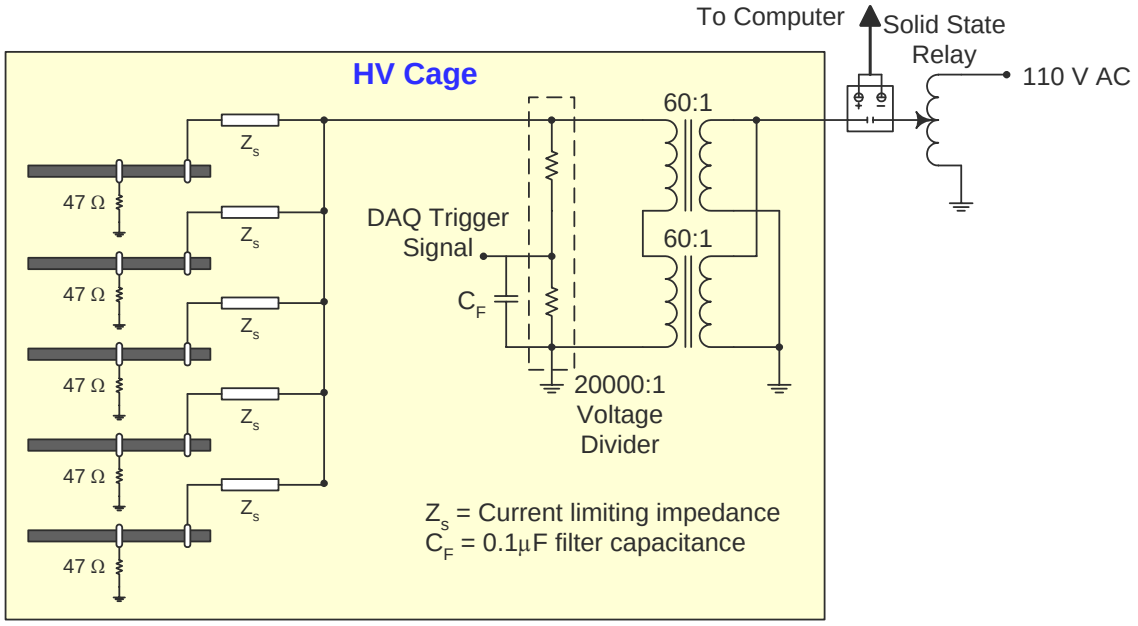

Figure 12. Electrical setup

IV. CABLE SETUP

The cable samples tested had end plugs at both ends to prevent the interior of the fiber optic cable from getting wet. The end plugs were made of a commercially available, flexible rubber-coating compound (Plasti Dip®). If the interior of the cables get wet, then the cables fail at the end instead of the area of interest. The test cables were 66 cm long[1]. Two electrodes were attached to the fiber optic cables, namely the high voltage and low voltage electrodes. The electrodes were spaced about 20 cm, 15 cm, and

[1] 36-cm long cables failed at the end plugs when tested.

3.8 cm (± 0.5 cm) apart for different set of experiments. The low voltage electrode was connected to ground through a 47 Ω shunt to measure the leakage current flowing on the cable's sheath. Back to back zener diodes (1N4732A) are used to suppress overvoltage spikes that might occur across the shunt resistors. These spikes were suppressed to prevent damage to measuring equipment (e.g. oscilloscopes and DAQ cards). The exact resistance values of the current measuring shunts are given in Appendix B. The high voltage electrode was connected to the output side (high side) of the transformers and then through a current limiting impedance and then unto the cable's sheath. Each cable has it's own series impedance. The cables were placed inside a galvanized metallic tank.

V. SPRAY SYSTEM

To simulate the environmental conditions of rain, salt-water solutions were sprayed onto the cables. The pump periodically sprayed salt-water on the cables every five minutes; 1.5 minutes on and 3.5 minutes off, using two nozzles for the tests reported in the "Half Yearly Report 1 For 1999". Test performed later had shorter spray cycles and a modified spray pattern, consisting of five lateral-spread nozzles. This technique is depicted in Figure 13. The figure shows the top view of three spray nozzles. Two other nozzles are on the other side (not shown) are equally spaced in between the three shown in the figure. The figure shows the water solution being sprayed.

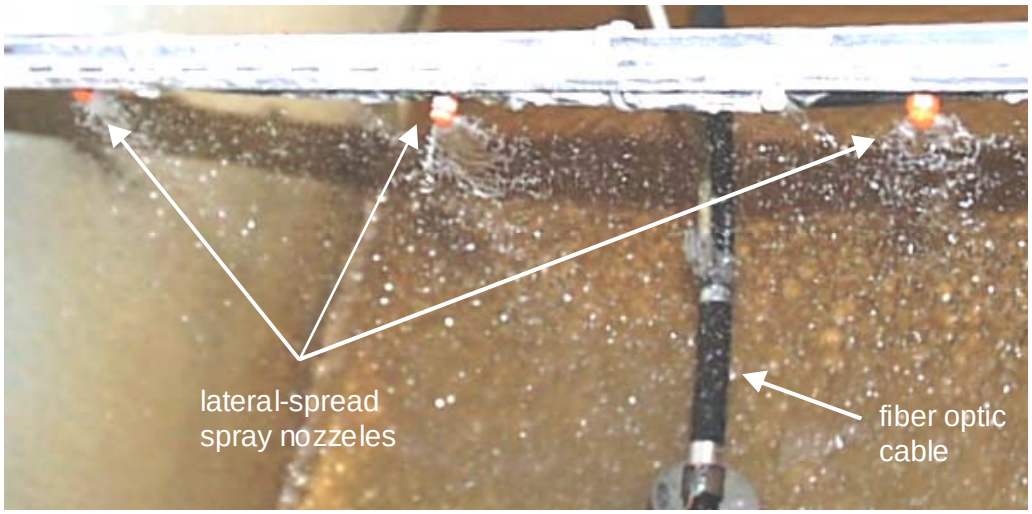

Figure 13. Brand-new spray pattern

The salt-water solution is stored in a 5-gallon water reservoir (bucket). The spray nozzles were setup so that each cable received approximately the same amount of water. The setup was improved to the spray system shown in Figure 13 because in the previous system the cables near the walls of the galvanized tank received more water than the cables in the middle. The water spray creates a wet conductive layer on the fiber optic cable sheath. The longitudinal field generated by the high voltage drives a current through this conductive layer. The current-limiting impedance limits the current. This current initiates the dry-band arcing process. The excess salt-water solution is collected at the bottom of the tank and recycled back to the reservoir. The pump is turned on and off by the LabVIEW™ computer program. With the modified spray technique the current limiting impedances do not get wet. A filter is used to filter the solid particles to reduce clogging of the spray nozzles.

VI. GALVANIZED METALLIC TANK

A galvanized metal tank was used as the container for the fiber optic cables and to collect the salt-water spray. A galvanized container was used to reduce metallic rusting due to the salt-water. The dimensions of the 1/8" thick steel container are shown in Figure 14. The metal tank was grounded for safety reasons. The metal tank can also sustain the heat generated by fires and prevent it from spreading better than a plastic tank. The tank had a 1/4" hole on its side for drainage. The tank was placed in an inclined plane position to allow the water to exit through the drained plug. The tank also supports the mounting brackets used to brace the high voltage insulators, spray nozzles, and cable suspension within the tank.

VII. PROTECTION SYSTEM

Dry-band arcing can cause some of the cables under test to heat up and possibly catch fire. Cables tested are sometimes known to fail in this manner. This results in a fire-hazard for personnel and property damage. A number of safety features were built into the experimental setup to enable the experiment to be run 24 hours a day, without human intervention. This ensures that all cables can be tested within a reasonable time frame, while providing proper and reliable results. The hardware and other logic electronic circuits used in the safety system have been not given any problem, to this date. The design and operation of the system is shown in Appendix A. Figure 15 shows a photograph of the test setup with four cables each with a 2.5nF current limiting capacitance inside the metallic tank. Also shown is a fire shield for added protection, the

HV connections, and the water line. This setup has been modified to the existing setup shown in Figure 16 in order to have a spray pattern that is evenly distributed on the each of the cables. Shown is the modified spray system and cable brace along with the temperature sensor near the nylon support. This setup has a cable sample with the *short-gap* and without the fire shield. The fire shield is made of galvanized sheet metal. It is placed over the galvanized tank to prevent fire from spreading the in the case of a fire. The temperature sensor is located right above a nylon cable support. If a fire were to spread unto the nylon cable support, the sensor would sense the heat generated and sends a signal to the computer. The cable support protection scheme is shown in Figure 16 and Figure 18. If the temperature sensor reaches the set point it will cause a series of events to occur. The computer will simultaneously shut off the high voltage and turn on the spray system for a six minutes and the cable under test will drop into the galvanized tank. The fire will be contained within the tank until cable burns out or is put out by the fire protection scheme.

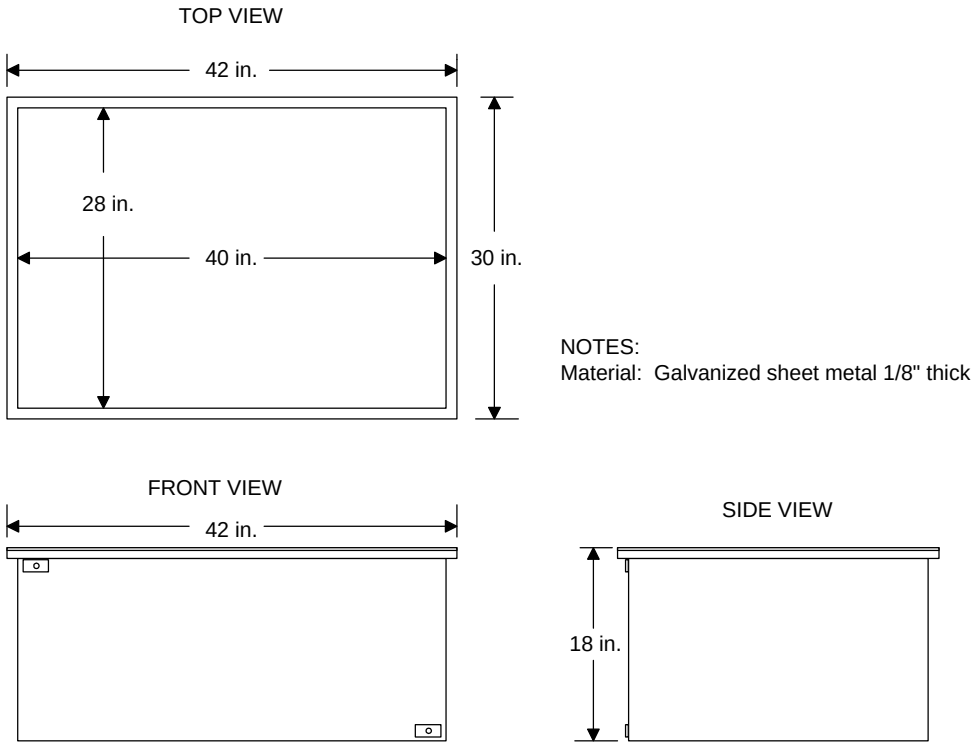

Figure 14. Galvanized metal tank used in the test setup

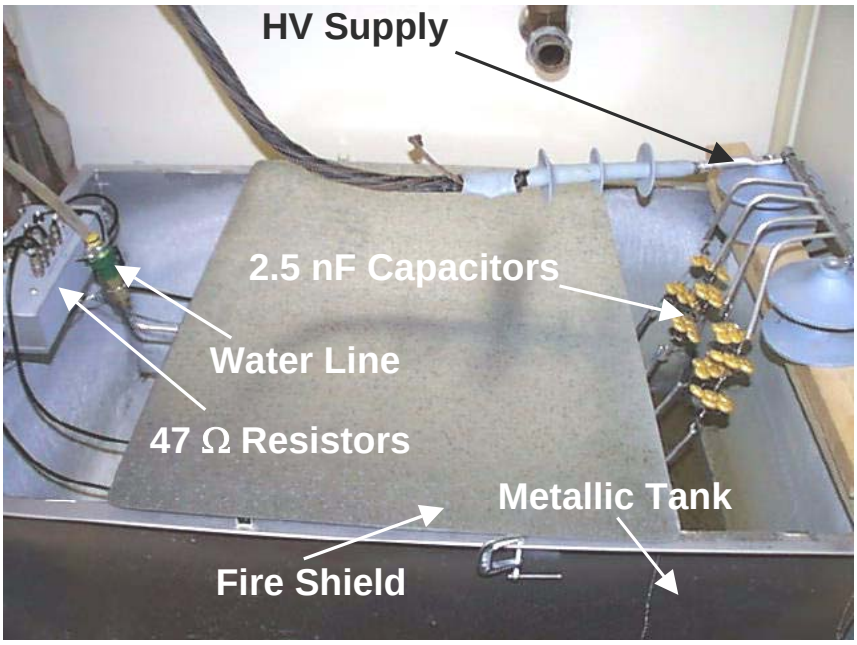

Figure 15. Photograph of test setup with 2.5 nF capacitors and fire shield

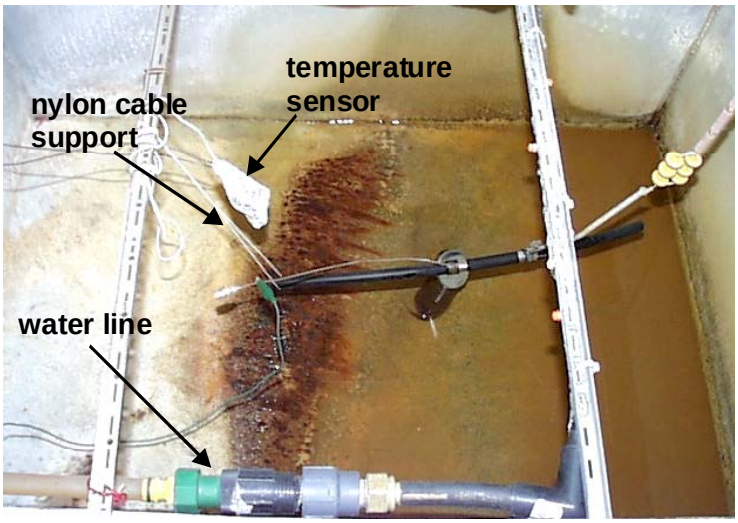

Figure 16. Modified fiber optic cable setup

Figure 17 shows a one-line diagram of the *Interface HV Control Box*. The lower left corner shows a comparator that monitors the set trip temperature and the actual temperature near the cable under test inside the galvanized metallic tank. This is one of the safety features included in the test setup. The comparator sends a transistor-transistor-logic (TTL) signal to the computer that corresponds to a high or low signal that depends on the relative comparison of the temperature sensor's output and the set temperature set point. The actual shematic of the *Interface HV Control Box* is shown in Appendix A. Figure 18 shows the cable suspension safety feature. If the cable were to catch fire and spread to the nylon string, the string will burn and the cable under test will drop into the galvanized metallic tank. The temperature sensor will sense the increase in temperature and send its output signal to the comparator mentioned above to be compared to the trip temperature.

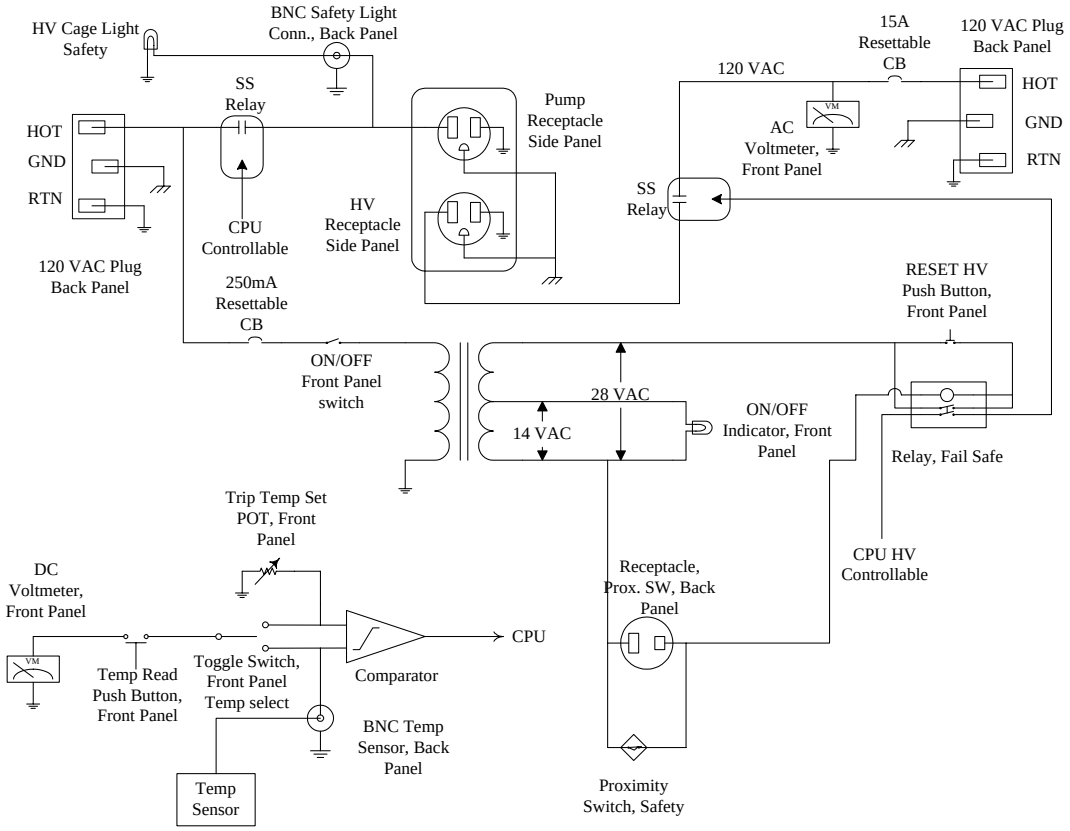

Figure 17. HV Control interface one-line diagram

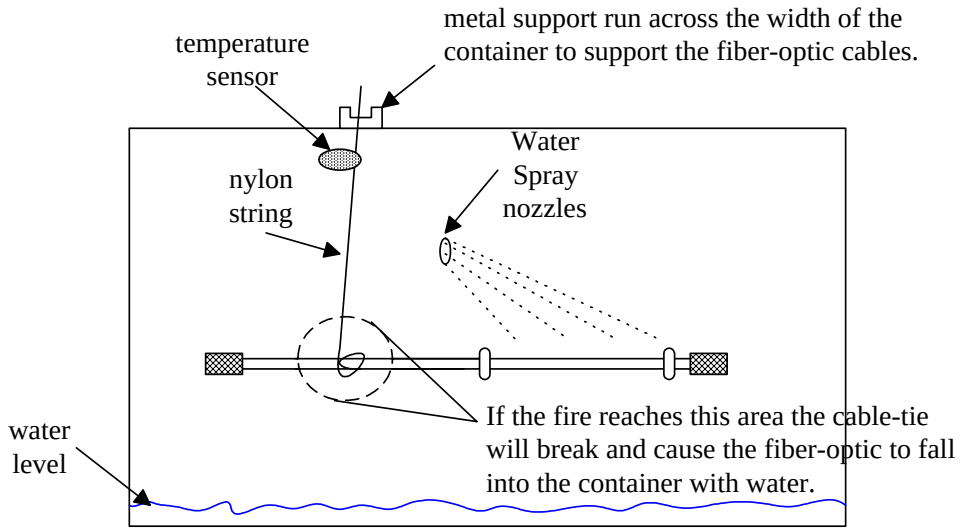

Figure 18. Cable suspension protection scheme

VIII. CABLES, IMPEDANCE, AND SALINITY

The cables are cut to a length of 66 cm. The electrodes are installed on the cables. The ends of the cables were dipped in the rubber-coating compound to form the end plugs and left to dry for a day. This procedure was not necessary with the brand-new spray technique, because the water spray was controlled to spray just on the gap space between the high and low voltage electrodes of the cable(s) under test. The cables are then installed in the metallic tank with the proper current limiting impedance.

The salt-water solution used for spraying is prepared in a 5-gallon bucket. The salt percentage of the water solution increases as the experiment progresses due to water evaporation. Hence, the range of salt percentages was observed for the tests performed and discussed in Chapter 4 and 5. The percentage of NaCl in the water is monitored periodically during the test with a portable conductivity meter. Water is added to the solution to keep the conductivity within the specified range

The rate of flow was between 350 to 375 ml/minute (0.92 – 0.99 gpm) for each nozzle used in the old spray system and approximately 1 gallon-per-minute (gpm) for the brand-new spray system. An in-line flow meter has been installed for the purpose of measuring this metric. The cable(s) is sprayed until saturated; i.e., there is no dry-band arcing and the leakage current is predominately sinusoidal (60Hz AC signal). The time required for full saturation was measured to be approximately 1 minute for a flow rate range of 0.5 to 1.0 gpm. The spray is then turned off, thereby letting the water film on the cable's sheath to dry naturally and eventually lead to dry-band arcing. The drying time is dependent on various parameters such as, the cables hydrophobicity (or lack of)

heating due to the current flow along the cable's sheath, and the incline of the cable. The incline or grade used for these experiments was set to 0° with respect to the horizontal axis. The incline is basically the only metric that can be measured and controlled in a repeatable manner.

IX. LABVIEW™ DATA ACQUISITION AND CONTROL SYSTEM

A PC with an AT-MIO-16E1 multi-function IO card in conjunction with LabVIEW™ software from National Instruments is used to control the experimental setup. The LabVIEW™ front panel used to interface with the high voltage, pump, and other safety functions is shown in Figure 19. The path and filename of the data file where the trip temperature, start and stop time, water cycle, and %NaCl information is stored is specified as an input. The %NaCl and trip temperature is used only for record puposes and will not affect the operation of this VI (virtual instrument) control panel.

The IO card is setup to monitor the trip temperature and indicates the appropriate indications on the front panel. The trip temperature signal is sent from the *Interface HV Control Box* shown in Figure 20. See the operator's manual "Dry-band arcing Experimental Procedure" for detailed information and operation in Appendix A.

The cables are sprayed periodically. The ON and OFF times for the pump can be set in the front panel based on a priori knowledge gained from previous experiments. For the set of experiments reported in the "Half Yearly Report 1 For 1999" submitted to WAPA, the ON time was set to 1.5 min and the OFF time was 3.5 min. As for the subsequent tests refer to Appendix B. A 'water cycle' is defined as the ON time plus the

OFF time. Time to failure, as compared to the number of water cycles, is therefore one of the metrics used to compare and rank the different fiber optic cables. The "High Voltage Override" can be used to turn off the high voltage any time during the test or in case of emergencies. The STOP button turns off the high voltage, the pump and stops the experiment. Presently the *PMP/HV CTRL.vi* and the *RECORDING REV0.3.vi* shown in Figure 19 and Figure 21 respectively are run independently from each other. These are two completely different software programs, which in the future will be merged into a single VI along with other functions to improve the reliability and safety while reducing the risk of lost time or loss of other resources.

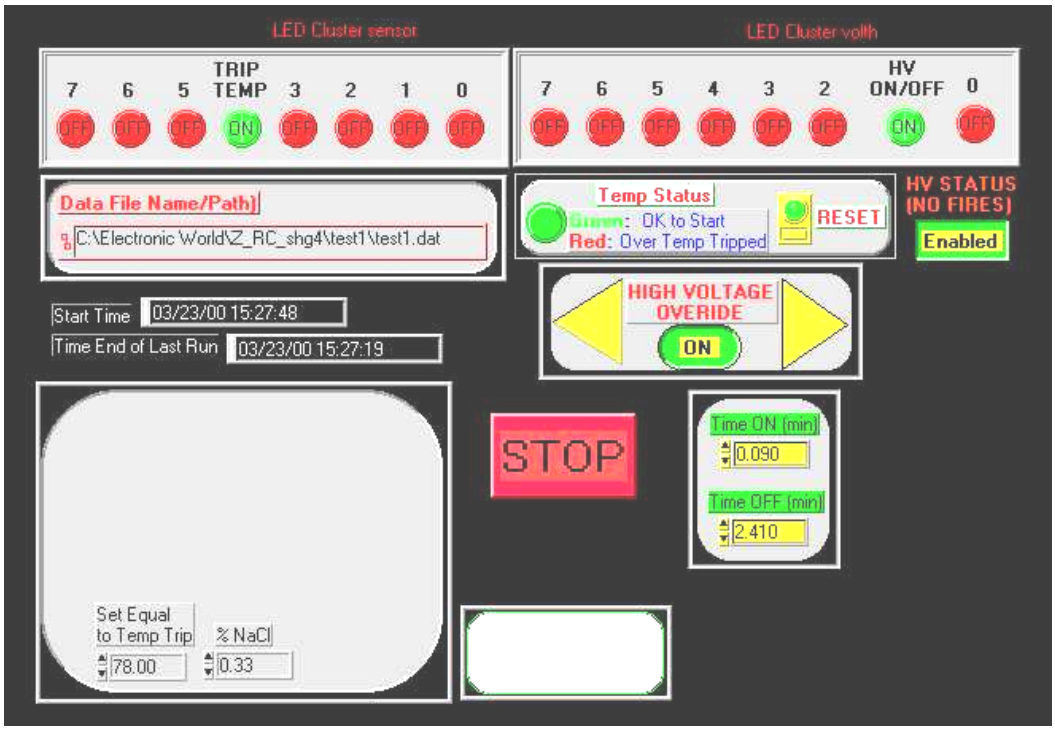

Figure 19. LabVIEW™ front panel for controlling the experiment

Figure 20. HV Control Interface Box, Front Panel

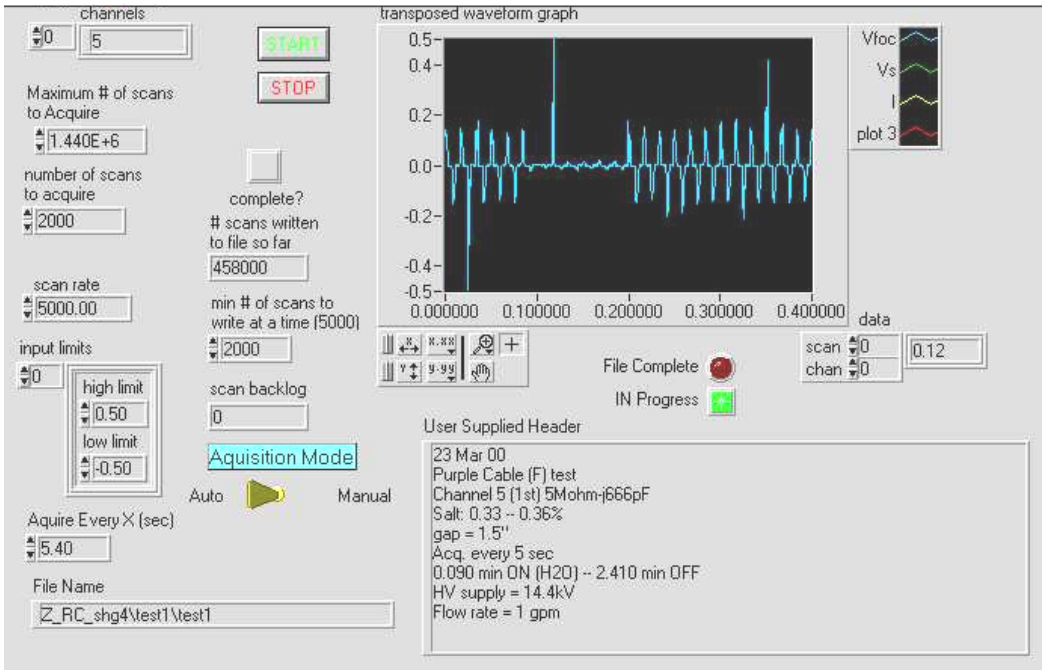

Figure 21. LabVIEW™ front panel for recording leakage current data

X. HARDWARE AND SOFTWARE INTERFACE

The 'heart' of the safety features lies in the hardware, namely the *Interface HV Control Box* that coexists with the functionality of the LabVIEW™ computer program(s). These two entities work together to make the whole system as robust as possibly feasible because the AT-MIO-16E1 multi-function IO card is robust enough to handle all the needs used in this test setup. The hardware is the underlying building block in the design, which can be considered as being standardized. The next step to make the system more robust begins with the software. The software can in most situations be configured to match the desired specifications determined by the signals being measured. In this case the measured signals are the leakage current and a TTL signal. In this sense, it could be developed into a system that obtains and processes the acquired leakage current data. The information can then be transformed or molded in order to reach the ultimate goal of understanding the natural occurrence of dry-band arcing on fiber optic cables in high voltage environments.

The LabVIEW™ program acquires and records the voltage signals measured across the 47Ω shunt resistor. This data can then be processed and analyzed off-line. The experiment is run until one of the cables fail. A cable is considered to have failed when it is either in flames or perceptible damage (e.g. puncture of the cable sheath) can be seen, but this may be subject to change based on the results. Once a cable failed, it was disconnected from the high voltage and removed from the setup. The experiment is then continued with the remaining cables till all the cables fail. In the case of a cable(s) not failing, they are included in evaluating the time-to-failure analysis. They are

considered as suspended data in a distribution function (e.g. Weibull distribution[2]) based on previous work pertaining to failure analysis. The method of analyzing the data is part of the ongoing research. The results of the present analysis technique will be given in the results section of Chapter 4. The experiment can be run 24 hours a day. The cables are also visually inspected to categorize the cable ranking.

XI. CONCLUSIONS

An automated laboratory experimental test setup has been developed and used to test, qualify, and rank different manufacture's fiber optic cable against dry-band arcing damage. The system is based on National Instrument® products, which include the LabVIEW™ software package and a AT-MIO-16E1 multifunction data acquisition PC card. A test can be run 24 hours-a-day with minimal operator intervention and collect leakage current data that can be used later to correlate the damage incurred to the time-to-failure of the fiber optic cable(s) tested. A procedure for testing fiber optic cables is implemented and documented using this apparatus as shown in Appendix A. The system has evolved extensively over the past couple of years and has become the only one of its

[2] Invented by Waloddi Weibull (1887-1979) in 1937.

kind known to function as this one. The *Interface HV Control Box* was built to accommodate necessary safety features and interface between the pump and high voltage to the LabVIEW™ computer program.

Chapter 4

Initial Dry-Band Arcing Verification Tests

I. INTRODUCTION

This chapter describes the initial tests and test setup used to subject the fiber optic cable(s) to dry-band arcing and discusses the results obtained. Various modifications are also discussed that were used to improve the setup. These preliminary tests were used to compare six anonymous manufacture's cables and rank them according to time-to-failure, which was also reported to WAPA as part of the joint research effort. A description of some the findings that resulted in modifications of the setup is discussed. The results obtained led to further tests with the modified system discussed in Chapter 3 and the results are given in Chapter 5. The results of the preliminary tests discussed herein did show that dry-band arcing could be produced on fiber optic cables but the damage caused by dry-band arcing could not be directly related to the time-to-failure. The time-to-failure for these experimental tests under the same conditions varied, but a distinctive decision could be drawn as to which fiber optic cable outperformed the rest of the cables tested.

II. INITIAL METRICS AND APPARATUS

An experimental set-up was built in ASU's High Voltage Laboratory. Figure 22 shows the fiber optic cable with the armor rods and electrodes, together with the major parts of the setup. The setup was designed to test five cables simultaneously. Three

electrodes were installed on each of the fiber optic cables. Thirteen 3/8-inch diameter brass rods, with rounded ends were placed in the middle of the cable to simulate the support system. On each side, a rod was extended by one inch, to simulate the unevenness that occurs at the ends of the armor rod assembly found in actual installations. Two aluminum electrodes were placed at 20 cm from the end of the brass rod assembly on each side to generate the longitudinal field and drive the current through the pollution layer.

The following metrics were used:

Water:

1. Conductivity: 1.45 mS/cm @ 20°C (tap water from ASU Tempe, Arizona)
2. Flow: 350-375 ml/min per nozzle (0.92-.99 gpm)

Electric:

1. Voltage: 14.4 kV_{rms}.
2. Short circuit current: 5.4 A @ 15 kV (Without limiting impedance)

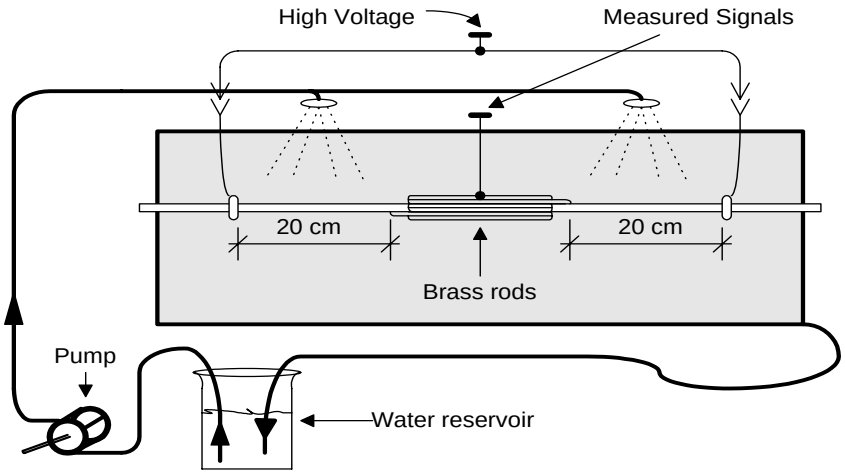

Figure 22. Original test setup with armor rod assembly and electrodes

III. SERIES 1: 0 Ω LIMITING IMPEDANCE, TAP WATER WETTING

A voltage level of 14.4 kV_{rms} was applied to the electrodes on each cable under test. The cables were subjected to alternate dry and wet periods. The wet period was of 5 minutes duration and the dry period was of 15 minutes duration. A cycle of one wet and one dry period define a water cycle. Hence, the duration of a water cycle is 20 minutes. The water cycle operation was controlled using LabVIEW™.

The experiment ran for several hundred cycles or till the cable failed. A cable is considered to have failed when it is either in flames or perceptible damage (e.g. puncture of the cable jacket) can be seen on the insulation. Once a cable 'failed', it was disconnected from the high voltage. The cables were inspected visually at the beginning and end of every day. The five fiber optic cables, 'A' through 'E', were exposed to the same level of high voltage and water cycle till one or more of the cables failed.

The five cables were installed in the open plastic container and energized to 14.4 kV_{rms} without any series limiting impedance as shown in Figure 23. The cables were periodically sprayed with tap water as explained before. The test results are shown in Table 3.

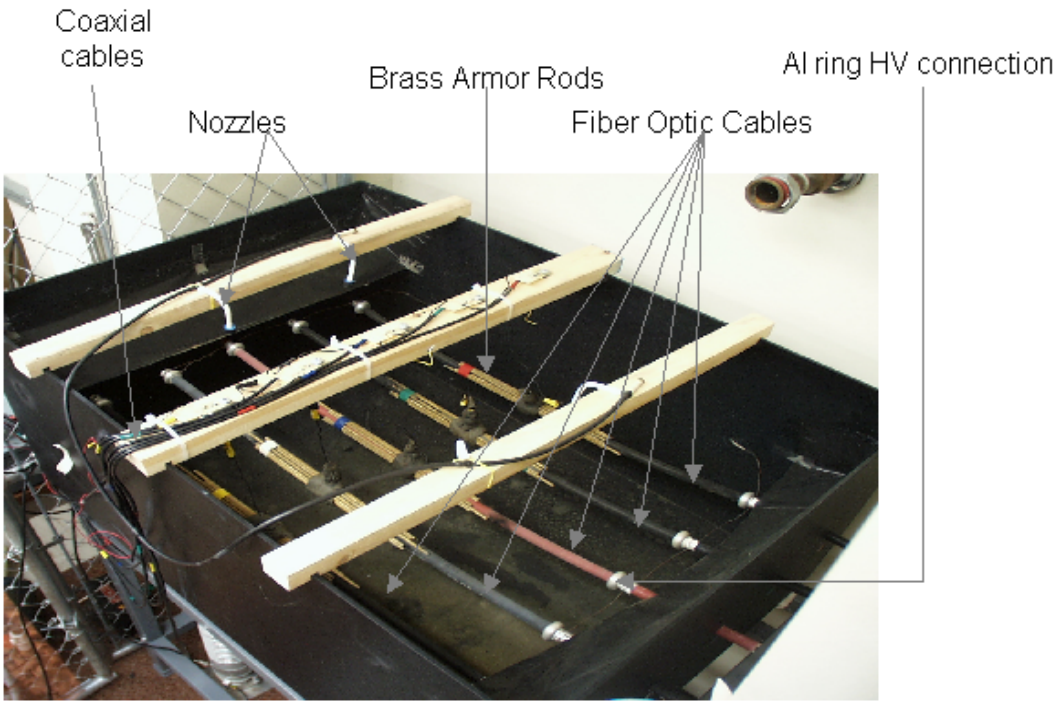

Figure 23. Top view of original experimental setup

Table 3. Series 1 test results

Cable	Cycles to failure	Observation
A, White	253 No failure	Discoloration, light-white deposits and loss of the black shine; surface mat.
B, Yellow	1	Severe burning, carbon deposit, jacket disintegrated.
C, Green	144	Severe burning, carbon deposit.
D, Blue	2	Puncture of the sheath at the middle.
E, Red	2	Severe burning, carbon deposit, sheath disintegrated.

The visual observation of cables 'B' and 'C' showed that random discharge occurred on the wet area (spot discharge). As the test progressed, the cables lost their hydrophobicity, which resulted in dry-band formation and dry-band arcing. The location of the arc changes throughout the test. Most frequently the dry band was formed adjacent to the high or low voltage electrodes. In other instances, the arc was between the electrodes near the center of the gap. The typical length of the arc were an estimated 1-1.5 inches.

At the beginning of the experimental test the cable sheaths were shiny and then in time disappeared. The surface became weathered and dull in color. The arcing caused discoloration of the cable sheath, and white deposits of NaCl covered the surface on some cables. Burn spots occurred at the arc root. Some of the cables burst into flames, while

others were punctured. The burning disintegrated the jackets. Figure 24 shows the damaged cables after completion of the test.

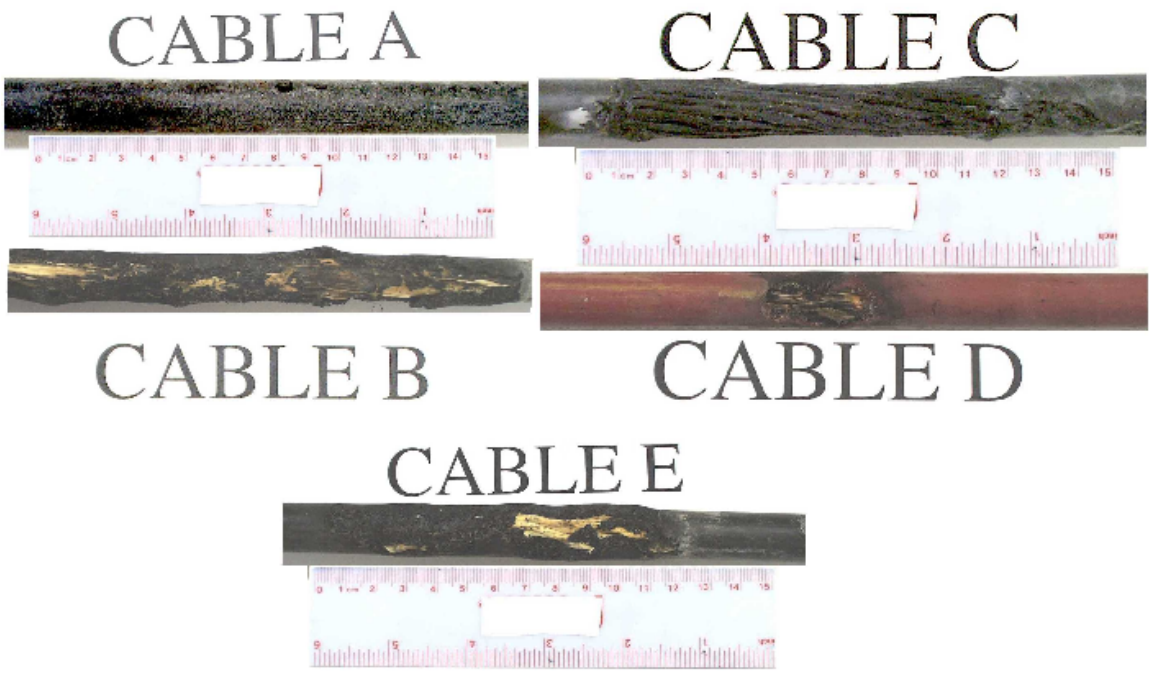

Figure 24. Series 1: damaged cable samples

IV. SERIES 2: 0 Ω LIMITING IMPEDANCE, TAP WATER WETTING

The first series was repeated to increase the reliability of the data. The test results are tabulated in Table 4. The damage caused by the discharge is demonstrated in the photographs shown in Figure 25.

Table 4. Series 2 test results

Cable	Cycles to failure	Observation
A, White	257 No failure	White textured discoloration between the armor rod and electrode.
B, Yellow	6	Severe burning between the electrode and armor rod, carbon deposit, jacket disintegrated.
C, Green	257	Discoloration, light white deposit and loss of the black shine, punctured track along the bottom side where water droplets formed.
D, Blue	257 No failure	White textured discoloration between the armor rod and electrode.
E, Red	163	Severe burning, carbon deposit, sheath disintegrated.

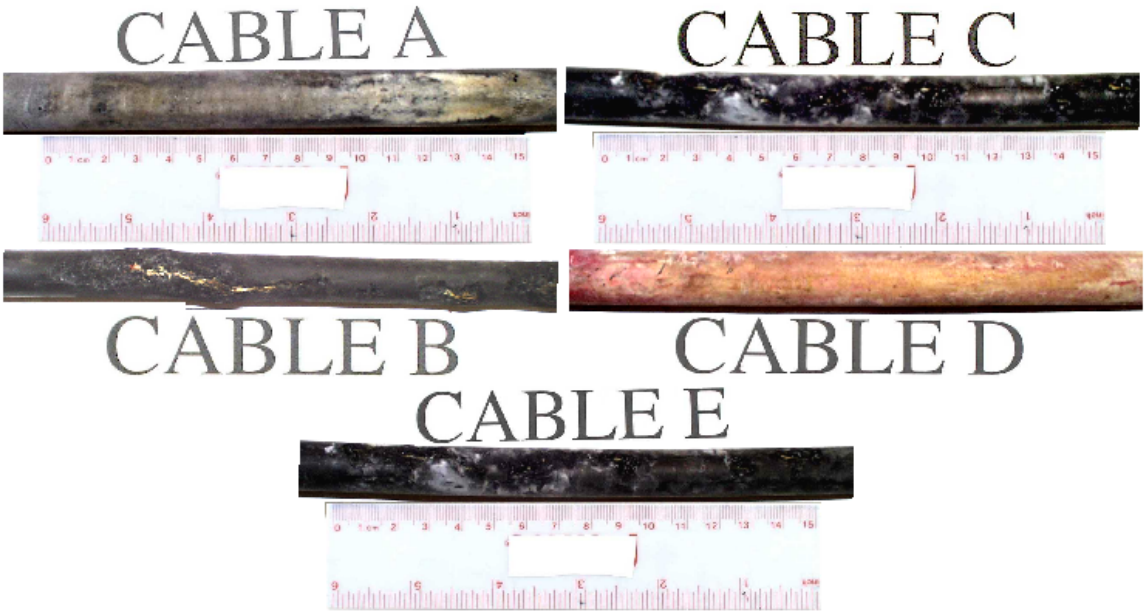

Figure 25. Series 2: damaged cable samples

V. SERIES 3: 1.65 MΩ LIMITING IMPEDANCE, TAP WATER WETTING

Each cable has a current limiting impedance of 1.65 MΩ connected in series to limit the current. This impedance limited the short circuit current to 9.1 mA at 14.4 kV_{rms}. The test results are shown in Table 5. The damage produced by discharge on cable C and E is similar to what was observed during the previous tests. However only discoloration and slight damage was observed on the other cables. During the tests some of the 1.65 MΩ resistors failed. Although the resistors were replaced, the failures reduced the reliability of this test series.

Table 5. Series 3 test results

Cable	Cycles to failure	Observation
A, White	>615 No failure	Discoloration and slight damage.
B, Yellow	>615 No failure	Discoloration and slight damage.
C, Green	615	Several punctures along the underside where water droplets formed.
D, Blue	>615 No failure	Discoloration and slight damage.
E, Red	163	Opened and burnt sheath, disintegrated material.

VI. SERIES 4: 150 kΩ LIMITING IMPEDANCE, SALT WATER WETTING

In order to investigate the effect of pollution, the tap water was replaced by higher conductivity salt water that represents a higher pollution level. This resulted in certain problems with the test set up. The main problems were:

1. The protection system switched off the system frequently due to an increase in the current during wetting. A 150 kΩ current limiting resistance was connected in series. This reduced the short circuit current to 100 mA. A new circuit breaker with a higher current rating was also installed.

2. It was observed that the test cables were damaged on only one side, even though the two sides were visually symmetrical. The test object was built using only one 20 cm gap. Figure 26 shows the new test object with mounted electrodes.

3. The conductive water caused electrical activity to occur outside the cage. Arcing was observed on the water pump. This was a potential health hazard. The acrylic plastic tank was replaced with the galvanized metal tank, described in Chapter 3, and the system was rebuilt. Grounded metal pipe sections were used to eliminate outside arcing. Figure 27 and Figure 28 show the new test arrangement from the outside and the inside.

4. It was visually observed that the discharge stops for a few minutes during the dry part of a water cycle. Hence, the dry cycle was shortened to 3 minutes. The new water cycle was now 2 minutes wet and 3 minutes dry.

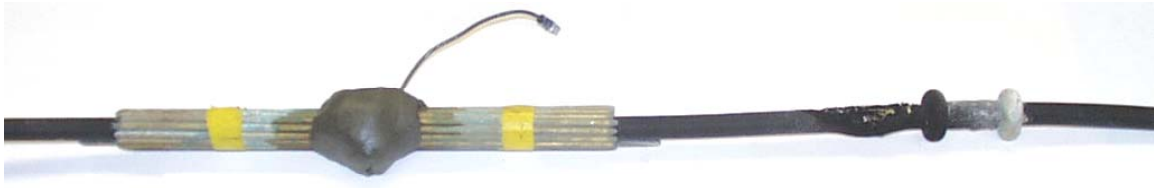

Figure 26. New and improved test object electrode arrangement

Figure 27. New and improved test arrangement

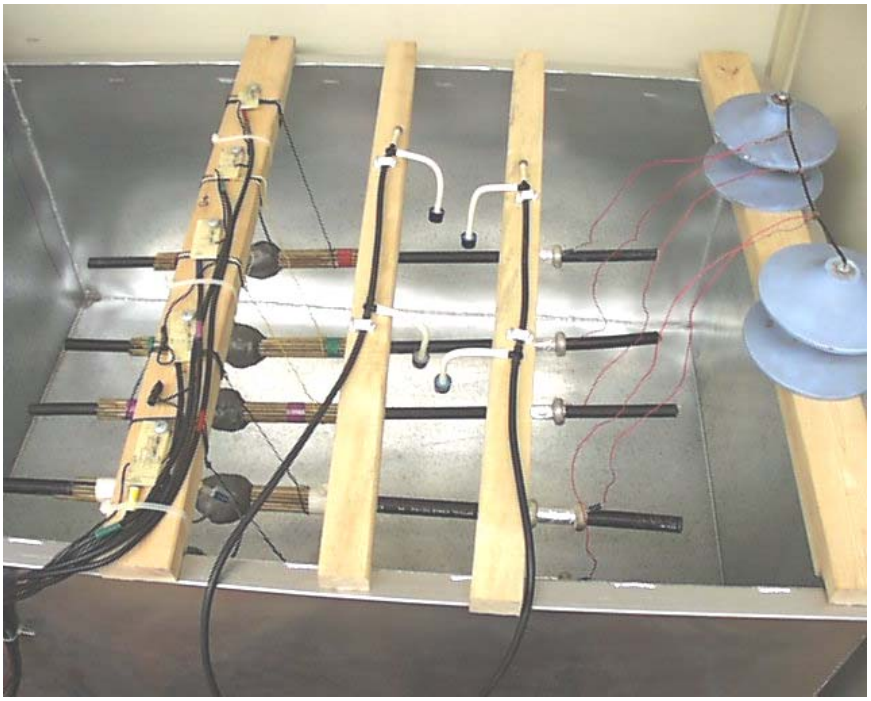

Figure 28. Inside view of new and improved test arrangement

The cables were energized continuously and cyclically wetted. Severe discharge was observed during wetting. The discharge gradually disappeared as the cable dried. No discharge was observed at the end of the dry period. The test was continued till one of the cables failed. At that point the failed cable was disconnected and the test with the remaining cables was resumed. The test results are presented in .

Table 6. Series 4 test results

Cable	Cycles to failure	Observation
A, White	884	Puncture near the HV electrode, burnt sheath.
B, Yellow	1021	Severe burning between electrode and armor rod, carbon deposit, jacket disintegrated
C, Green	1220	Sheath burned, punctured track along the bottom side where water droplets formed.
D, Blue	296	Sheath bulged like a balloon and broke open.
E, Red	1020	Severe burning, carbon deposits, sheah disintegrated.

Long term arc discharge on the severely polluted cables produced fire, when cables ‘A’, ‘B’, ‘C’, and ‘F’ failed. The fire in case of cable ‘A’ and ‘B’ extinguished when the electricity was switched off. The fire in case of cable ‘C’ and ‘F’ continued when the electricity was switched off. Cable ‘E’ did not burn. We can conclude that some of the cables are made of flammable material. Disregarding the fire, the type of damage is similar to what was observed previously. The fire destroyed the cable as shown in Figure 29. The fires prevented overnight testing. A fireproof test setup is

needed. The practicality of this test method was questioned and led to the concept of the *short-gap* arc test. Hence, the 20 cm gap is defined as the *long-gap*.

Figure 29. Series 4: damaged cable samples

VII. COMPARISON OF SERIES 1 – 4 TEST RESULTS

The use of a current limiting resistance increases the time to failure due to the decreased current magnitude. Cable ranking is possible but inconsistencies are observed. As an example the blue cable failed immediately during Series 1 and did not fail during Series 3. Some of the cables caught fire when they failed. This created a safety hazard, which prohibited overnight testing and increased the time needed to complete the test. The reliability of the results can be improved by repeating the test several times. However, this required a fire resistant test set up. It is suspected that the reason for the inconsistencies is due to the fact that the short circuit current was over 200 mA during the first 3 series causing adverse failure rates. Theoretical simulation studies have revealed that the short circuit current in natural conditions is less than 10 mA even in the case of heavy pollution. The first three test series used a relatively high short circuit current to accelerate the aging. However the results show that this large current results in extreme deterioration and fire that is not known to occur in nature.

The results suggest the repetition of the tests with a current limiting impedance to limit the short circuit current below 10 mA. These preliminary tests showed promising results, which gave rise to the development of a different test procedure.

Table 7. Series 1-4 test results comparison

Cable	Series 1	Series 2	Series 3	Series 4
A, White	253 No failure	257 No failure	No failure	884
B, Yellow	1	6	615	1021
C, Green	144	257	163	1220
D, Blue	2	257 No failure	No failure	N/A
E, Red	2	163	No failure	296
F, Purple	N/A	N/A	N/A2	1020

VIII. LONG-GAP TESTS WITH 10 kV_{RMS} SUPPLY

Three series of tests were performed on the cables as shown in Table 8. The use of a current limiting resistance increases the time to failure due to the decreased current magnitude. Cable ranking is possible but inconsistencies are observed. As an example the blue cable failed immediately during Series 1 and did not fail during Series 3. Some of the cables caught fire when they failed. This created a safety hazard, which prohibited overnight testing and increased the time needed to complete the test. The reliability of the results can be improved by repeating the test several times. However, this required a fire resistant test set up. It is suspected that the reason for the inconsistencies is due to the fact that the short circuit current was over 200 mA during the first 3 series causing adverse failure rates. Theoretical simulation studies have revealed that the short circuit current in natural conditions is less than 10 mA even in the case of heavy pollution. The first three test series used a relatively high short circuit current to accelerate the aging.

However the results show that this large current results in extreme deterioration and fire that is not known to occur in nature.

The results suggest the repetition of the tests with a current limiting impedance to limit the short circuit current below 10 mA. These preliminary tests showed promising results, which gave rise to the development of a different test procedure.

Five cables were tested under Series A and B. Four cables were tested under Series C. The cables were assigned letters 'A' through 'F' (six cables total) to maintain anonymity of the manufacturers. The cables were also color coded with electrical tape for easy identification. All cables were energized to 10 kV_{rms} for each series. The cables were tested to failure. The times to failure and some observations about the failure modes are given in Table 9 through Table 11.

Cable 'B' in series A was replaced by cable 'D' due to a lack of cable 'B' samples. Cable 'C' was removed from the test setup for series C due to a lack of cable 'C' samples. Three tests were performed for cables 'B' and 'C' in series A and an average value was used for the time to failure.

Table 8. Tests performed using the long-gap method

Cable	Limiting Impedance	Salinity
Series A	1.0 MΩ resistance	0.09 % (Tap Water)
Series B	1.0 MΩ resistance	0.48 % to 0.65 %
Series C	2.50 nF capacitance	0.48 % to 0.65 %

In series C, the cable samples were shortened in length in order to conserve on cable. This was done, in spite of the knowledge that they tend to fail at the end caps. As a result, two of the cables failed at the end caps as noted in Table 11.

Table 9. Series A test results

Cable	Cycles to failure	Observation
A, White	2539	Cable did not fail. White discoloration was observed.
B, Yellow	104 86 127	Severe burns between the hgh and low voltage electrodes. Carbon deposits can be observed. Sheath was completely disintegrated where water droplets form after wetting.
C, Green	194 33 147	Sheath melted and caught fire. A punctured track along the bottom side was observed, where water droplets formed.
E, Red	320	Sheath broke open exposing the fiber materials inside of the cable.
F, Purple	1354	Burnt sheath with carbon deposit and tracks.

Table 10. Series B test results

Cable	Cycles to failure	Observation
A, White	842	Cable punctured, became hard and porous. Bubbles were formed on the sheath.
C, Green	16	Sheath melted and also caught fire.
D, Blue	382	Damage was observed on the underside where water droplets form. The cable sheath became porous looking.
E, Red	382	Porous looking punctures near the high voltage electrode.
F, Purple	1032	An eroded track about 4 inches long occurred near the high voltage.

Table 11. Series C test results

Cable	Cycles to failure	Observation
A, White	1207	Cable did not fail. White discoloration was observed.
D, Blue	723	Sheath bulged and failed near the high voltage electrode.
E, Red	240	Tracks observed at the edge. The end caps failed and the test was stopped.
F, Purple	1089	Tracks observed at the edge. The end caps failed and the test was stopped.

Times to failure grouped by cables are plotted in Figure 30 and the following observation can be deduced. In cable ‘A’, increasing the salinity reduced the time to failure. In cable ‘C’ and ‘F’, increasing the salinity reduced the time to failure. However, for cable ‘E’, increasing the salinity increased the time to failure. The time to failure for cable ‘A’ and cable ‘D’ is greater for capacitive impedance compared to resistive impedance.

Times to failure grouped by series are plotted in Figure 31. For series A and series B, cables ‘A’ and ‘F’, are more resistant to damage due to dry-band arcing than the other cables tested. Comparing results from series B and C, cable ‘A’ outperforms cable ‘D’ for both tests in regard to dry-band arcing damage.

Based on the above observations, Figure 30, and Figure 31 a rough ranking of the cables can be derived as follows:

Rank 1: ‘A’, ‘F’

Rank 2: ‘D’

Rank 3: ‘E’

Rank 4: ‘C’, ‘B’

These rankings are partially inconclusive and further tests were performed, which are discussed in Chapter 5 to correlate the dry-band arcing to the time-to-failure of the cable’s sheath.

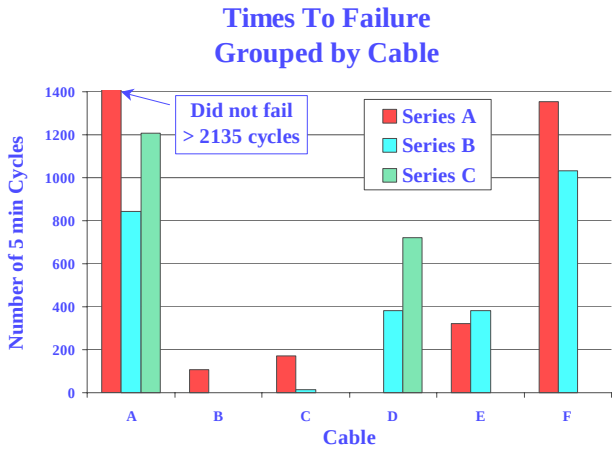

Figure 30. Series A – C; time-to-failure grouped by cable

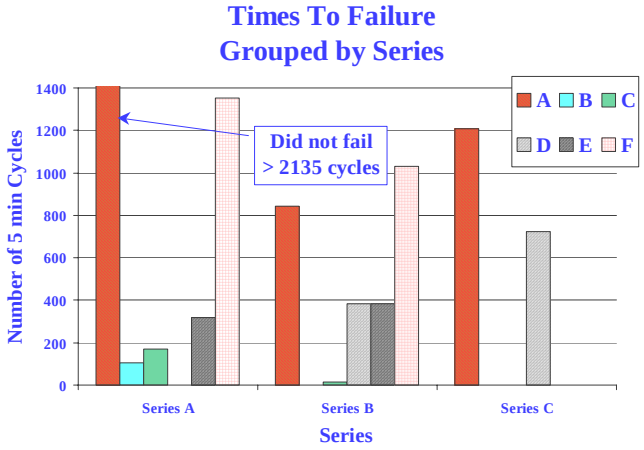

Figure 31. Series A – C; time-to-failure grouped by series

IX. TEST ON CABLES 'A' AND 'F'

Since the results of the above series were partially inconclusive, further tests need to be performed on all the cables to ensure data reliability. Based on the results obtained above, cables 'A' and 'F' seem superior to the other cables, with respect to dry-band arcing failure. Hence, these cables were selected for another test to compare them. Four

cables were installed in the test setup with the corresponding current limiting impedance as shown in Table 12. A 0.22 % salt solution was used as a pollution level.

Before starting the test, voltage and current oscillograms were captured to measure the impedance of the salt water layer on the fiber optic cable sheath. The oscillograms were captured for cable 'A' using the capacitive current limiting impedance. The voltage across and the current through the polluting layer and the capacitive limiting impedance are shown in Figure 32 and Figure 33 respectively. The values calculated from the oscillogram are shown in Table 13. Two important observations from these results indicate that the layer is purely resistive, and the capacitance has a resistive component (loss factor[3] at 60 Hz~ 2.1 %). In Table 13, the subscript 'foc' represents the fiber optic cable and the subscript 'c' represents the current limiting capacitance. The term R_c represents the effective series resistance (ESR) of the capacitance.

Table 12. Cables 'A' and 'F' with 0.22 % NaCl and corresponding impedance

Cable	Limiting Impedance
A, White	1.0 MΩ resistance 2.50 nF capacitance
F, Purple	1.0 MΩ resistance 2.50 nF capacitance

[3] Loss factor is calculated here, as the ratio of the resistance to the capacitive impedance at 60 Hz. Loss factor is also called dissipation factor and represents ALL (dielectric and resistive) losses in the capacitor at a single specified frequency.

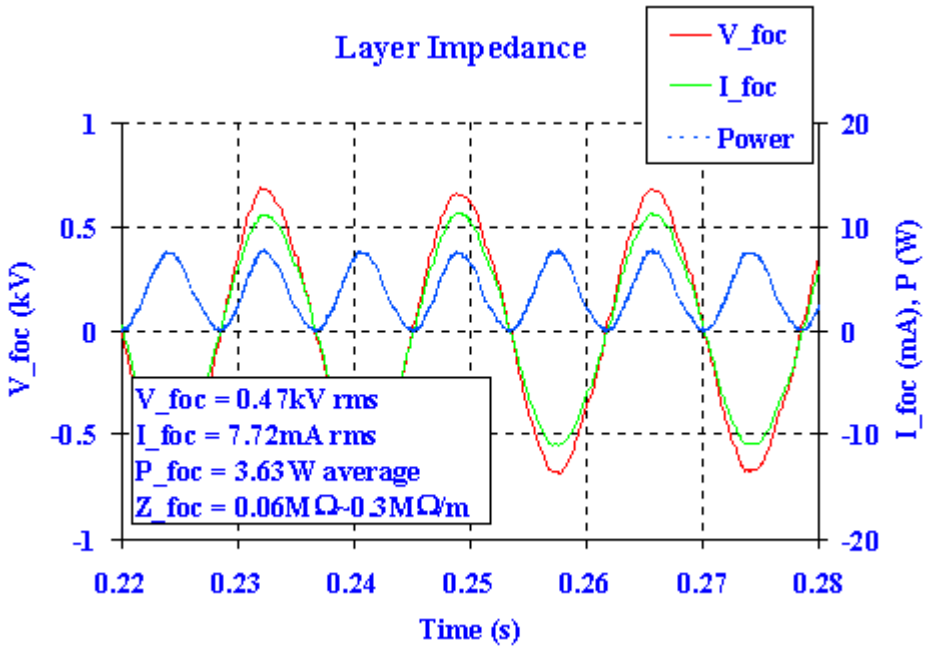

Figure 32. Voltage and current measurements on layer impedance

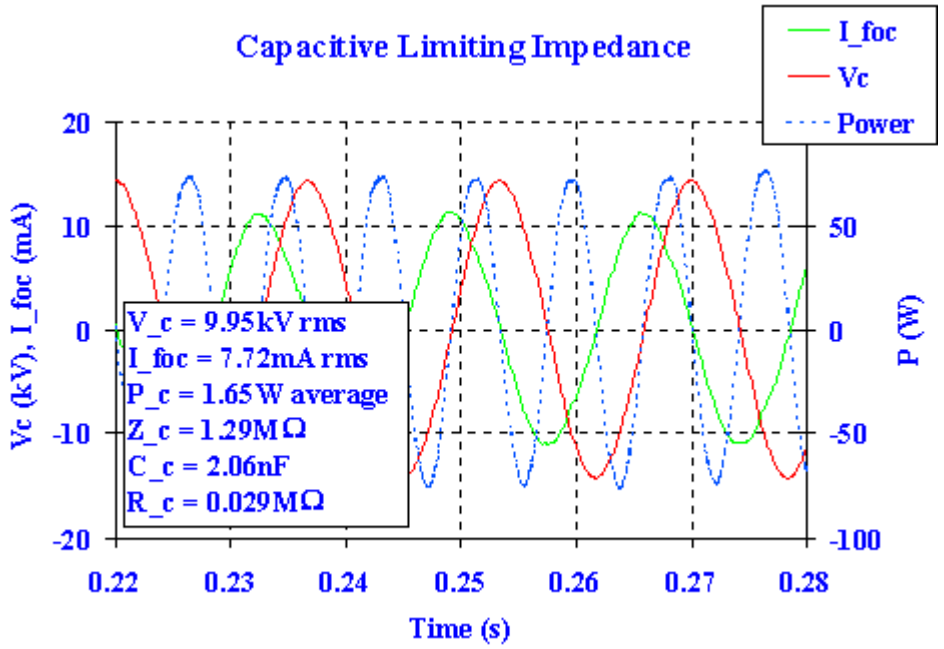

Figure 33. Voltage and current measurements on capacitive impedance

Table 13. Electrical measurements of layer impedance and limiting impedance

Layer		Capacitive Limiting Impedance	
V_foc	0.47 kV rms	V_c	9.95 kV rms
I_foc	7.72 mA rms	I_foc	7.72 mA rms
P_foc	3.63 W average	P_c	1.65 W average
Z_foc	0.06 MΩ~0.3 MΩ/m	Z_c	1.29 MΩ
		C_c	2.06 nF
		R_c	0.029 MΩ

The times to failure of the four cables are given in Table 14. From Table 14, we can conclude that cable 'A' is better than cable 'F' in resisting dry-band arcing. In addition, the cables with resistive limiting impedance fail faster than with capacitive limiting impedance. Some current oscillograms are shown in Figure 34 through Figure 37.

Figure 34 and Figure 35 show the current waveforms for cables 'A' and 'F' with 1.0 MΩ current limiting impedance. Figure 36 and Figure 37 show the current waveforms for cables 'A' and 'F' with 2.5 nF current limiting impedance. These figures indicate that the current waveform does not depend on the cable sheath.

For the 1.0 MΩ impedance, the maximum current magnitude observed is about 10 mA, which is consistent with the applied voltage and the limiting impedance.

Table 14. Cable ‘A’ and ‘F’ test results

Cable	Limiting Impedance	Cycles to failure	Observation
A, White	1.0 MΩ resistance	20	Cable sheath became hard and porous and bubbles were formed
	2.50 nF capacitance	446	Cable did not fail
F, Purple	1.0 MΩ resistance	10	Burnt sheath with carbon deposit and tracks.
	2.50 nF capacitance	74	Tracking occurred on the cable.

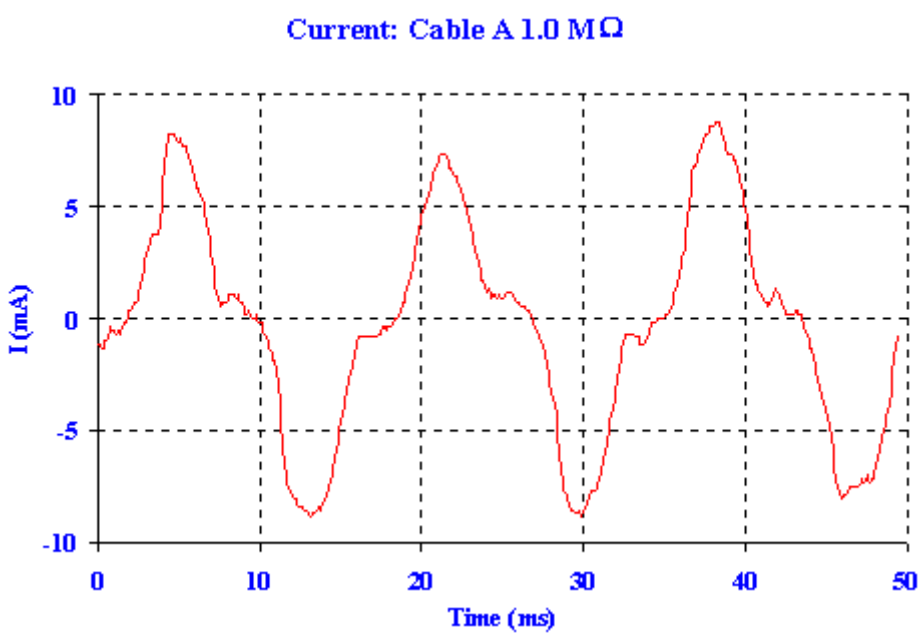

Figure 34. Current: Cable ‘A’, 1.0 MΩ, arcing

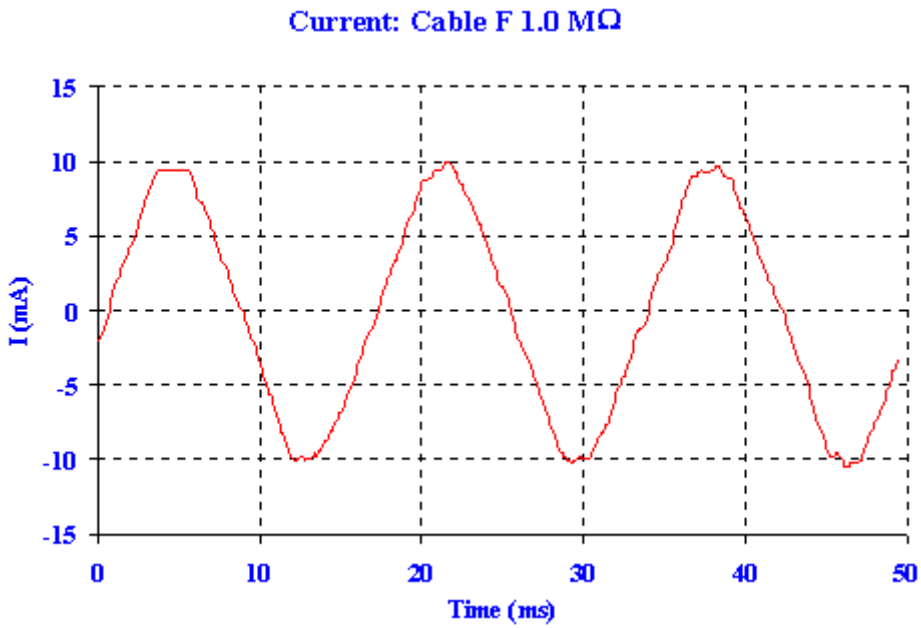

Figure 35. Current: Cable 'F', 1.0 MΩ, no arcing

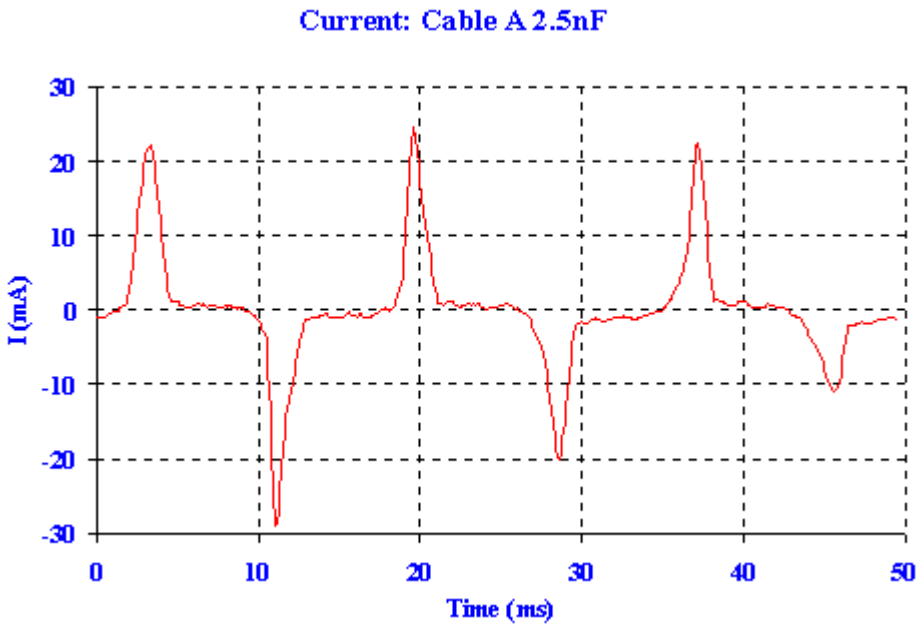

Figure 36. Current: Cable 'A', 2.5 nF, arcing

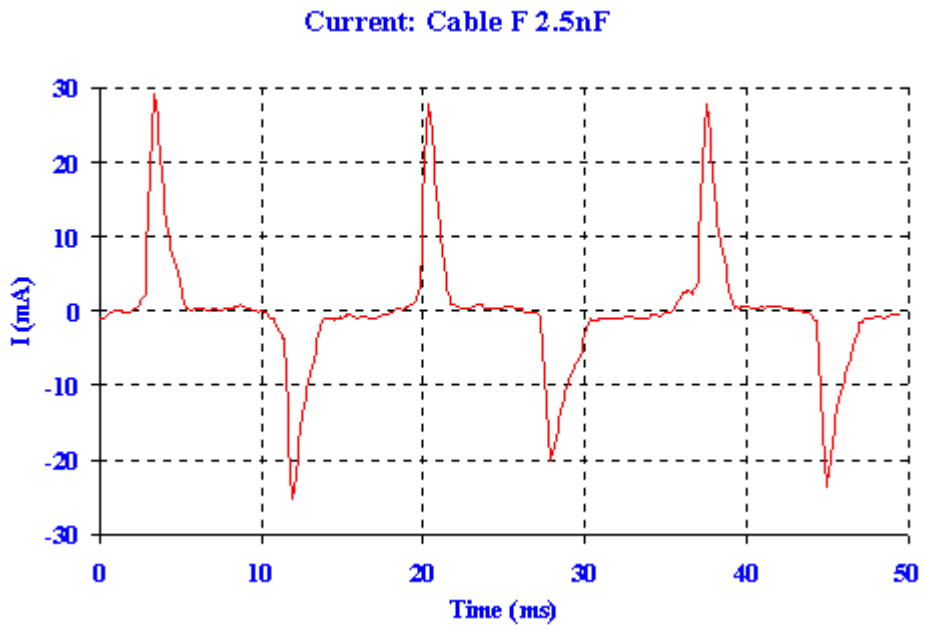

Figure 37. Current: Cable 'F', 2.5 nF, arcing

The current waveforms, when using a 2.5 nF limiting impedance, are narrower than the 1.0 MΩ waveforms, but have a higher amplitude (Figure 34 and Figure 36). The typical amplitude of the current pulses was around 30 mA. This increased to a limit of about 100 mA, for cable 'A', as time progressed. Cable 'A' did not fail after 446 cycles.

The current in the capacitance case has shorter bursts of energy than the resistance case during the dry-band arcing event. The amplitude is also larger for the capacitance case than the resistance case. Figure 38 shows the progress of the current waveform before arcing, at the onset of arcing, and during steady arcing. The oscillograms in Figure 38 show waveforms of the current through cable 'A' with a 2.5 nF limiting impedance. The current amplitude is limited to about 15 mA at the onset of arcing. The current increases to 30 mA during steady arcing.

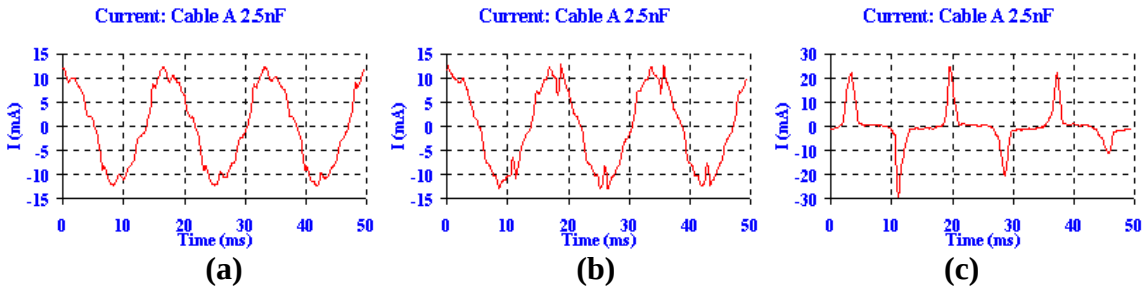

Figure 38. Arc current in cable 'A': (a) before arcing, (b) onset of arcing, (c) steady arcing

X. CONCLUSIONS

Dry-band arcing can be reproduced in the laboratory by directly applying the high voltage to a sectional piece of fiber optic cable and wetting the cable with a water solution. The current induced using this method needs to be limited to avoid the large current magnitudes that presently are not known to occur on installed fiber optic cables near high voltage transmission networks.

The current limiting impedances of 1.0MΩ resistance and 2.5 nF capacitance were used to compare the dry-band arcing current magnitudes and damage incurred on the cable. A voltage source with a frequency of 60 Hz makes the 2.5 nF capacitance have an equivalent impedance as the 1.0 MΩ resistance. The damage and current waveforms of these two current limiting impedances is different in magnitude and shape due the high frequencies present during dry-band arcing..

There were some inconsistencies in evaluating the time-to-failures. The time-to-failures varied but a decisive observation about cable ‘A’ and cable ‘F’ could be made, namely they outperformed the other cables overall.

Chapter 5

Correlation Between Dry-Band Arcing and Time-To-Failure

I. INTRODUCTION

This chapter defines the categorization of the dry-band arcing events into three distinctive events. A series of tests along with the results are given based on an analysis which correlates the events of dry-band arcing damage to the time-to-failure. These tests have evolved from the previous tests discussed in Chapter 4. A set of eight metrics are also defined used as conditional and qualitative factors that are related to the natural condition as might be encountered by fiber optic cables installed in high voltage transmission networks. The main variable or metric used to correlate dry-band arcing damage to the time-to-failure is the leakage current.

II. CATEGORIZATION OF DRY-BAND ARCING EVENTS

One of the main factors being considered is the magnitude of the mean of the current squared, i.e., $imsq = \sum_{k=1}^{N} \frac{i_k^2}{N}$. This is directly proportional to the power being developed between the high and low voltage electrodes on the fiber optic cable under test. This region is where the damage occurs. The distribution of the *imsq* is categorized into three distinct forms of activity:

1. *AC period*, this occurs when the current is predominantly sinusoidal. This type of activity takes place during the time prior to the onset of dry-band arcing. The reason

for this is because the cable is fully saturated by the pollution (H_2O salt solution) and no dry bands exist in the region of interest forming a conductive layer. It is proposed that this type of activity be one of the sequence of events used to characterize dry-band arcing on fiber optic cables. The *imsq* for this activity can be estimated or measured based on the supply voltage and current levels. In addition it may be considered deterministic for data analysis. Previous studies have shown that *AC period* currents do not account for the damage on the cable's sheath in an adverse nature

2. *Arcing period*, this event follows the *AC period* activity. In this period the cable has undergone the drying process and dry bands have formed to initiate dry-band arcing. The mechanics and the development of dry-band arcing during this period may be regarded as a random process; and will be treated as such. The random variable, which will be used, is *imsq*. The use of random variables enables notions of probability[4] to be put into a mathematical framework and hence apply mathematical techniques. Both types of arcing are considered under the same definition of the *Arcing Period.*

   a. *60 Hz type.*

   b. *Pulse type.*

Another idea is to try and contain the arcing to a specific region on the cable's sheath that can be repeated from sample to sample and then relate the damage to the acquired data, namely the leakage current. The advantage of restricting the activity of dry-band arcing is that it localizes the damage to a specified region of interest.

3. *Noise period*, this occurs when negligible current is induced through the cable's sheath and is regarded in the same category as the *AC period* activity in terms of the amount of damage caused. Small current magnitudes during this period are not enough to sustain dry-band arcing to cause any appreciable amount of cumulative damage, relative to the current magnitudes in the *Arcing period*. This is the floor level for the signals being considered since the data acquisition system can not accurately measure these current levels. These low leakage current levels are considered to be negligible since their respective damage is not considered to be a dominant factor on the overall damage.

These three qualitative aspects will be the rationale used in the process of analyzing the data and thereby conveying the acquired data into an intelligible and useful form of information. The three categories effectively account for one hundred percent (100%) of the dry band arc's sequence of events undergone on the cable's sheath. The three events are basically counted and then sorted in a set of bins to form a histogram. It

---

[4] *At the bottom of the theory of probabilities is only common sense expressed in numbers.* Essai philosophique des probabilités –P.S. Laplace (1814)

is now a matter of capturing the events as they are happening, which can be done by the acquisition system, but would require a very large amount of memory for data storage. Therefore the leakage current is sampled in 5 second intervals at a rate of 5 ksps (samples per second). The goal here is it to account for the three dry-band arcing events and categorize them into numerically different characteristics that encompass the whole notion of dry-band arcing on fiber optic cables. These three set of events, give rise to an ensemble of statistics for the *AC*, *Arcing*, and *Noise periods* which are then correlated to the time-to-failure. By building upon this data, one can apply them to complement the known knowledge obtained thus far of dry-band arcing damage caused on different cables. To date, the nature of the failures due to dry-band arcing tend to be elusive and not very lucid in its relation to time-to-failures. The results obtained should be of no surprise, since the very nature of dry-band arcing itself is random and thereby giving an outcome of relatively the same level of complexity; in terms of time-to-failure. The tests discussed in Chapter 4 have been relatively inconclusive. The new technique implemented will try to circumvent the quintessence of dry-band arcing and its damage to fiber optic cable's sheath under a prescribed test method. The results seem to be quite encouraging leading to a much better grasp of the ongoing research goals.

III. DATA ACQUISITION PARAMETERS

There are a number of parameters that must be defined prior to the acquisition of data. These parameters have been used in the LabVIEW™ data acquisition program, *RECORDING REV0.3.vi*, shown in Figure 21. These sets of values have been determined from practical limitations on the amount of data that can be stored to disk,

sampling rate, and other hardware limitation. These issues have lead to the following values used in the tests discussed and listed below:

1. *Channels*: used as a hardware selection from the set of channels to be used for the measurement of leakage current (e.g., 0,1).
2. *Maximum # of scans to Acquire*: defaults to $1.44*10^6$.
3. *Number of scans to Acquire*: defaults to 2000.
4. *Scan rate*: defaults to 5000.
5. *Acquire every X (sec)*: this is the sampling interval and should not be mistaken as the sampling rate. The value used was 5.4 seconds. This corresponds to a sampling interval of 5 seconds. The fractional part of 0.4 sec corresponds to the acquisition time ($time_{acquisition}$).
6. *Min # of scans to write at a time*: defaults to 2000.
7. *Input limits*: ±1.0 Volt that corresponds to the peak-to-peak voltage of the measured signals.

NOTE: The following equations describe the relationship of the data acquisition scanning setup.

$$time_{acquisition} = \frac{2000}{5000} = 0.4\,\text{sec} = 24 cycles(60Hz) \tag{1}$$

$$1.44 \cdot 10^6 \frac{scans}{hour} = 3600 \frac{\text{sec}}{hour} \cdot \frac{2000 scans}{5\,\text{sec}} \tag{2}$$

IV. TESTS PERFORMED AND METRICS USED

A series of tests were performed on cable 'A' and cable 'F' using both the *long-gap* and *short-gap* test methods. The *long-gap* is the 15cm gap length and the *short-gap* the 3.81cm gap length.

The first test, Series I, was to investigate the failure modes between the resistive (1.0 MΩ) and capacitive (2.5 nF) current limiting impedances. This is a continuation from the previous tests reported using cable 'A', and the metrics for this set of measurements are given in Table 15 below.

Table 15. Metrics used for Series I

METRIC	VALUE	COMMENTS
%NaCl	0.48% to 0.65%	Based on qualitative pollution levels
Supply Voltage	$10kV_{rms}$	Settings based on induced currents required.
Current limiting impedance	1MΩ and 2.5nF	Used for comparison purposes
Gap (between electrodes)	15.0 ± 0.5cm	Long gap method
H_2O flow rate	1gpm (gallon-per-minute)	Enough to saturate and initiate dry-band arcing
Acquisition time	Every 5 seconds	24 60Hz cycles or 0.4 seconds
Spray cycle	ON/OFF time	0.5 minute ON / 1.5 minutes OFF
Incline	0° w.r.t. the horizontal	To have a drying process as evenly distributed as possible.

The second test, Series II, conducted involved cable ‘A’ again but with the thevenin equivalent *RC* current limiting impedance representing a high pollution level, 5.0MΩ – *j*666pF. The metrics used in this test is given in Table 16 below. In this test the ON/OFF times were varied due to the system’s response to dry-band arcing with the new current limiting impedance. During the *test1.dat* data set no dry-band arcing occurred. The H_2O salt solution on the FOC (fiber optic cable) was not drying fast enough for the allotted time between the on and off periods of the spray. The ON/OFF times varied, in order to obtain dry-band arcing. The cable did not fail. This cable is to be considered as one of the best and less prone to damage caused by dry-band arcing.

Table 16. Metrics used for Series II

METRIC	VALUE	COMMENTS
%NaCl	0.33% to 0.36%	Based on qualitative pollution levels
Supply Voltage	$10kV_{rms}$	Settings based on induced currents required.
Current limiting impedance	5.0MΩ - *j*666pF	Used to represent a high pollution level.
Gap (between electrodes)	15.0 ± 0.5cm	Long gap method
H_2O flow rate	1gpm (gallon-per-minute)	Enough to saturate and initiate dry-band arcing
Acquisition time	Every 5 seconds	24 60Hz cycles or 0.4 seconds
Spray cycle	ON/OFF time	See the time summary, Appendix B
Incline	0° w.r.t. the horizontal	To have a drying process as evenly distributed as possible.

The third test, Series III, conducted involved cable 'F'. It was concluded that the time needed for cable 'A' would be too long to be able to conduct a time-to-failure analysis test in a timely fashion. Therefore the next choice of cable was one which was surmised to fail in a shorter length of time, namely cable 'F'. This cable is considered to be ranked second, as compared to cable 'A' in its performance to dry-band arcing. The metrics for this test is shown in Table 17 below. The ON/OFF spray periods for this test were such that only enough H_2O salt solution was sprayed to initiate dry-band arcing.

The cable was for the most part not fully saturated with the H_2O salt solution. The reason was because the drying process was not occurring fast enough to cause a failure. A suite of five runs was performed using this spray technique which resulted five failures with various time-to-failure data points. The acquired leakage current data for these runs was also analyzed using the criteria based on the *imsq* and categorizing the values into the *AC period*, *Arcing period*, and the *Noise period*.

Table 17. Metrics used for Series III

METRIC	**VALUE**	**COMMENTS**
%NaCl	0.33% to 0.36%	Based on qualitative pollution levels
Supply Voltage	$10kV_{rms}$	Settings based on induced currents required.
Current limiting impedance	5.0MΩ - *j*666pF	Used to represent a high pollution level
Gap (between electrodes)	15.0 ± 0.5cm	Long gap method
H_2O flow rate	1gpm (gallon-per-minute)	Enough to saturate and initiate dry-band arcing
Acquisition time	Every 5 seconds	24 60Hz cycles or 0.4 seconds worth
Spray cycle	ON/OFF time	See the time summary, Appendix B
Incline	0° w.r.t. the horizontal	To have a drying process as evenly distributed as possible.

The fourth test, Series IV, performed conducted involved cable 'F' again. Since a decision was made concerning the sequence of events that should occur during the testing period, the cable was now sprayed to fully saturate it. This will make the first event in the sequence to be the *AC period*. Another change was the supply voltage metric, changed from 10 kV_{rms} to 14.4 kV_{rms}. All other metrics was unchanged. The ON/OFF time periods of the spray cycle is given in the summary table in Appendix B.

The fifth test, Series V, complements Series III and Series IV. The cable used in the test is cable 'F'. The same metrics as in Series IV, except that the cable was not fully saturated. The spray technique as used in Series III was followed for this case. The supply voltage level applied was 14.4 kV_{rms}. This test was performed to find out if the cable would fail in the same mode as to those conducted in Series III. The ON/OFF time periods of the spray cycle is given in the summary table in Appendix B.

Finally the sixth test, Series VI, is performed using the *short-gap* test method. The metrics used in this case study are given in Table 18 below. The idea here is to try and contain the arcing to a restricted region of interest and thereby the damage incurred during the testing process is limited to a localized region of interest. There were different failure modes in this series of tests. The cables failed prematurely based on the Weibull plots, b is less than 1, which is indicative of infant mortality failures. The Weibull plot is used to show the failure modes and is an analysis technique that is incorporated into this form of application-specific form of failure analysis. The results can be used to compare and be associated with actual data observed in failures in the field as it becomes available.

Table 18. Metrics used for Series VI

METRIC	VALUE	COMMENTS
%NaCl	0.33% to 0.36%	Based on qualitative pollution levels
Supply Voltage	14.4 kV_{rms}	Settings based on induced currents required.
Current limiting impedance	5.0MΩ - *j*666pF	Used to represent a high pollution level
Gap (between electrodes)	15.0 ± 0.5cm	Long gap method
H_2O flow rate	1gpm (gallon-per-minute)	Enough to saturate and initiate dry-band arcing
Acquisition time	Every 5 seconds	24 60Hz cycles or 0.4 seconds worth
Spray cycle	ON/OFF time	See the time summary, Appendix B
Incline	0° w.r.t. the horizontal	To have a drying process as evenly distributed as possible.

V. TEST ON CABLE 'A' – SERIES I RESULTS

The results for Series I follow. The test sample, current limiting impedance, time-to-failure (TTF), and observations are given in Table 19. This series of tests is based on cables 'A' and 'F' since this were the cables that were considered the better overall from the initial tests performed and discussed in Chapter 4.

Table 19. Series I summary table

Cable	Limiting Impedance	Cycles to failure	Observation
A	1.0 MΩ resistance	7588	Cable sheath became hard and porous and bubbles were formed near both electrodes but much more prevalent near the LV electrode extending to a length of approximately 6.5cm and a width average of 0.75 cm on the bottom side.
	2.50 nF capacitance	5088	Circumferencial erosion of approximately 1.5 to 2.5 (cm) near LV electrode and three visible punctures next to the LV electrode. Some bubble formation on the bottom side near the HV electrode with approximate dimensions 1.0 x 0.5 (cm)

The graphs shown in Figure 39 and Figure 40 are the *imsq* distribution plotted as a percentage versus the number of cycles. Figure 39 is for the 2.5 nF and Figure 40 is for the 1.0 MΩ tests. These plots are in some sense analogous to the power spectrum. It is basically a discrete running histogram of the variable *imsq*. The plots show how the *imsq* power distribution changes over time and can be used to detect when cable failures occur.

Figure 39 (a) shows all of the *imsq* data from the beginning of the test, 0 cycles, to the end of the test, 5088 cycles, and the range of the *imsq* is from 0 μA^2 to 100 μA^2. This plot accounts for the total range that the current may fluctuate during the test. From this plot it can also be seen that the majority of the activity was in the *Noise period*, approximately 75 % of the time. Figure 39 (b) is for and *imsq* range of 45 μA^2 to 90 μA^2,

which shows that in the beginning of the test much of the activity fluctuated corresponding to the hydrophobicity of the cable. This initial type of arcing activity diminished to the point where most of the activity was either in the *AC* or *Noise period*.

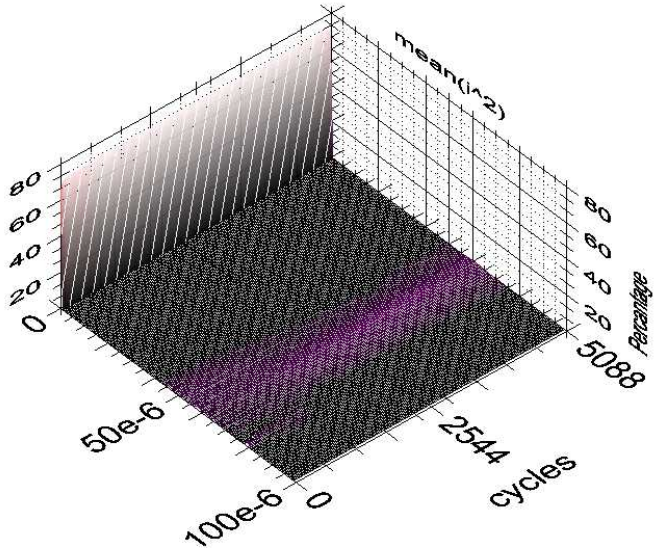

(a)

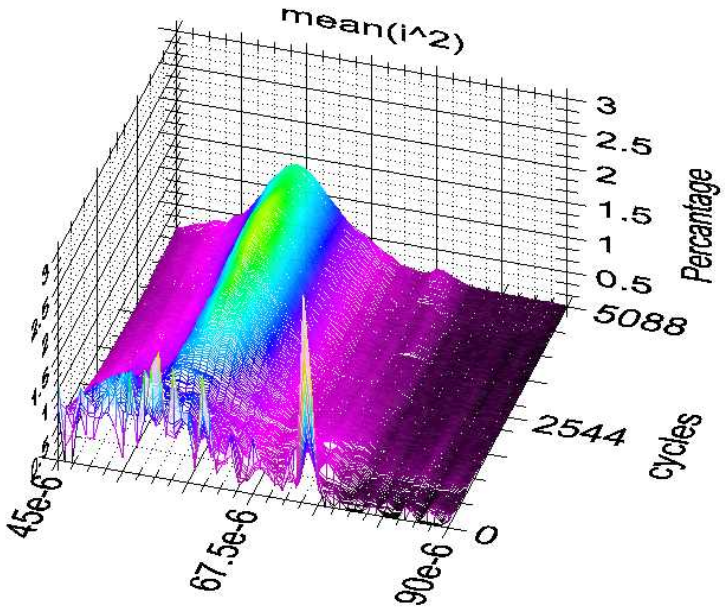

(b)

Figure 39. Series I: 2.5 nF *imsq* distribution (a) all, (b) 45e-6 to 90e-6

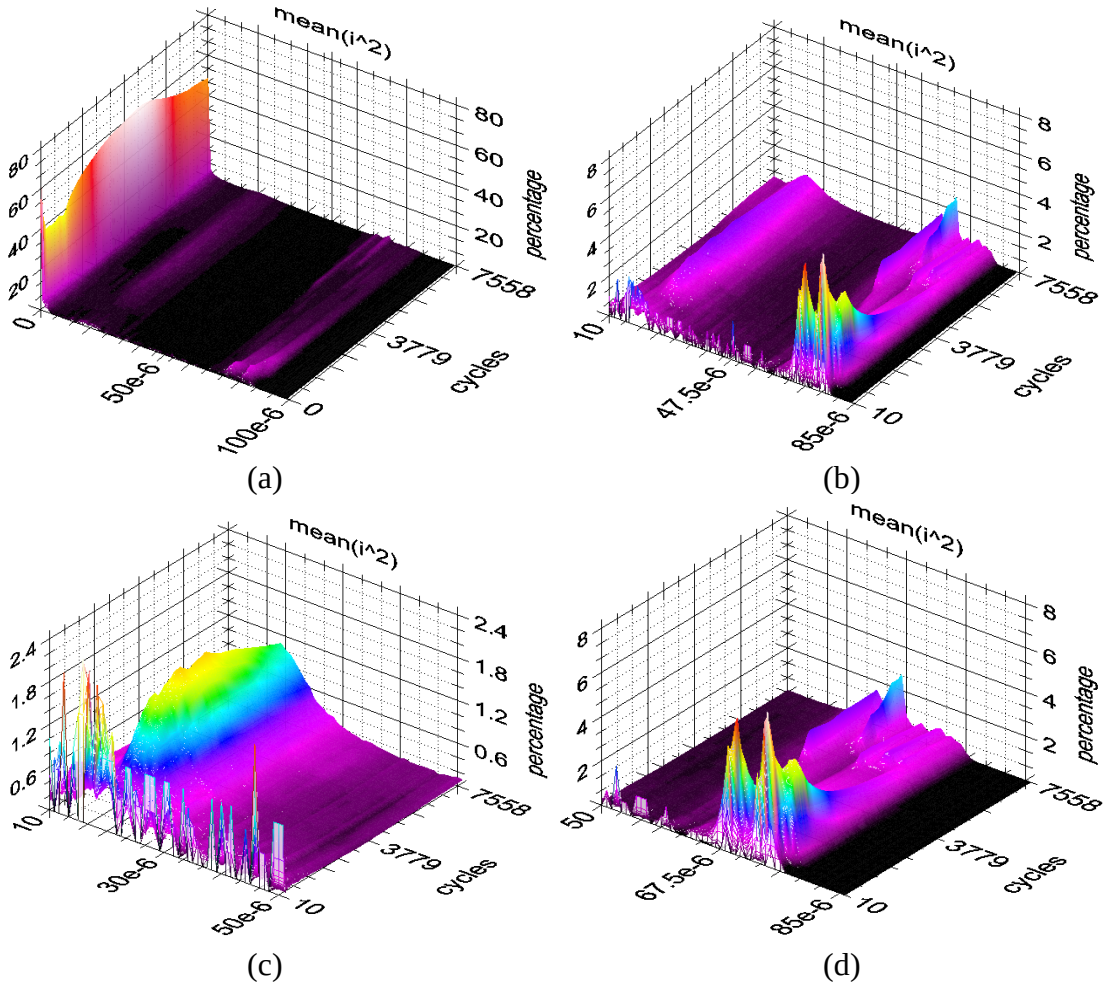

Figure 40. Series I: 1.0 MΩ *imsq* distribution (a) all, (b) 10e-6 to 85e-6, (c) 10e-6 to 50e-6, (d) 50e-6 to 85e-6

Figure 40 (a) shows the entire *imsq* distribution for the 1.0 MΩ limiting impedance test of Series I. It can be seen that the majority of the leakage current's activity falls into the *Noise period*, which fluctuates approximately from 38 % to 64 % of the time. Figure 40 (b) shows the *imsq* distribution from the range of m 10 μA^2 to 85

μA^2. It can be seen that the *imsq* distribution has two dominant ranges; a low range as shown in Figure 40 (c) (10 μA^2 to 50 μA^2), and high range as shown in Figure 40 (d) (50 μA^2 to 85 μA^2). These plots show that in the beginning the *imsq* activity ranges widely and then diminishes indicating that the cable is initially hydrophobic and eventually losses it. The low range of Figure 40 (c) a type of arcing activity, while the high range of Figure 40 (d) is sinusoidal current with arcing acitivity.

These plots could even be extended further and called the probability distribution function (pdf) of a random variable, which in this case is *imsq*. In terms of probability theory, the pdf defines the probability distribution. The pdf outlines the distribution of probability over the range of the random variable, namely *imsq*. The height (percentage axis) is proportional to the probability distribution function, $p_{imsq}(x)$, where $p_{imsq}(x)=P(imsq=x)$. It is of interest to know the pattern of outcome or set of outcomes that result from the failures with respect to the *imsq* distribution. In this case the outcomes, namely the three qualitative categories that dry-band arcing undergo on a fiber optic cable's sheath, are the set of an event. The event being the individual test performed on the cable.

The *imsq* may also be called the $power_{imsq,}$ since it is directly proportion to the real power developed by the leakage current and assuming it to be normalized to a resistance of 1 Ω. The *imsq* for the 2.5 nF case is consistently in the range between 55 μA^2 and 75 μA^2, with a percentage range between 0.5 % and 1.9 % as shown in Figure 41. This directly translates into a current between 7.41 mA and 8.67 mA. As for the 1.0

MΩ case the $power_{imsq}$ has several modes. The obvious ones fall in a low range between 15 μA^2 and 32 μA^2 and a high range between 66 μA^2 and 86 μA^2, with a fluctuating percentage range as shown in Figure 41. These values translate into a low current range between 3.87 mA and 5.66 mA and high current range between 8.12 mA and 9.27 mA. A third mode can be seen to show up below 15 μA^2 and into the noise.

An interesting observation noted from Figure 42, which is a plot of energy (J) versus time-to-failure in cycles, is that the power delivered to a resistance of 1 Ω (i.e., normalized to 1) corresponds to 475.6 μW and 493.5 μW for the 2.5 nF and 1.0 MΩ current limiting impedances respectively. These values are given in Table 20. Although no conclusions could be made whether this is a coincidence or of value that could be used to compare TTF of different cables.

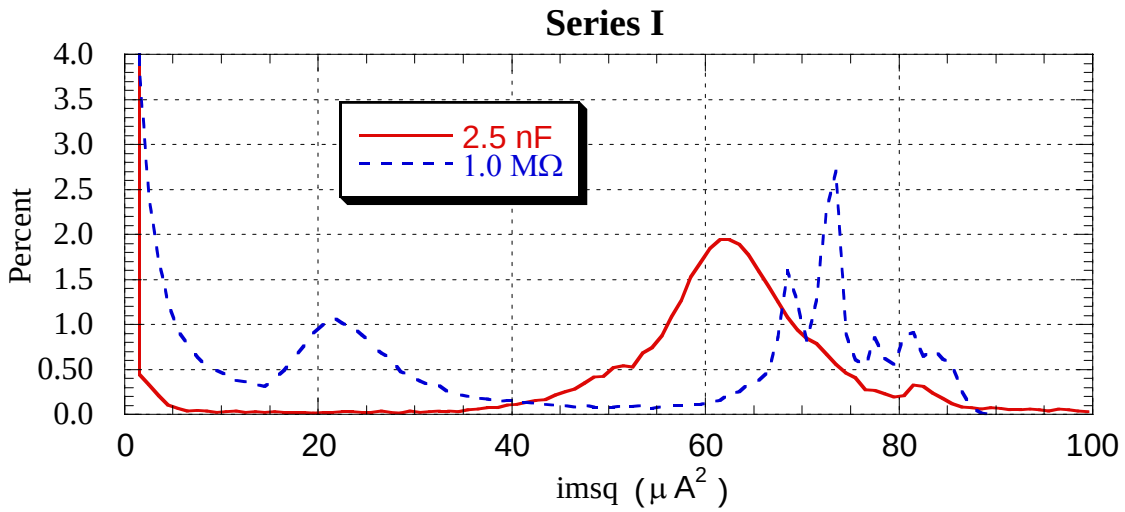

Figure 41. Series I: *imsq* histograms

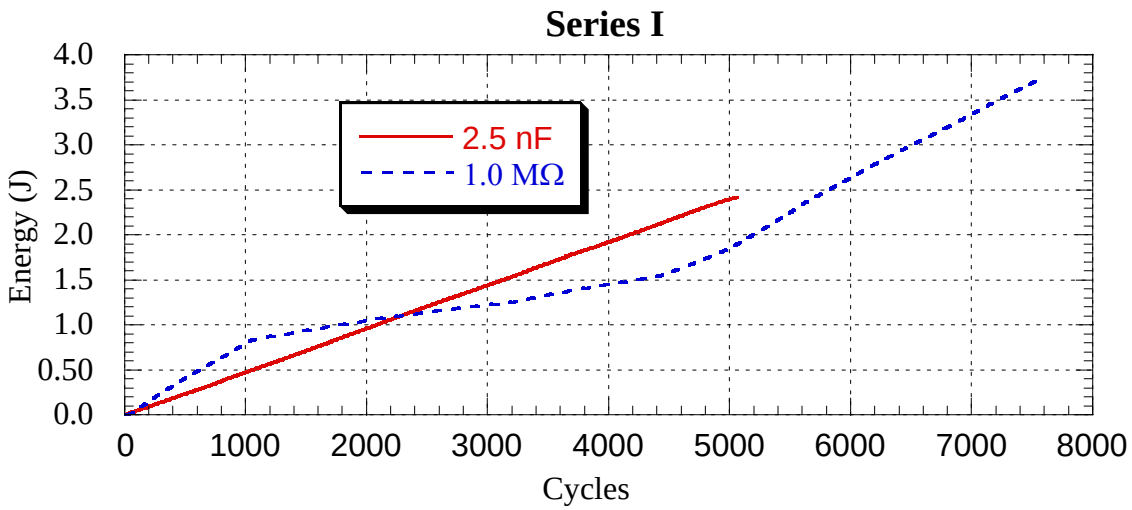

Figure 42. Series I: Energy vs. time-to-failure

Table 20. Comparison of Relative power and TTF %CHG values; Series I

Relative Power – Time-to failure	Absolute % Change
475.6μW (2.5nF) 493.5μW (1.0MΩ)	3.63 %
5088 (2.5nF) 7558 (1.0MΩ)	48.54 %

VI. TEST ON CABLE 'A' – SERIES II RESULTS

The results for Series II are given in this section. The test sample, current limiting impedance, TTF, and observations are given in Table 21. The graphs shown in Figure 43 are the *imsq* distribution over time for Series II. There are two dominant ranges in which the *imsq* falls into, namely a high range and a low range. The high range corresponds to the qualitative category, *AC period*, and the low range corresponds to the *Noise period* of the dry-band arcing process. It can be seen that there is a small amount of the *Arcing period* activity as compared to the other two activities. This can be shown both qualitatively and quantitatively in Figure 44 and Figure 45. From these plots, it can be observed that for the majority of the time the activity is occurring in the *AC* and *Noise period* approximately 82 % of the time. This is some form of evidence that can be related to the cable's performance due to dry-band arcing. The plots in Figure 44 and Figure 45 are extracted from the running histogram data. The cumulative *imsq* distribution as a percentage is shown in Figure 46. The *AC period* range is between 2.1 μA^2 and 2.3 μA^2. The *Noise period* range is from 0 to 40 nA^2.

Table 21. Series II summary table

Cable	Limiting Impedance	Cycles to failure	Observation
A, White	5.0MΩ - *j*666pF	No failure (9736)	Cable became discolored, but no obvious damage or erosion can be seen.

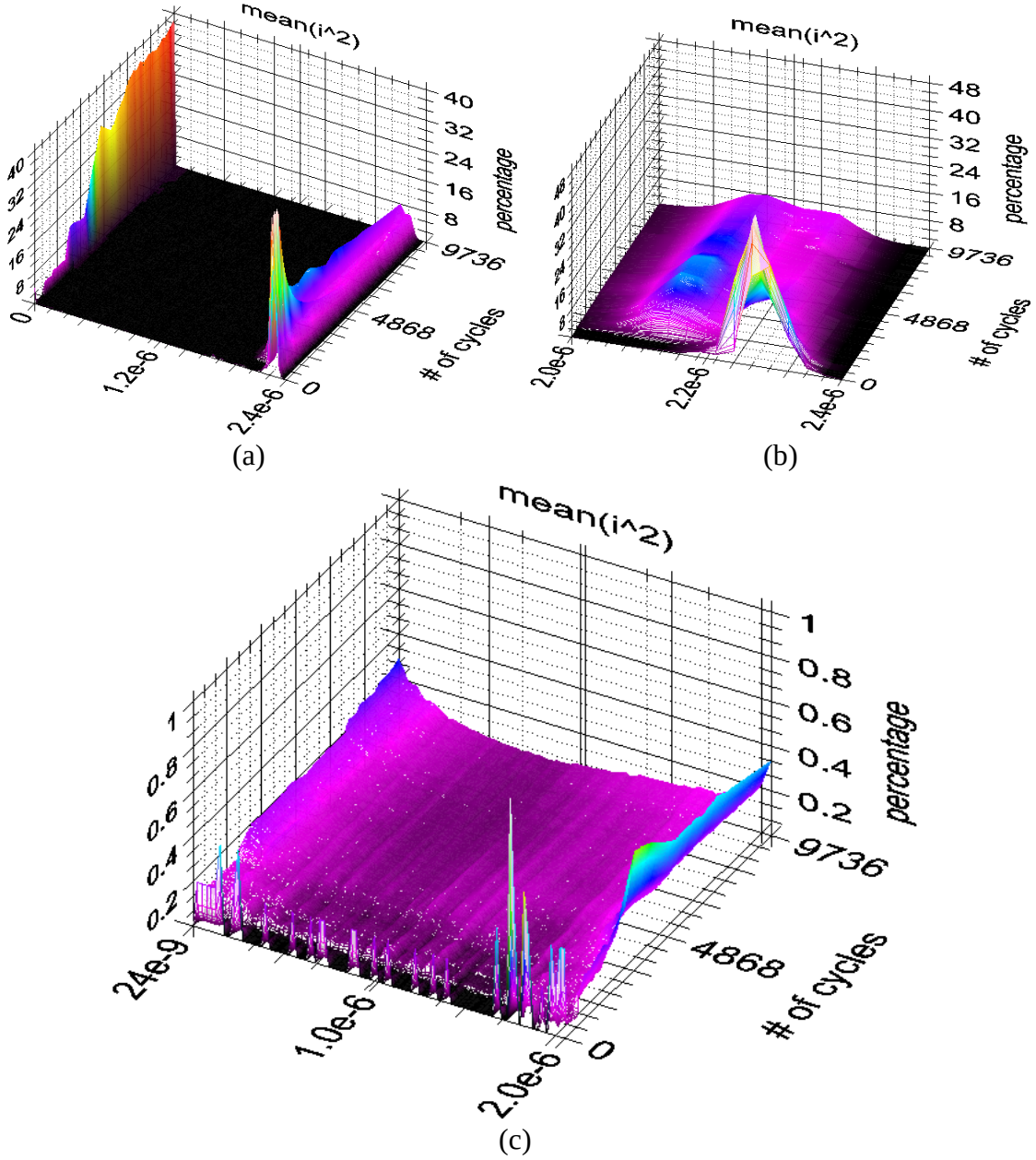

Figure 43. Series II: 5.0MΩ - *j*666pF *imsq* distribution (a) all, (b) 2.0e-6 to 2.4e-6, (c) 24e-9 to 2.0e-6

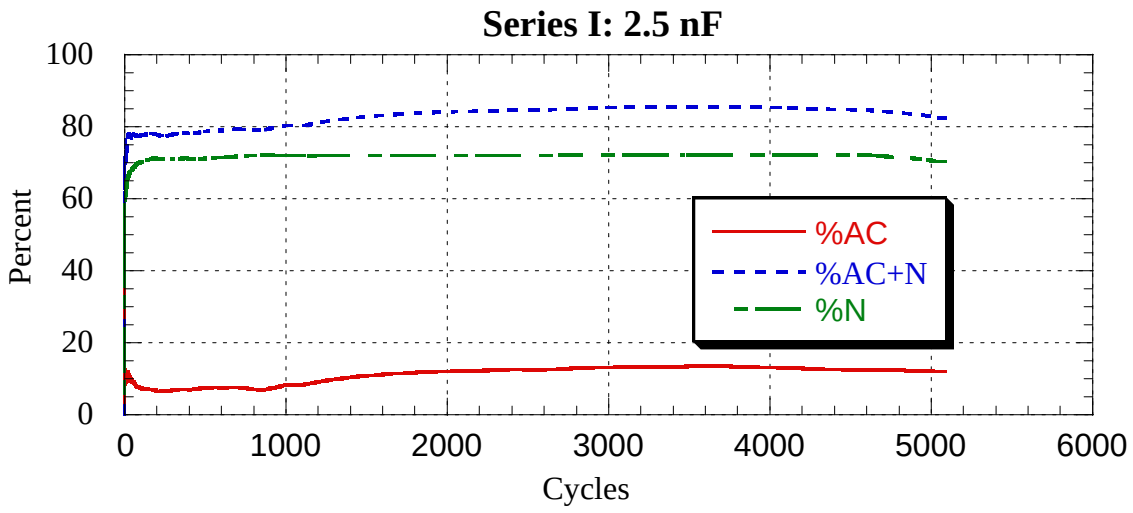

Figure 44. Series I: 2.5 nF, Percent vs. TTF of *AC*, *Noise*, and *Arcing*

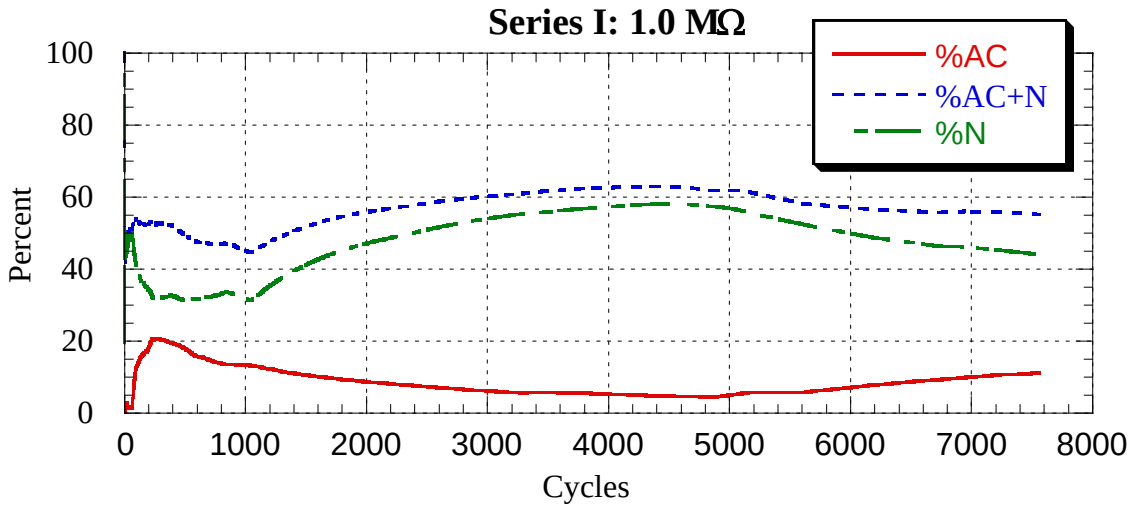

Figure 45. Series I: 1.0 MΩ, Percent vs. TTF of *AC*, *Noise*, and *Arcing*

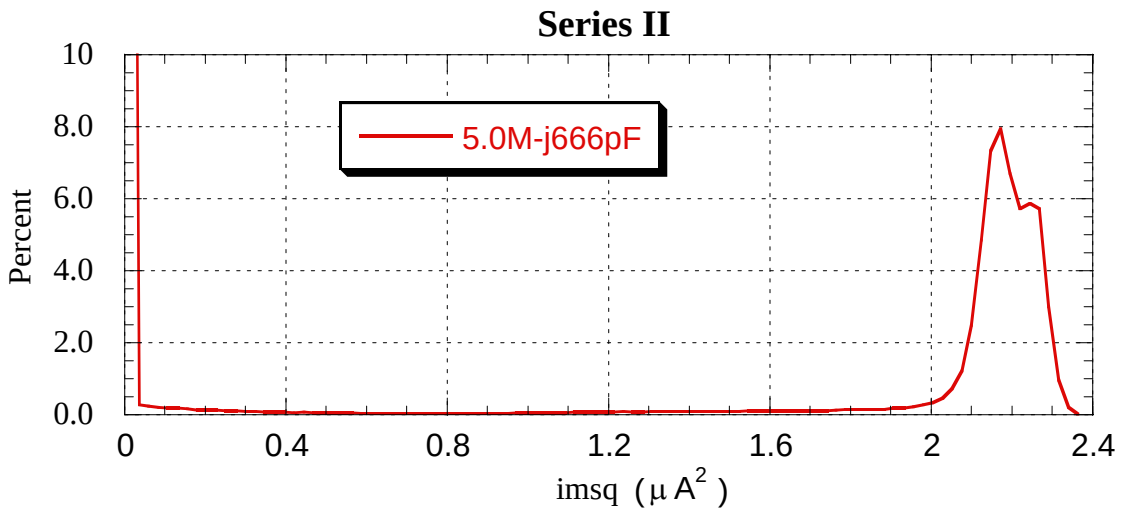

Figure 46. Series II: 5.0MΩ - *j*666pF percent vs. *imsq* histogram

For comparative purposes see the plot shown in Figure 47 between Series I and Series II tests. From this plot, it can be surmised that the cable would fail at approximately 131k cycles by extrapolation. This is under the assumption that the energy trajectory continues in the same fashion, i.e., at a rate of 35 μW per 10k cycles. It would also be assumed that the cable fails within the same power range as to those of Series I as was shown in Table 20.

The percentage of dry-band arcing events is shown in Figure 48. The plot shows that approximately 80 % to 90 % of the activity occur in the *AC* and *Noise period*. This also supports to the fact that the cable did not fail since a low percentage of the time arcing did not occur to cause enough damage to fail the cable. This also indicates that a small percentage of the energy developed between the electrodes was not related to dry-band arcing but to the *AC* and *Noise period* that do not cause considerable damage.

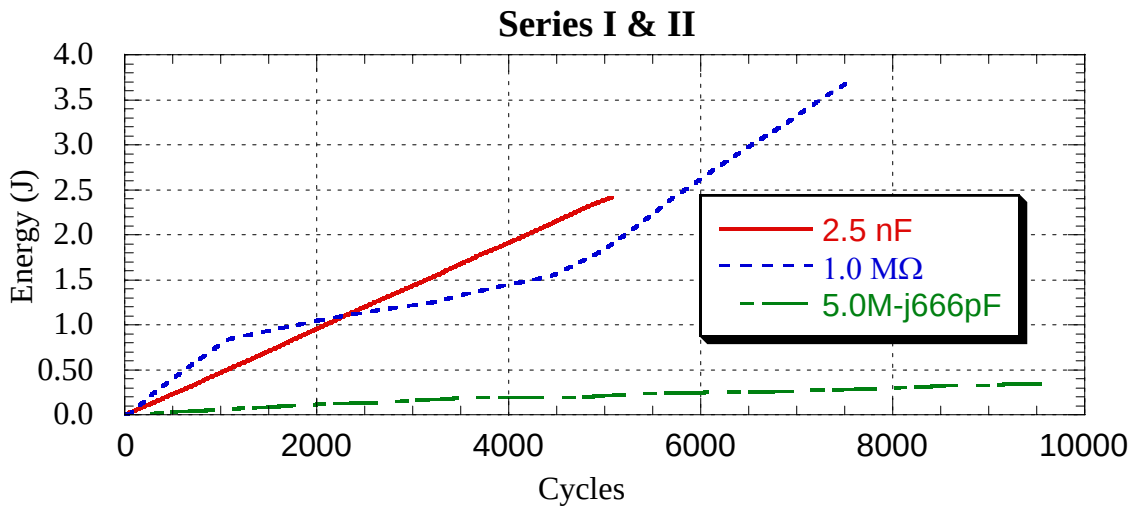

Figure 47. Series I and II: Energy vs. TTF comparison

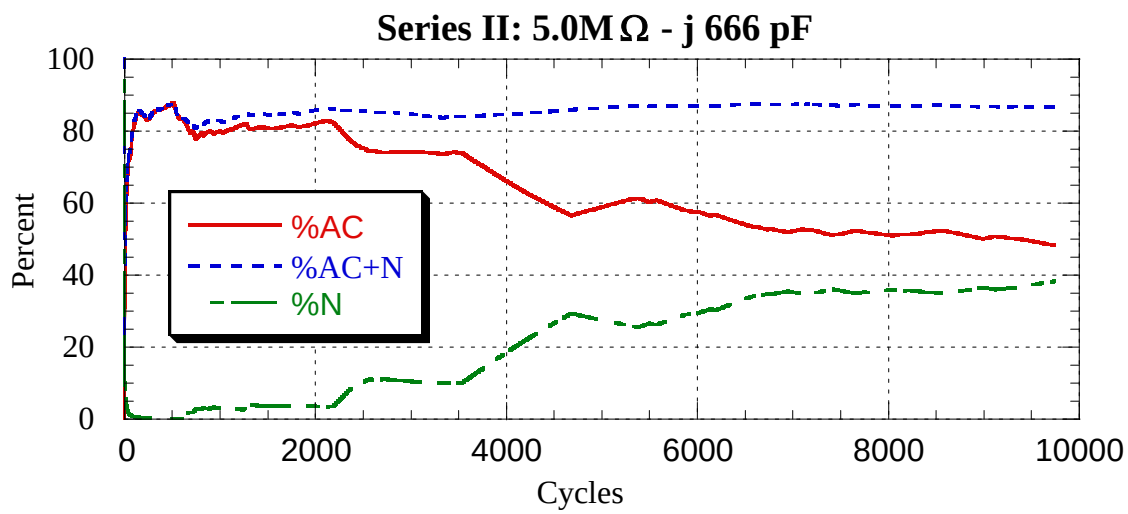

Figure 48. Series II: 5.0MΩ-j666pF, Percent vs. TTF of *AC*, *Noise*, and *Arcing*

VII. TEST ON CABLE 'F' – SERIES III RESULTS

The results for Series III follow. The test objects, current limiting impedance, TTF, and observations are given in Table 22. It should be noted that in all of the tests the damage occurred near the low voltage electrode. The TTF data was plotted on a Weibull plot that indicates the failures to be random.

Table 22. Series III summary table

Cable	**Limiting Impedance** 5.0MΩ - *j*666pF	**Cycles to failure**	**Observation**
F, Purple	Run 1	2804	Incineration and tracking on the bottom side where water droplets would have formed. Tracks branched out longitudinally about 3.5cm. Circumferencial wear extending 1.0cm from the LV electrode.
	Run 2	2453	Same as Run 1
	Run 3	342	Less circumferencial wear as compared to Run1 and 2. Puncture on bottom side near the LV electrode extending about 0.75cm longitudinally and a width of 0.25cm.
	Run 4	462	Same as Run 1 but not as much incineration.
	Run 5	4346	Same as Run 3 except with damage with dimensions of 1.0cm longitudinally and a width of 0.3cm.

The graphs shown in Figure 49 are the *imsq* distributions over the number of cycles as a percentage. It can be seen that the TTF for Run 1 and Run 5, Figure 49 (a) and (e) respectively, have a higher percentage of *AC period* activity. This accounts for the larger TTF values as compared to the other runs. This proves that the *Arcing period* in the dry-band arcing process is the dominant factor causing the fiber optic cable failures. This must be further investigated to be absolutely sure, but for the present time this will be considered as the principle reason for failure that can be justifiable based on the existing acquired data. Correlation of the degree of damage caused by the actual *Arcing period* could help in explaining the relationship of the TTF and dry-band arcing by this method of analysis. The root of the problem will require some other form of reasoning based on first principles, such as thermal dynamics.

In the meantime the acquired data will be the quantitative information used to find a pattern that will link the damage to the measured leakage current. This is one practical means by which actual fiber optic cables in the field could be monitored. From the monitored information it can then be determined if there are any risks present. This in turn would then make reliability, safety, and risk management more accurate to predict if necessary. This type of data mining is currently in progress and needs to be developed and refined. Obtaining more data samples would certainly make this method a very viable solution to the problem. Although this analytical technique will be subject to review.

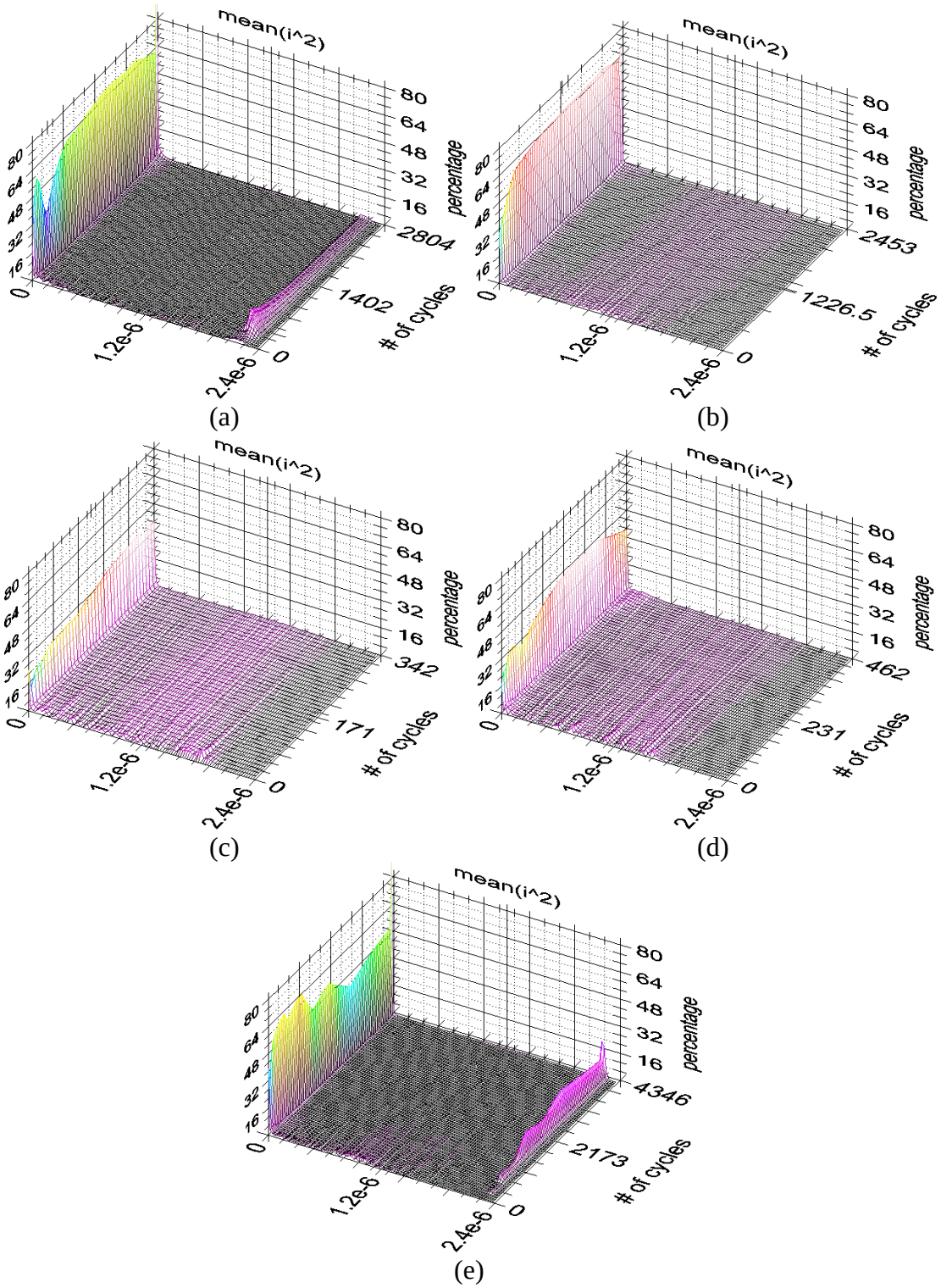

Figure 49. Series III: 5.0MΩ - *j*666pF (a) Run1, (b) Run2, (c) Run3, (d) Run4, (e) Run 5

The next plot shown in Figure 50 is the sum of *AC* and *Noise period* activity percentage versus TTF for Series III. All of the trajectories exhibit a peak value prior to cable failure. Also revealed in the trajectories is a *tail* with negative slope that is an indication of a breakdown in the cable's sheath. This corresponds to the fact that there is a continuous flow of leakage current through the cable's sheath as has been observed in prior experimental tests. Although, the leakage current during a failure is sinusoidal as categorized by the *AC period*, quantitatively they are different. The leakage current magnitude flowing during the failure is less than the *AC period* but greater than the *Noise period*. These characteristic indicators agree with the experiments performed and reported prior to this finding. The leakage current during the failure falls in the category of the *Arcing period* as defined by the activities respective value even though it is not really arcing in the strictest sense.

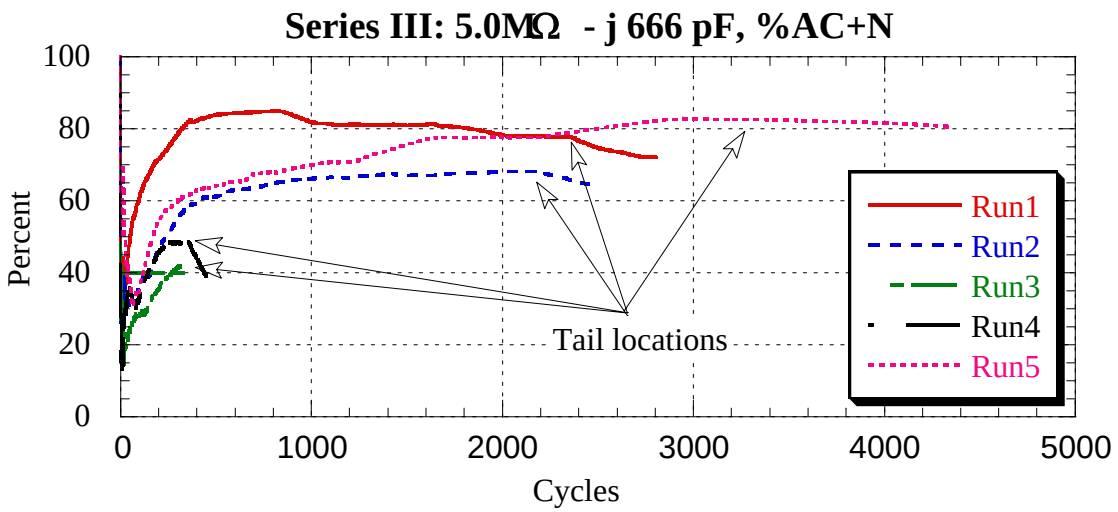

Figure 50. Series III: Percentage vs. TTF of *AC+N period*

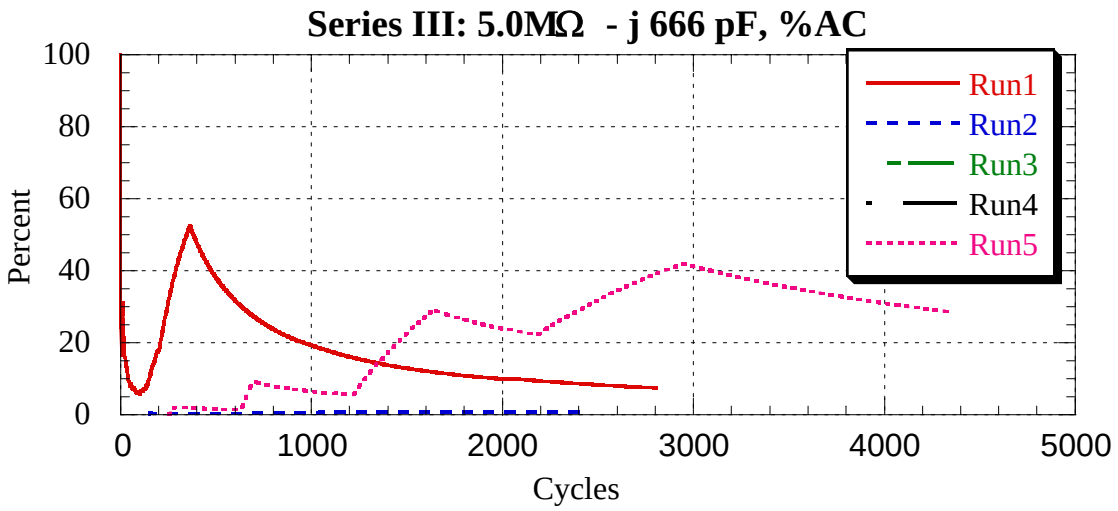

Figure 51. Series III: Percentage vs. TTF of *AC period*

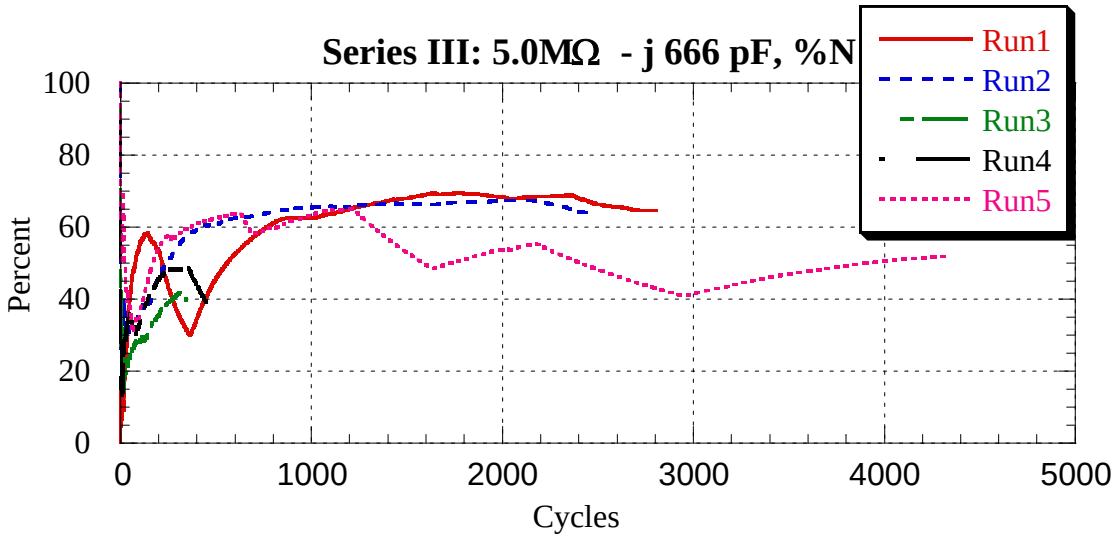

Figure 52. Series III: Percentage vs. TTF of *Noise period*

From the previous plot in Figure 50 has led to an interesting observation. The observation is that the TTF could be fitted by certain function. The function initially would appear to be either logarithmic, quadratic, or some other form. The function

selected to fit this is the Weibull distribution. Figure 53 shows the Weibull distribution fit versus TTF for Series III. The following equation defines the Weibull distribution, namely the cumulative distribution function (CDF), which may be explicitly defined mathematically as follows [27]:

$$F(t) = 1 - e^{-\left(\frac{t}{\eta}\right)^{\beta}} \tag{3}$$

where: *F(t)* is the fraction of device under test (DUT) failing

1. *t* is the time to failure (TTF)
2. η is the characteristic life or scale parameter
3. β is the slope or shape parameter
4. *e* is the constant, base for Naperian or natural logarithms

The parameters of the Weibull distribution has two degrees of freedom, namely the slope, β, and the characteristic life, η. The slope of the line, β, is associated with the physics of the failure. The characteristic life, η, is the normal TTF in this type of analysis. The distributions given by the Weibull analysis is advantageous by its capability to give accurate failure analysis while simultaneously providing good failure predictions with an extremely small amount of data samples. The slope parameter, β, is further classified into a class the failures may represent:

1. $\beta < 1.0$ is indicative of infant mortality
2. $\beta = 1.0$ typically means that the failures are random, i.e., independent of age

3. $\beta > 1.0$ is indicative of failures due to wear out

Weibull analysis is a whole class of analysis in its own right. The Weibull curve shown in Figure 53 is obtained using the parameters obtained from the Weibull analysis. The Weibull curve crosses the TTF on four of the five trajectories quite near the actual time of failure. The actual TTF is the onset of the *tail* of the independent trajectories characterized by a negative slope.

These percentage values could be extended to the energy plot and extract the amount of energy or power developed by each of the three events of the dry-band arcing process on fiber optic cables.

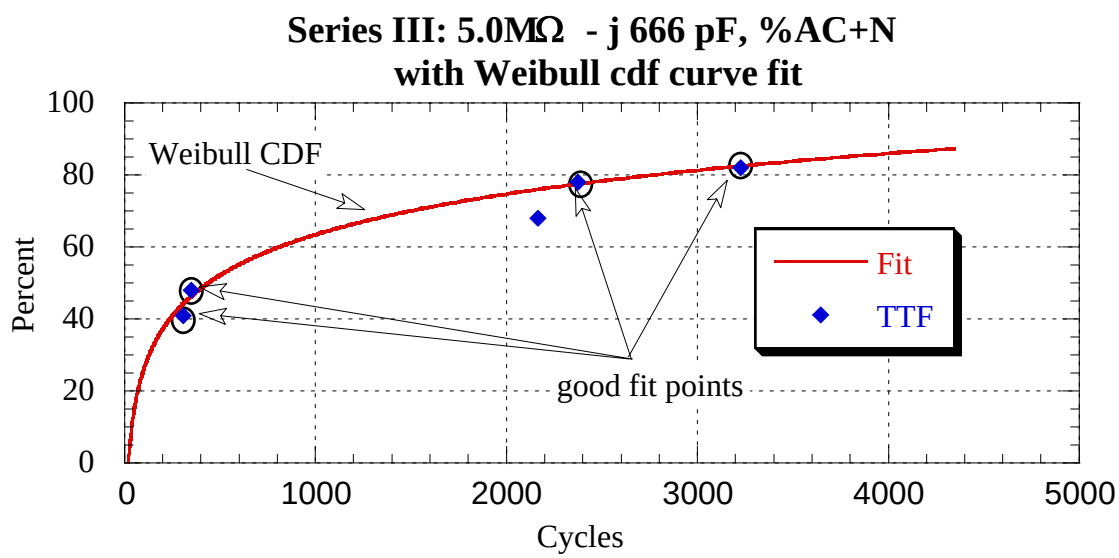

Figure 53. Weibull fit vs. TTF, Series 3

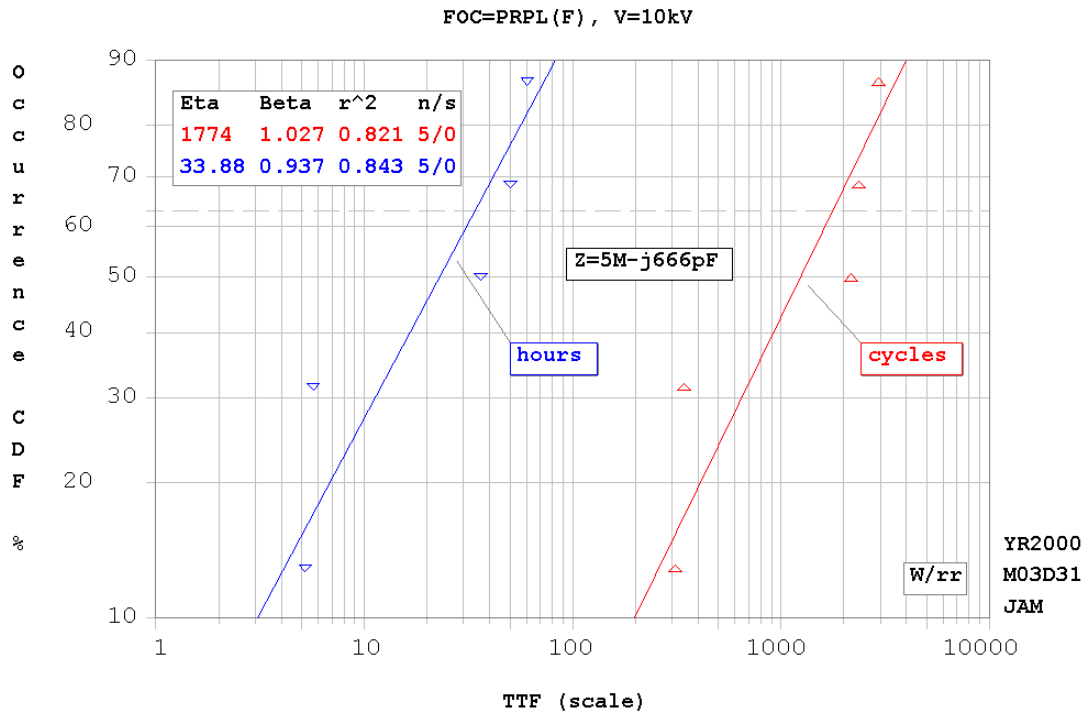

Figure 54. Weibull plot, Series III

The Weibull plot in Figure 54 confirms that the essence of the damage caused by dry-band arcing is a random phenomenon, since the slope, β, is approximately equal to one. This is a correlation between the nature of dry-band arcing and its effects on the fiber optic cable's sheath, i.e., the time-to-failure. The fact that the phenomenon is a random process allows the analysis to be considered as a method that appropriately deals with this type of random data, e.g., probability, statistics, etc.

VIII. TEST ON CABLE 'F' – SERIES IV AND V RESULTS

The following results are for Series IV and Series V. The test sample, current limiting impedance, TTF, and observations are given in Table 23. The current limiting

impedance used for both set of experiments is 5.0MΩ – *j*666pF. The difference between the tests is the ON/OFF spray periods. The HV applied to the cable sample is 14.4 kV_{rms}. One of the reasons for performing these tests was to determine if the cable would fail within a reasonable amount of time by forcing the development of the dry-band arcing to undergo all three of the defined activities; the *AC, Noise,* and *Arcing period*. The second reason, which was a result of the first, was to force the cable's sheath to fail and have a comparison to the test results of Series III. Series V test was subjected to the same spray pattern as the test for Series III. Notably, the TTF for Series V did not lessen, given the fact that the magnitude of the leakage current is greater than that of Series III, which is actually counter intuitive. The TTF of Series V is greater than all the runs in Series III.

Table 23. Series IV and V summary table

Cable	**Limiting Impedance** 5.0MΩ – *j*666pF	**Cycles to failure**	**Observation**
F, Purple	Series IV	4578 No Failure	No obvious visible damage. Comparable to a new sample.
	Series V	4600	Same type of failure as observed in Series III, Run 1, except that the tracking extended 7.5cm longitudinally and much wider. The circumferencial wear extended 1.7cm from the LV electrode. This is indicative that the dry band the arc can bridge is greater than for the lower induced voltage used in Series III.

The data file *test5.dat* of Series IV is lost and therefore not included in the analysis, although it is not a great loss. Another glitch in Series IV is the voltage was changed from 10 kV_{rms} to 14.4 kV_{rms} after *test2.dat*. The reason for this was because of the lack of arcing activity at the 10 kV_{rms} level. By increasing the voltage level, it was presumed that the arcing activity would increase. The *imsq* distribution over time for Series IV is shown in Figure 55 and the histogram is shown in Figure 57. As for Series V, the *imsq* distribution over time is shown in Figure 56 and the corresponding histogram is shown in Figure 57. The main difference between the two *imsq* running histograms is that for Series V there is minimal *AC period* activity, and the cable failed in this test. Figure 56 (b) shows the arcing activity of the *imsq* distribution from the range of 50 nA^2 to 5 μA^2.

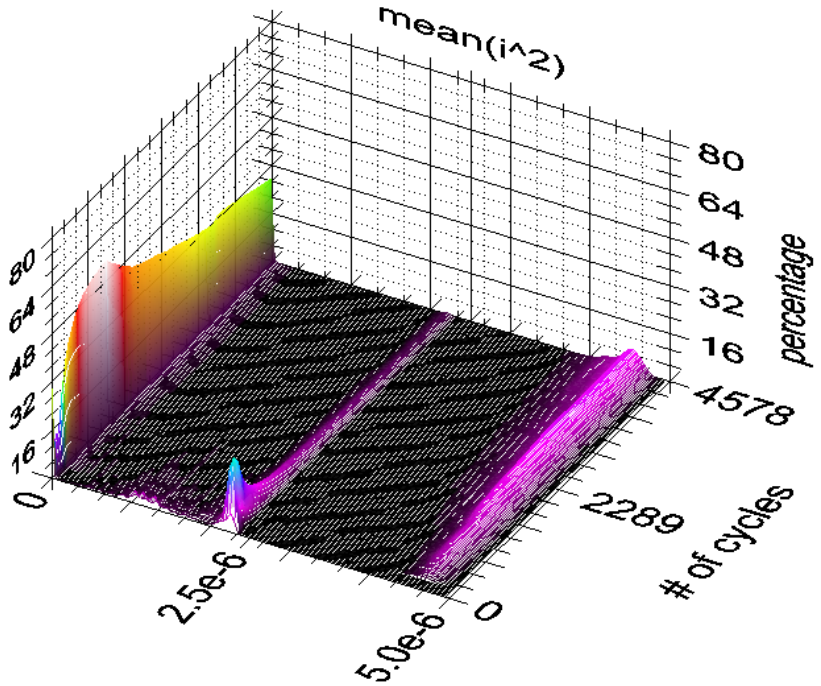

Figure 55. Series IV: 5MΩ-*j*666pF *imsq* distribution

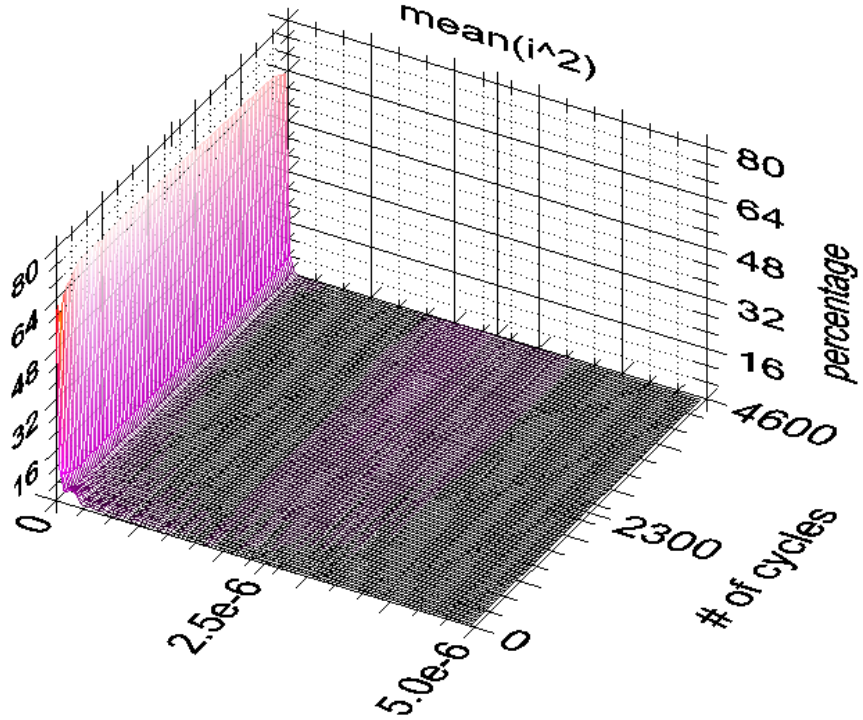

(a)

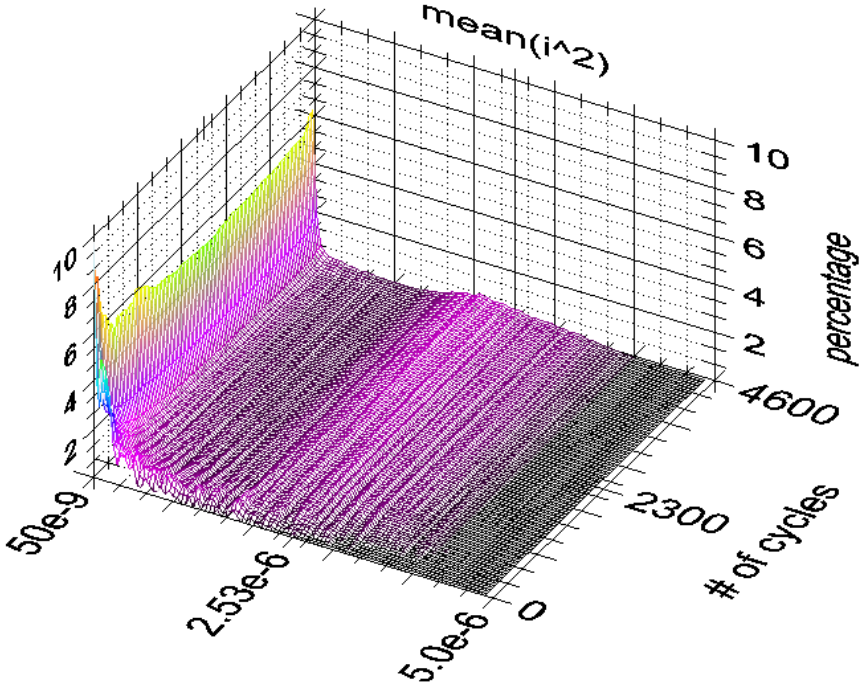

(b)

Figure 56. Series V: 5MΩ-*j*666pF *imsq* distribution (a) all, (b) 50e-9 to 5.0e-6

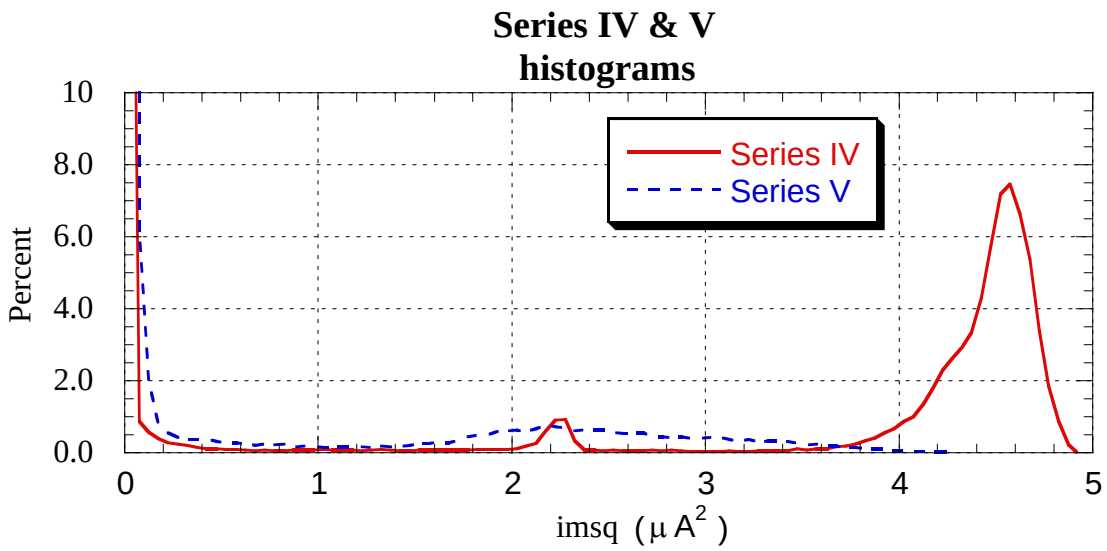

Figure 57. Series IV and V: Percent vs. *imsq* histogram 5MΩ-*j*666pF

From the energy versus TTF plot in Figure 58, it is obvious that a higher energy is not an indication of failure directly. The trajectory of Series IV in Figure 58 may be extrapolated to the actual number of cycles, 4578. The final energy value, assuming the same rate as shown, would be between 360 mJ and 400mJ. The plot in Figure 59 shows the percentage of *AC+Noise period* versus TTF. TTF is the number of spray cycles. Not much can be concluded from the *AC+Noise period* percentage plot due to reason that two different spray techniques were used.

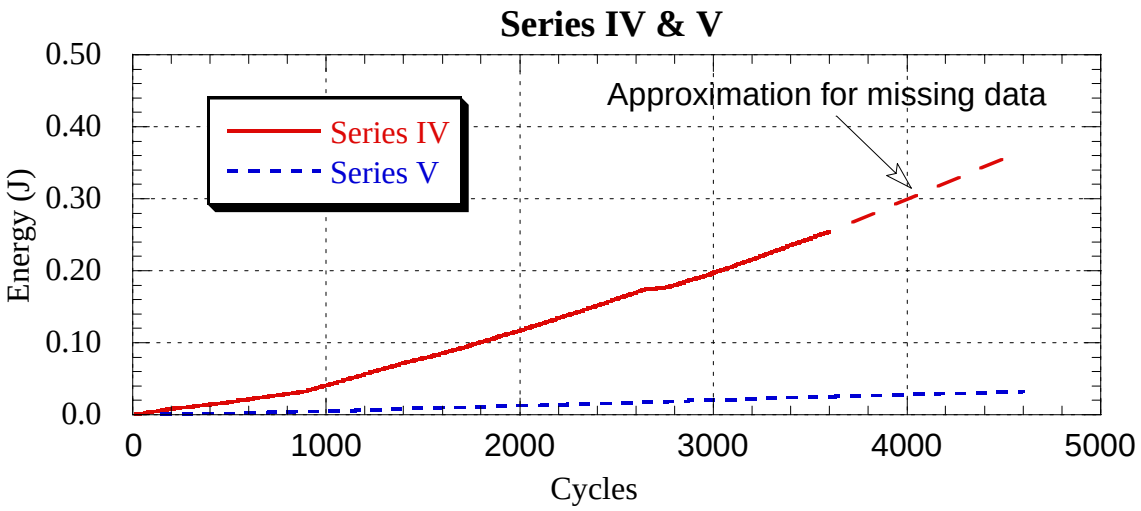

Figure 58. Series IV and V: Energy vs. TTF comparison

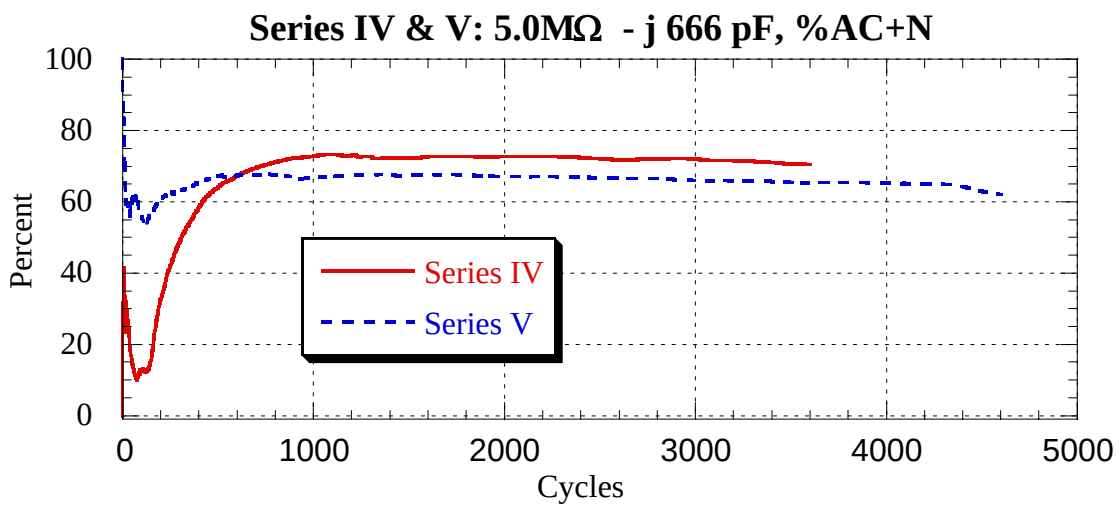

Figure 59. Series IV and V: Percentage vs. TTF of *AC+Noise period*

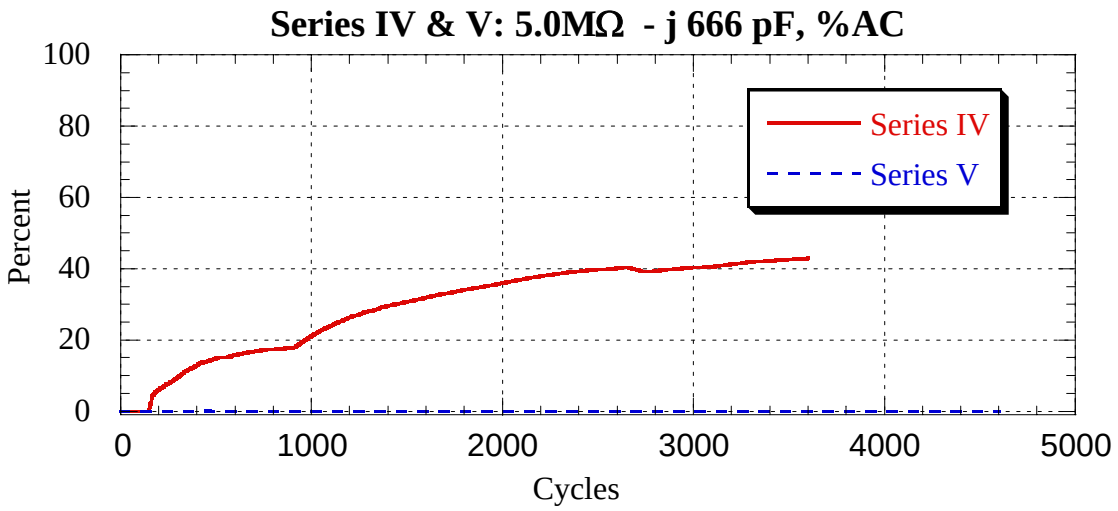

Figure 60. Series IV and V: Percentage vs. TTF of *AC period*

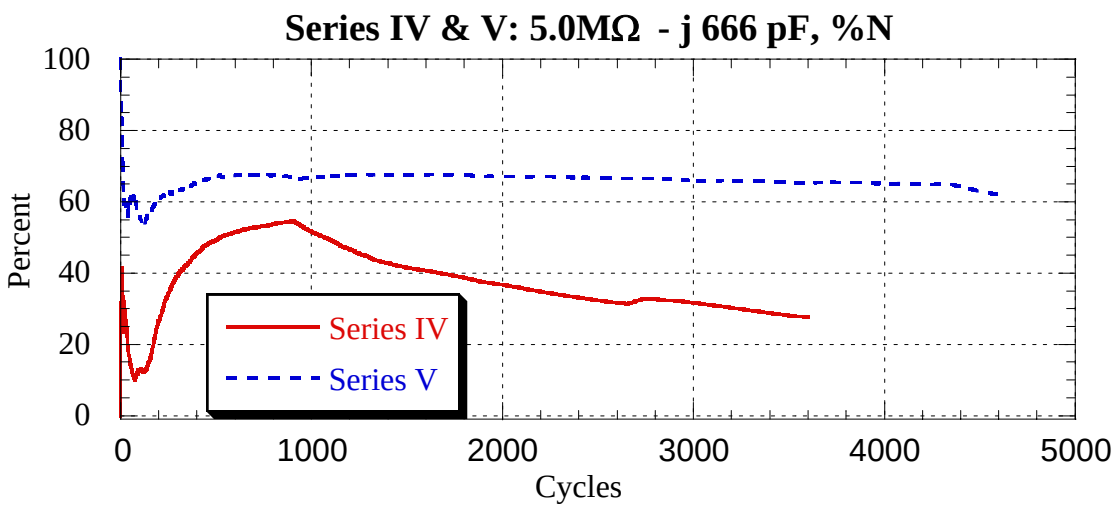

Figure 61. Series IV and V: Percentage vs. TTF of *Noise period*

Series V could be compared to the tests done in Series III. The energy versus TTF trajectories of Series III and V are shown in Figure 62. It is difficult to conjecture anything valid from this plot. From the plot of *AC+Noise period* versus TTF shown in

Figure 63 it can be concluded that the failure modes can not be categorized under the same criteria. In other words, the distribution of failures are described by different β and η parameter using the Weibull distribution function. This should not be surprising, since the power level being developed by the dry-band arcing process between the electrodes is twice as large for Series V than that of Series III. The *AC+Noise period* trajectory of Series V has the same characteristics noted in Series III. The characteristics are the tail near the TTF and the maximum peak achieved prior to failure. Therefore the analysis employed is independent of the voltage level used.

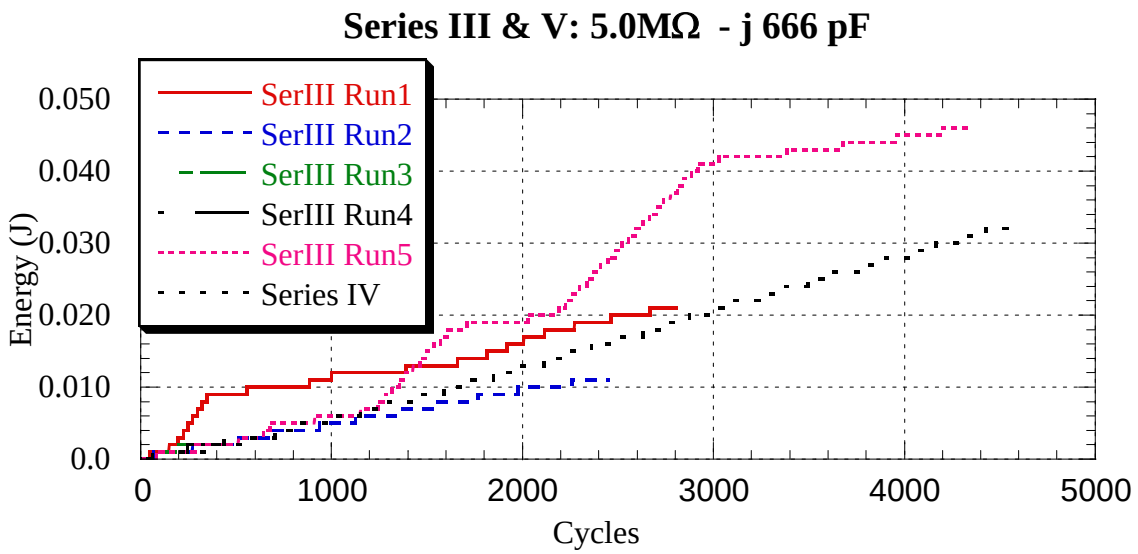

Figure 62. Series III and V: Energy vs. TTF comparison

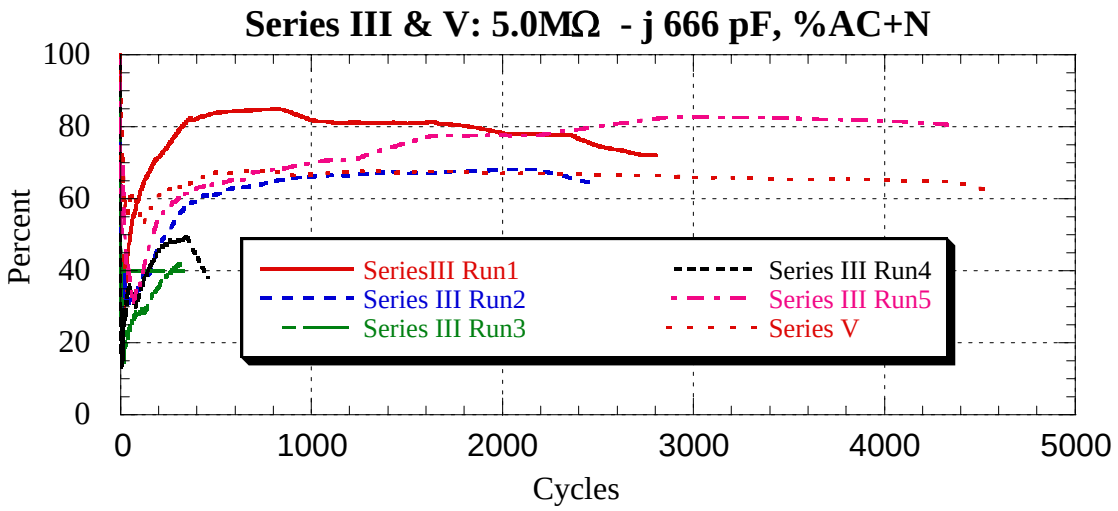

Figure 63. Series III and V: Percentage vs. TTF of *AC+Noise period*

IX. TEST ON CABLE 'F' – SERIES VI RESULTS

The following results concern the *short-gap* experiment, Series VI. The test objects, current limiting impedance, TTF, and observations are given in Table 24. The TTF was shortened considerably by the *short-gap* test setup but deciphering information corresponding to the TTF from the data is a bit more complicated. The failures seem to have more than one failure mode, which makes the analysis difficult. Some failures occurred at very short times with some possible reasons as noted in the observations in Table 24. The problem associated with this type of test is determining and classifying the failure modes. The definition of a failure might have to be revisited due to the possible failures encountered with the *short-gap* test. There could be some other interesting correlation based on these outcomes which could be looked into.

Table 24. Series VI summary table

Cable	Limiting Impedance	Cycles to failure	Observation
F, Purple	Run 1	95	Single track extending from the HV electrode 1.9cm with a nominal width of 0.2cm.
	Run 2	42	Same as Run 1 except with dimensions of 0.9cm x 0.2cm (*l x d*)
	Run 3	437	Test stopped due to an increase of leakage current during the *Noise period*, which is indicative of failures in previous experiments. An abrasion located 1.5cm from the HV electrode with some curved-like erosion that is convex shaped.
	Run 4	122	Same as Run 3 except that the erosion is perpendicular to the length of the cable.
	Run 5	279	Single track extending from the LV to HV electrodes. The nominal width being 0.2cm.
	Run 6	7	Single track extending from the HV electrode 1.3cm. Nominal width is 0.2cm.
	Run 7	338	Same as Run 6 except with a length of 0.8cm and a with a width of 0.25cm and some abrasion at 1.5cm from the HV electrode as in Run 3.
	Run 8	10	Single track of length 1.6cm equidistant from both electrodes. Nominal width is 0.25cm. This failure occurred on a manufacture hairline mark that runs along the cable's entire length.
	Run 9	2	Single track of length 2cm extending from the LV electrode with a nominal width of 0.2cm. The failure occurred near on a manufacture hairline mark that runs along the cable's entire length
	Run 10	612	Circular puncture that could be considered the onset of a track near the HV electrode. Abrasion and slight wear in the center between the two electrodes with an area of approximately 1.2cm in length and 0.6cm in width.

The graph shown in Figure 64 is the energy versus TTF for Series VI. All the energy trajectories have approximately the same increasing rate and in a linear fashion. There is no direct correlation between the TTF and the energy from this plot as for the previous series of tests reported thus far.

The plots in Figure 65 through Figure 67 show the percentage of *AC+Noise period*, *AC period*, and *Noise period* trajectories respectively. The trajectories in this case do not fit into a Weibull distribution as they did for Series III.. One characteristic that is prominent is the negative sloping *tail* prior to failure and a crest value is reached indicating the onset of the *tail*. Fitting a curve to the TTF is not straightforward and the plots are used just for illustrative purposes.

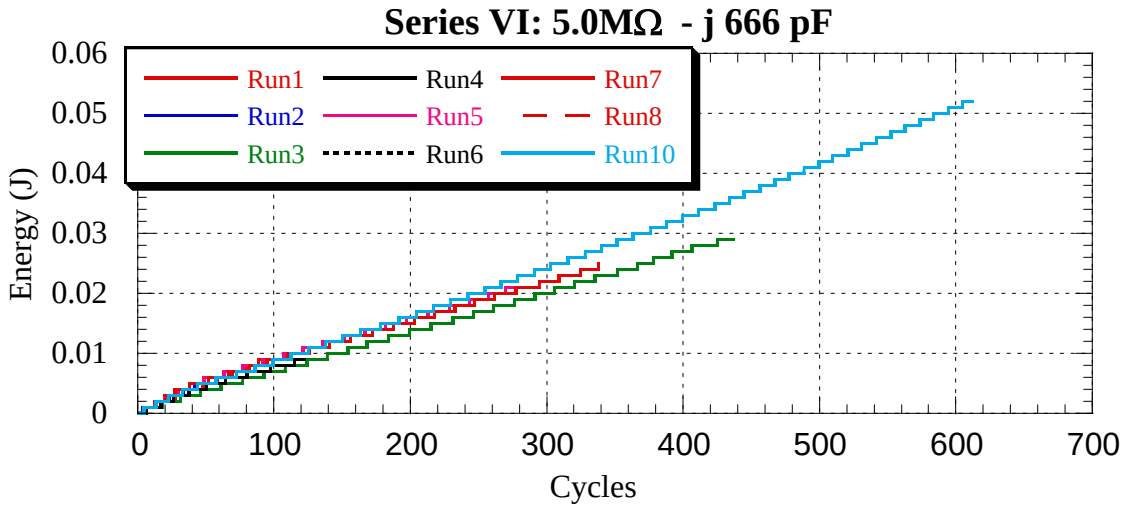

Figure 64. Series VI: Energy vs. TTF comparison

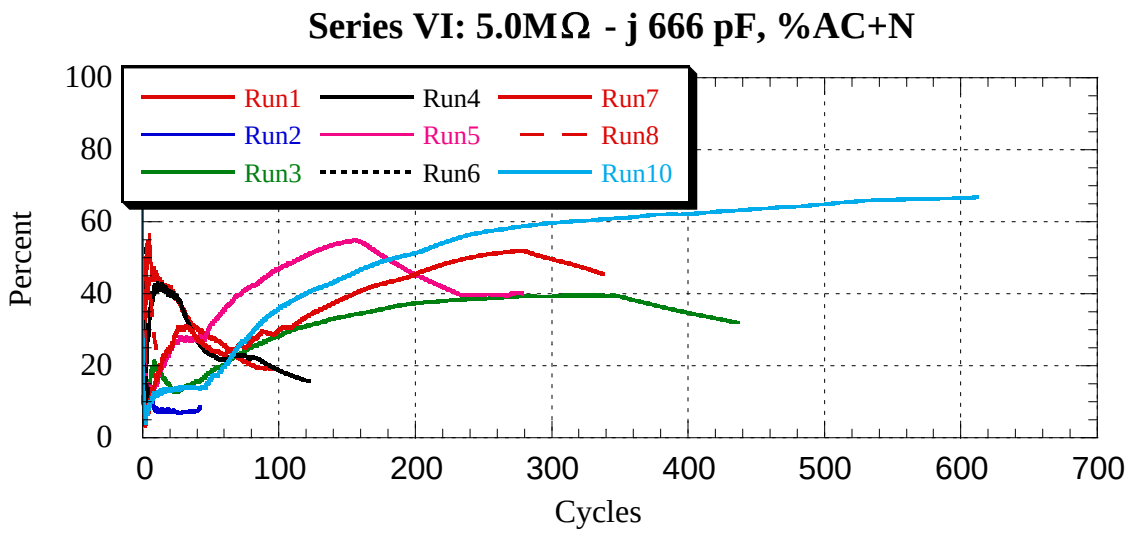

Figure 65. Series VI: Percentage vs. TTF of *AC + Noise period*

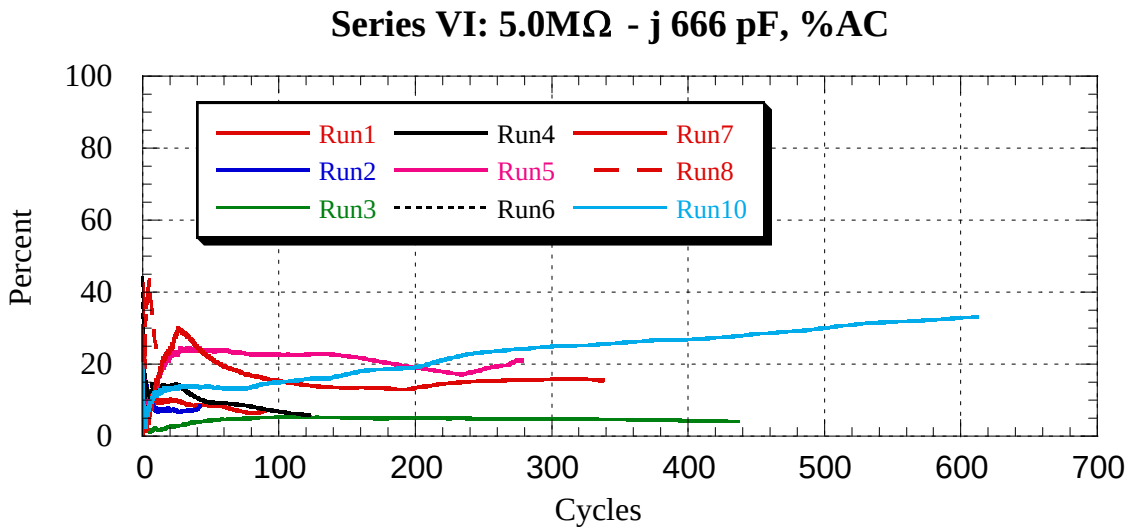

Figure 66. Series VI: Percentage vs. TTF of *AC period*

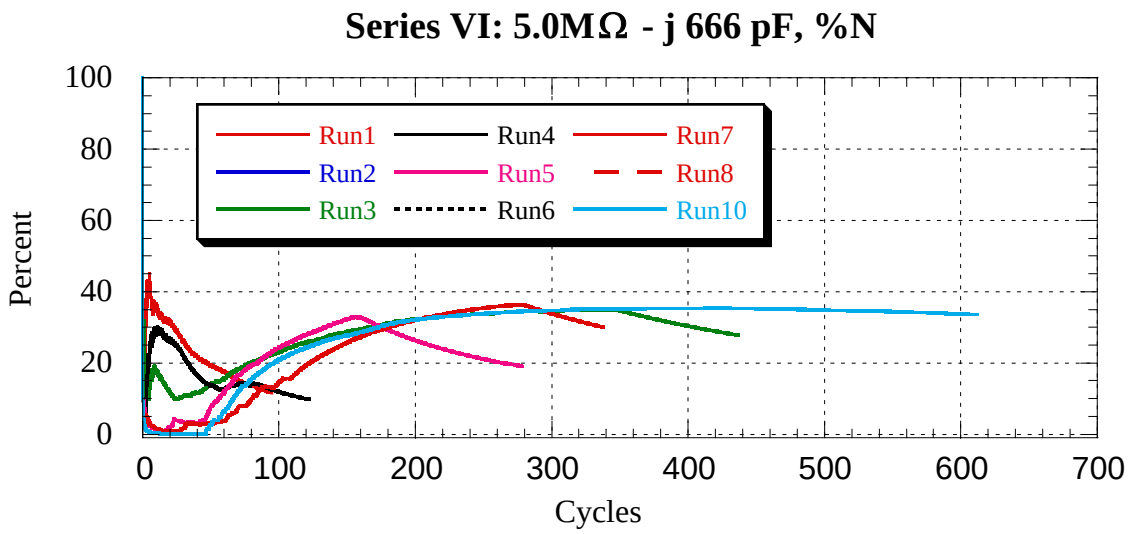

Figure 67. Series VI: Percentage vs. TTF of *Noise period*

The Weibull plot is shown in Figure 68 along with the table of values used. The values with the symbol, >, are suspended values. The suspended values are samples that have failed by a different failure mode. The different failure mode is not clearly defined at the moment, but are considered abnormal comparable to the previous series of tests. The suspended values are not ignored and are included in the analysis [27].

The β value is less than 1, indicating that the cables have failed prematurely. This makes sense based on the experimental conditions and the development of the dry-band arcing between the two electrodes. Other statements regarding the outcome can be surmised, although it would not be prudent at the present time.

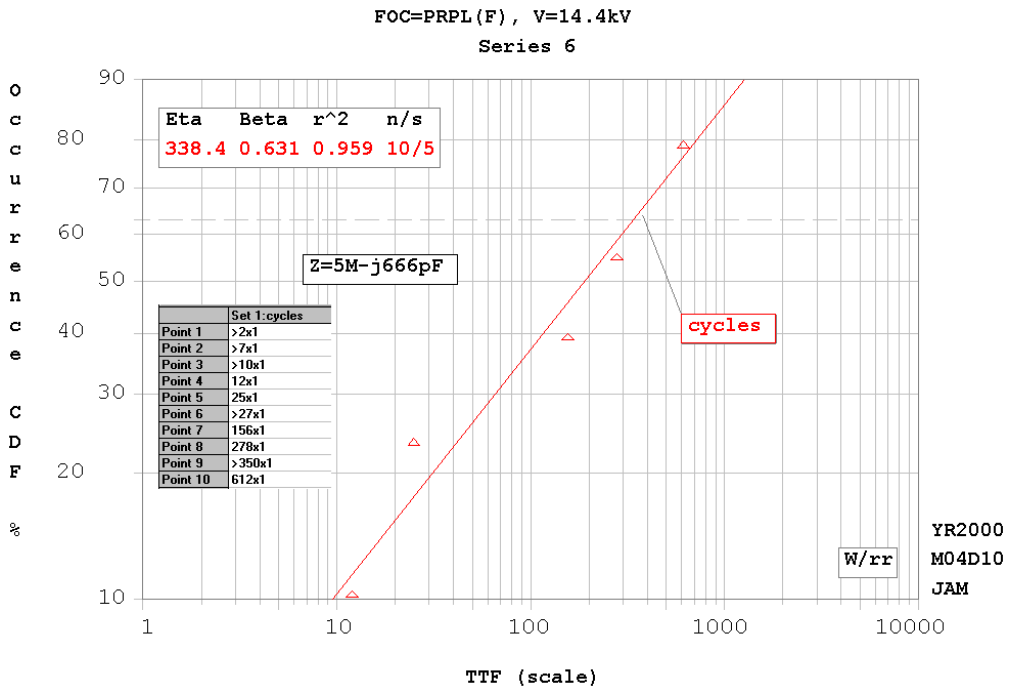

Figure 68. Series VI: Weibull plot with suspensions

The values used in the Weibull plot in Figure 68 are the onset points of the *tail* trajectory. The Weibull plot in Figure 69 shows the TTF plotted for the four possible ways of categorizing the failures. The plot using the 'suspensions only' data could be further categorized into two more failure modes. The reason for this is because the data does not fit a straight-line too well, $r^2 = 0.864$.. One thing that could be said for certain is that the cables fail quite differently under these test conditions. Therefore, the repeatability in this test procedure is not too good. There must be some other factor influencing the failure modes and would require further investigation in order to find the connection between the failures. In any case, the failure modes that are considered here all have a shape parameter, β, of less than one. This might be an indication that the severity of the dry-band arcing is concentrated too much in one area, which may or may

not actually occur in nature. These series of tests should be kept in mind in the development of a standard test method.

An interesting result would be a Weibull plot of the TTF with a shape parameter, β, greater than one, which is yet to be seen. This would definitely add a twist to the ongoing research and possibly be helpful information in understanding the development of the dry-band arcing phenomenon.

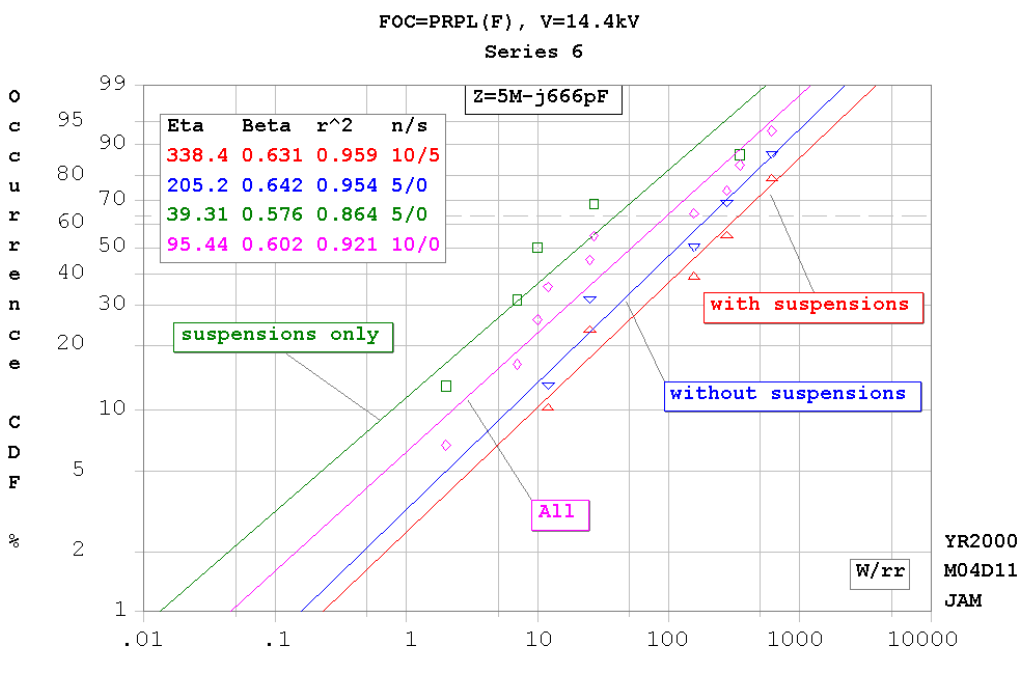

	Set 1:with s..	Set 2:withou..	Set 3:suspen..	Set 4:All
Point 1	>2x1	12x1	2x1	2x1
Point 2	>7x1	25x1	7x1	7x1
Point 3	>10x1	156x1	10x1	10x1
Point 4	12x1	278x1	27x1	12x1
Point 5	25x1	612x1	350x1	25x1
Point 6	>27x1			27x1
Point 7	156x1			156x1
Point 8	278x1			278x1
Point 9	>350x1			350x1
Point 10	612x1			612x1

Figure 69. Weibull plot of various failure modes, Series VI

The graphs in Figure 70 and Figure 71 show the *imsq* distributions for the ten runs in Series VI. One interesting observation to note is that for TTF of 42, 7, 10, and 2 have a very low percentage of the *Noise period* leakage current. This means that the majority of the time the current either in the *AC* or *Arcing period*. A known fact is that most of the damage is caused during the *Arcing period*. It should be noted that there were instances when the arcing was interrupted by the spray, otherwise the arcing could have continued and cause the failures to occur in a shorter number of cycles. There were other instances when the arcing self-extinguished. A possible reason for the duration of the arcing is due to the nature of the drying process and droplet formations on the cable's sheath. The drying process is itself random. Another interesting observation from the graphs in Figure 70 and Figure 71 is that the overall percentage of *Noise period* activity is less than those recorded in the *long-gap* series of tests.

All of this data may provide some further insight in the nature of dry-band arcing on fiber optic cables. As for now it seems that the *long-gap* test procedure provides results that are better understood, while the *short-gap* series of tests result are considerably less tangible.

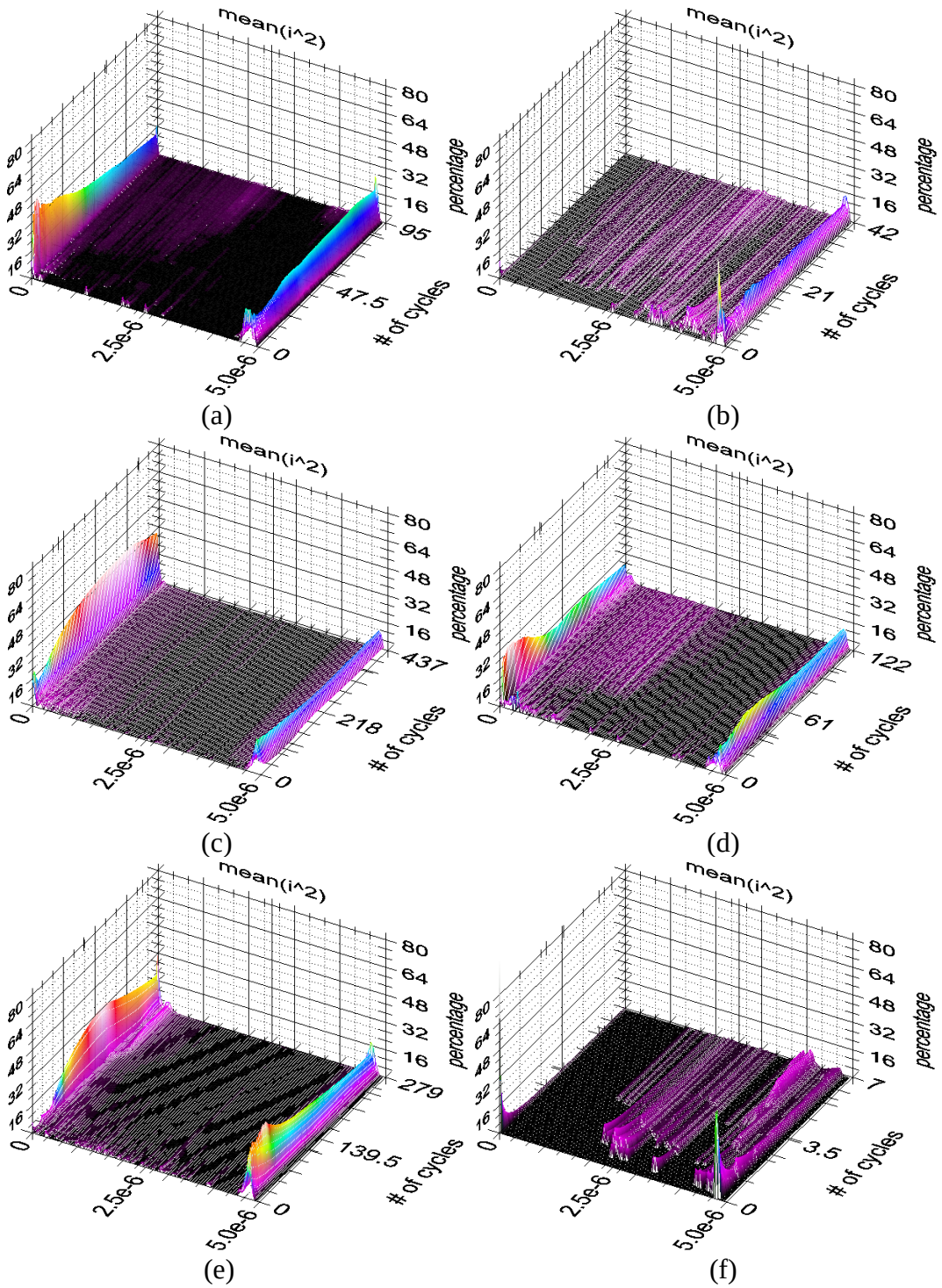

Figure 70. Series VI: *imsq* distribution, (a) Run1, (b) Run2, (c) Run3, (d) Run4, (e) Run5, (f) Run 6

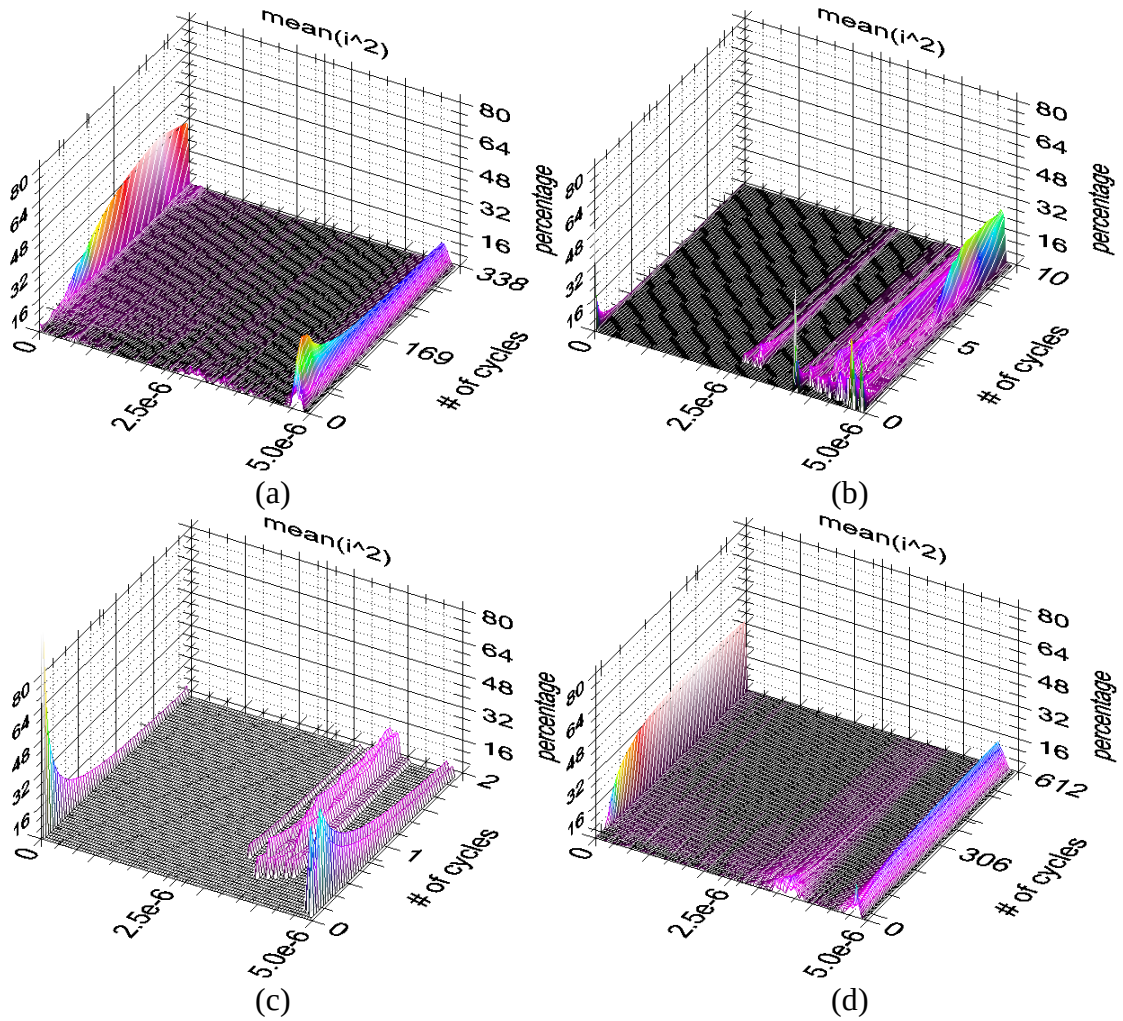

Figure 71. Series VI: *imsq* distribution, (a) Run7, (b) Run8, (c) Run9, (d) Run10

X. CONCLUSIONS

Three categories of events were defined for the activity of dry-band arcing on fiber optic cables:

1. *AC period*

2. *Arcing period*

a. *60 Hz type*

b. *Pulse type*

3. *Noise period*

From the leakage current data a random variable, $imsq = \sum_{k=1}^{N} \frac{i_k^2}{N}$, was defined and used to account for the three periodic events of dry-band arcing. The values of *imsq* were used to form a set of histograms, running histograms, energy plots, and percentage trajectories that are used to correlate dry-band arcing to the time-to-failure of the fiber optic cables.

Six series of test were performed and leakage current data was acquired. The acquired data was used to correlate dry-band arcing damage to the time-to-failure and show how the failure modes of the *long-gap* versus the *short-gap* methods differed by using the slope parameter, β, from the Weibull plots. The *short-gap* TTF data had a $\beta <$ 1 indicative of premature failures and with various modes of failure within this regime. The *long-gap* had a $\beta = 1$ indicative of random failures, as could be expected to actually occur in nature. The TTF data points were fitted with the Weibull cumulative distribution function (cdf) for the *long-gap* test of Series III quite well.

The percentage trajectories of the three periodic events undergone by dry-band arcing showed a definite pattern amongst the various series of tests performed. The trajectories showed to have a peak value prior to a negative sloping tail, at which point the cable's sheath were considered to have failed.

Chapter 6

Conclusions and Recommendations

I. DRY-BAND ARCING DAMAGE

Dry-band arcing is an electrical phenomenon acknowledged by numerous people who have studied it to cause failures of fiber optic cables installed near high voltage transmission networks and drop out of service. The fiber optic cables naturally become polluted and in effect forming a conductive layer to be formed on the cable's outer sheath. The high voltage conductors on the transmission towers cause an electric field that induces a current to flow on the conductive layer. During wet and dry periods that occur from rainfall will allow for the formation of dry bands on the fiber optic cable's sheath. The dry bands can, in some instances, have a large enough potential across it to cause an arc to be created and thereby cause damage to the sheath.

II. THE NEED OF A TEST PROCEDURE

A laboratory experimental test setup and procedure has been developed to qualify fiber optic cables and be able to find out which sheathing material is best suited to withstand dry-band arcing damage as would be encountered in the field. A test method needs to be standardized, which the IEEE joint working group is presently doing. The initial draft standard, IEEE P-1222, would benefit from the results obtained in this thesis in standardizing the test method. A set of metrics are defined for the test which can be used as base case conditions along with a method of measuring and acquiring leakage

current data. The data is used to correlate damage caused by dry-band arcing to the time-to-failure of the cable's sheath. From the correlated information, cables from different manufacture's could be compared and ranked to determine which cables has a better sheath to withstand dry-band arcing.

III. FUTURE RESEARCH AND DEVELOPMENT

An IEEE joint working group has been formed to study and create a standardized test procedure in evaluating ADSS fiber optic cables installed on overhead utility power lines. WAPA is currently helping in the research by funding ASU's electrical engineering power department to study dry-band arcing on fiber optic cables and has done so for the last 4 years. Other institutions involved in this study and other facets of this problems are EPRI, Bonneville Power Administration, Washington State University, and others outside of the United States. Concrete solutions for avoiding catastrophic failures caused by dry-band arcing and having a standard test method are still under investigation as follows:

1. Effects of gap length for different voltages and limiting impedance.
2. Failure modes caused by different %NaCl.
3. Effects of failures for different inclines.
4. Determine the ON/OFF times to efficiently test cables for a given time frame.
5. Verify pollution levels for various climates around the world.
6. Effects of electrode dimensions.

References

[1] M.W. Touminen, "3 Phase circuit model for ADSS optical fiber contamination currents," Engineering Report TNL3-99-1, Bonneville Power Administration, US Department of Energy, May, 1999.

[2] C.N. Carter, M.A. Waldron, "Mathematical model of dry-band arcing on self-supporting, all-dielectric, optical cables strung on overhead power lines", *IEE Proceedings - C*, Vol. 139, No. 3, May 1992, pp. 185-196.

[3] S.M. Rowland, K. Craddock, et. al., "The development of a metal-free, self supporting optical cables for use on long span high-voltage overhead power lines," *Proceedings of the 36th International Wire and Cable Symposium*, Arlington, 1987, pp. 449-456.

[4] The Furukawa Electric Co., Ltd., "Optical fibers and cables," http://www.furukawa.co.jp/english/product/jotsu1_e.htm, May 2000.

[5] Resource Site prepared by CAO Long Qing, "Fiber optic cable resource site," http://csadfa.cs.adfa.edu.au/~mariamf/int-tele/assign1/cao/cao.htm, May 2000.

[6] Telecommunication Industry Association, "Communications in the 21st Century," http://www.atalink.co.uk/tia/, June 2000.

[7] American National Standards Institute, "Standards and conformity assessment information," http://www.ansi.org/, April 2000.

[8] International Organization for Standardization, “ISO online,”, http://www.iso.ch/, May 2000.

[9] International Electrotechnical Commission, “Standards and assessment of electrotechnology,” http://www.iec.ch/, April 2000.

[10] P-1222: IEEE Standard for All-Dielectric Self-Supporting Fiber Optic Cables (ADSS) for use on Overhead Utility Lines. Draft, April 1995.

[11] Corning Cables, “AirLite ADSS optical fibre cable,” http://www.corningcables.com.au/airlite.htm, May 2000.

[12] C.N. Carter, “Dry band electrical activity on optical cables separately strung on overhead power lines,” *Proceedings of the 37th IWCS*, Reno, November 1988, pp. 117-121.

[13] A.G.W.M. Berkers, J.M. Wetzer, “Electrical stress on self-supporting metal-free optical cable in high voltage networks,” *Proceedings for the 5th DMMA*, Canterbury, June 1988, IEE Conference publication No 286, pp. 69-72.

[14] R.G. Olsen, “An improved model for the electromagnetic compatibility of all-dielectric self-supporting fiber optic cable and high voltage power lines,” *IEEE Transactions on Electromagnetic Compatibility*, Vol 41, No 3, August 1999.

[15] G.G. Karady, S. Devarajan, M. Tuominen, B. Han, “Computer simulation of fiber optic cable failures due to dry-band arcing,” *Proceedings of the 1999 Power Engineering Society Summer Meeting*, July 1999, 99SM-127.

[16] C.N. Carter, "Arc control devices for use on All Dielectric Self Supporting optical cables," *IEE Proceedings-A*, September 1993, Vol. 140, No 5, pp. 357-361.

[17] G. Carlton, C.N. Carter, A. Peacock, "Progress in the long term testing of an all dielectric self supporting cable for power system use," *12th International Conference on Electricity Distribution CIRED*, London, UK, IEE Conference publication No. 373, Vol. 3, 1993 pp. 3.16/1-4.

[18] C.N. Carter, J. Deas, N.R. Haigh, and S.M. Rowland, "Applicability of all-dielectric self supporting cable system to very high voltage overhead power lines," *Proceeding of the 46th International Wire and Cable Symposium*, 1997, pp. 622-631.

[19] K.S. Edwards, P.D. Pedrow, R.G. Olsen, "Portable ADSS surface contamination meter," *1999 Annual Report Conference on Electrical Insulation and Dielectric Phenomena*, Piscataway, NJ, USA; IEEE Cat. No. 99CH36319, Vol.1, 1999, pp. 158-61.

[20] J.C.G. Wheeler, M.L. Lissenburg, J.D.S. Hinchliffe, M.E. Slevin, "The development and testing of a track resistant sheathing material for aerial fiber cables," *Proceedings of the 5th DMMA*, Canterbury, June 1988, IEE Conference publication No. 286, pp. 69-72.

[21] S.M. Rowland, C.N. Carter, "The evaluation of sheathing material for an all dielectric self-supporting communication cable, for use on long span, overhead power lines," *5th International Conference on Dielectric Materials, Measurements*

and Applications, London, UK; IEE Conference publication No. 289, 1988; pp. p.77-80.

[22] L.A. Dissado, M.J. Parry, S.V. Wolfe, A.T. Summers, C.N. Carter, "A new sheath evaluation technique for self-supporting optical fibre cables on overhead power lines," *Poceedings of 39th International Wire and Cable Symposium*, Shrewsbury, NJ, USA, 1990, pp. 743-51.

[23] D.A. Brewer, L.A. Dissado, M.J. Parry, "Limitations on the damage mechanism in dry-band arcing on all dielectric self supporting cables," *6th International Conference on Dielectric Materials, Measurements and Applications*, 1992, pp. 49–52.

[24] S.M. Rowland, F. Easthope, "Electrical ageing and testing of dielectric self-supporting cables for overhead power lines," *IEE Proceedings – A*, Science, Measurement and Technology, Vol.140, No.5, September 1993, pp.351-56.

[25] S.M. Rowland,I.V. Nichols, "Effects of dry-band arc current on ageing of self-supporting dielectric cables in high fields, *IEE Proceedings,* Science Measurement and Technology, Vol.143, No.1, January 1996, pp.10-14.

[26] LabVIEW, National Instruments Corporation, 11500 N. Mopac Expwy, Austin, TX, 78759-3504.

[27] R.B. Abernethy, The New Weibull Handbook, 2nd edition, Robert B. Abernethy, Florida, 1993.